Ethiopian
Academy
of Sciences
የኢትዮጵያ ሳይንስ አካዳሚ

PCC
ETHIOPIAN PANEL ON
CLIMATE CHANGE

ETHIOPIAN PANEL ON CLIMATE CHANGE

FIRST ASSESSMENT REPORT

WORKING GROUP I REPORT ON CLIMATE CHANGE OVER ETHIOPIA

I

PHYSICAL SCIENCE BASIS

ETHIOPIAN ACADEMY OF SCIENCES

ETHIOPIAN PANEL ON CLIMATE CHANGE

FIRST ASSESSMENT REPORT

WORKING GROUP I REPORT ON
CLIMATE CHANGE OVER ETHIOPIA

I

PHYSICAL SCIENCE BASIS

Lead Author: Tesfaye Gisila
Authors: Jemal Seid, Andualem Shemelis, Temesgen Gebremariam, Gebru Jember, Aklilu Amsalu (PhD)
Review Editor: Gizaw Mengistu (PhD)
Substantive Editor: Seyoum Mengitou (Prof.)

Citation- This document may be cited as follows:

Ethiopian panel on Climate Change (2015), First Assessment Report, Working Group I *Physical Science Basis,* Published by the Ethiopian Academy of Sciences

About the Ethiopian Academy of Sciences

The Ethiopian Academy of Sciences (EAS) was launched in April 2010 and recognized by an act of parliament (Proclamation No. 783/2013) as an independent institution mandated to provide, inter alia, evidence-based policy advice to the Government of Ethiopia and other stakeholders. Its major activities include undertaking consensus studies, conducting convening activities such as public lectures, conferences, workshops and symposia on issues of national priority; as well as promoting science, technology and innovation.

Acknowledgements

Table of Contents

Preface

The Working Group I is one of the key working groups established by Ethiopian Academy of Science to compile and assess the physical science aspect of climate change over Ethiopia. The contribution of the working group to Ethiopian Panel on Climate Change (EPCC) is a more detailed assessment of the physical aspect of current and future climate change and variability over Ethiopia while ensuring consistence with the Intergovernmental Panel on Climate Change (IPCC) AR5 report. As a result, the assessment expands existing new evidence of past, present and projected future climate change reported by IPCC Working Group I, based on analysis of in-situ observations and outputs from Coordinated Modeling Inter-comparison Project Phase 5 (CMIP5) models over Ethiopia.

The report is a compressive review of the physical aspect of climate variability and change and it is based on IPCC report, other published and unpublished scientific literatures on Ethiopian climate variability, change and its drivers available up to the end of March, 2015 and ongoing investigations from analysis of in-situ observations and data from CMIP5 models over Ethiopia.

The report has short summary for policymakers and seven chapters plus annex. The first chapter presents an overview of observed extreme events attributable to climate variability and change over Ethiopia, global climate change in general, efforts to unravel evidences of climate change and its links to anthropogenic factors as well as global initiatives to create awareness and to tackle the problem. The second and the third chapters assess the observed changes in mean climate and extremes over Ethiopia based on analysis of instrumental records and climate archives. Chapters 4-5 describe observed changes in the hydrological cycles and impact of climate change through shift on onset, cessation of rainy seasons and length of growing season. The introduction of climate models used in simulating past and present climate is presented in Chapter 6. The seventh chapter covers analyses of the 21st century projected changes in precipitation and temperature based on the ensemble mean of fourteen CMIP5 models.

A new element in this Working Group I review assessment is the inclusion of studies at local scales based on in-situ observations that resolve small

scale features peculiar to Ethiopia. Moreover maps of Climate Projections (in Chapter 7 and in the Annex) containing future temperature and precipitation projections for Ethiopia strengthens existing AR5 IPCC report on East Africa with country level detailed evidences. However, the limitations of this report is that it is based only on coarse resolution CMIP5 models since the models are not downscaled either dynamically or statistically to resolve small scale features spatially.

1. Introduction

The increased frequency of extreme weather events which faced Ethiopia in the 20th century may be one major impetus for enhancing the visibility of climate change issues over the country, Thus, research activities dealing with finding the major causes of these increasingly occurring extreme and severe weather and climatic events in the country date from the 1980s onwards (Gissila et al, 2004).

The major land marks of official research reports on Climate change over Ethiopia include climate change assessment reports coordinated by the National Meteorological Agency which included, US country climate change study report on climatic trend and vulnerability to climate change in 1996, the Initial National Communication Report of Ethiopia to the conference of the parties in 2001 and the National Adaptation Plan of Action (Ethiopia's NAPA report) in 2007. Since the publication of the NAPA report, various research reports have confirmed that the country should face climate change issues, and one of the objectives of this synthesis report is to undertake a general review and assessment of the results of climate change research over the country.

Anthropogenic climate change is one of the most pressing problems, which have emerged on our planet in the 20th century, needing serious attention on the part of Governments, the United Nations Organization and the Public. The major milestones in the science of climate research that brought the immensity of the problem to the attention of the public were the first and the second World Climate Conferences in 1979 and in 1990, where solid evidences on global warming and climate change were presented by Climate scientists and researchers based by the study of direct and proxy climate data.

The first official admission of the UN Body on the problem of global warming and climate change was, when the two specialized agencies of the United Nations, the United Nations Environmental Program(UNEP) and the World Meteorological Organization(WMO) decided in 1988 to set up an Inter Governmental Panel on Climate Change (an international panel of climate scientists, researchers and experts delegated by their Governments) to undertake a more thorough investigation on this newly emerging problem of

global warming and climate change, and come out with concrete proposals for the decision makers.

In 1990, the first Assessment report on global warming and climate change was released by the Intergovernmental Panel on Climate Change (IPCC), and a call for a global treaty regarding global warming and climate change was put as a proposal by the IPCC. In the same year, the issue was raised in the United Nations General Assembly and negotiations on a framework convention began. In 1991, the first meeting of the Inter-Governmental Negotiating Committee (INC) took place and in 1992, the Inter Governmental Negotiating committee adopted the UNFCC text, and at the earth summit in Rio, the UNFCC was opened for signature and in 1994 the UNFCC entered force.

By 2013, the IPCC has reached its fifth assessment report and all the studies undertaken so far have reconfirmed that global warming and climate change has become one of the most important problems facing mankind.

1.1 Background

There is now increased scientific consensus that climate change is happening. Observations and historical records provide strong evidence that the global climate has already started to change. In its Fifth Assessment Report, the IPCC (2013) has indicated that warming of the climate system is unequivocal, and since the 1950s, many of the observed changes are unprecedented over decades to millennia; the atmosphere and ocean have warmed, the amounts of snow and ice have diminished, sea level has risen, and the concentrations of greenhouse gases have increased. The trend in recent years show increasing temperatures in various regions, and/or increasing extremes in weather patterns.

During the last century, the average global temperature rose by 0.74°C which is the largest and fastest warming trend in the history of the Earth. Current projections show that the trend will continue and accelerate. The best estimate indicates that the earth could warm by 3°C during the 21st Century. Furthermore, the number and intensity of extreme events might increase further as the global temperature continues to warm as a result of climate change (WMO 2006). The radiation budget of the earth is a central element

of the climate system. On average, radiative processes warm the surface and cool the atmosphere, which is balanced by the hydrological cycle and sensible heating. Spatial and temporal energy imbalances due to radiation and latent heating produce the general circulation of the atmosphere and oceans. The major landmark in this direction has been the detection of an increasing trend of downward thermal radiation, based on data from observatories.

Climate changes prior to the Industrial Revolution in the 1700s can be explained by natural causes, such as changes in solar energy, volcanic eruptions, and natural changes in greenhouse gas (GHG) concentrations. However, research indicates that recent climate changes cannot be explained by natural causes alone; it is now certain that most of the change is due to human interference. This is evident from the increasing greenhouse gas concentrations in the atmosphere, positive radiative forcing, observed warming, and understanding of the climate system (IPCC, 2013). Greenhouse gases, of which CO_2 is the most important, trap heat in the earth's atmosphere, leading to the overall rise of global temperatures, which are liable to disrupt natural climate patterns. Modeling studies based on observations indicate an increase of 2.6 Wm^{-2} per decade over the 1990s, in line with model projections and the expectations of an increasing greenhouse effect (Wild et al., 2008). It is found out that human pollution mainly from fossil fuels, has added substantially to global warming in the past 50 years (Fowler et al 2004; UNEP 2006). With global warming on the increase and species and their habitats on the decrease, chances for ecosystems to adapt naturally are diminishing.

Climate change is already having significant impacts in certain regions, particularly in developing countries, and on most ecosystems. Africa is the most vulnerable continent to the impacts of projected changes because of widespread poverty which is a significant limitation to adaptation capabilities. The climate of the continent is controlled by complex maritime and terrestrial interactions that produce a variety of climates across a range of regions, e.g., from the humid tropics to the hyper-arid Sahara (Boko et al., 2007). There is already evidence that Africa is warming faster than the global average, and this is likely to continue although the overall trend is geographically variable (Conway, 2009). According to the IPCC (2007), average temperatures in Africa are predicted to increase by 1.5 to 3°C by 2050, and will continue further upwards beyond this time. Over the next century, this warming

trend and changes in precipitation patterns are expected to continue and be accompanied by a rise in sea level and increased frequency of extreme weather events. Such changes are expected to put huge pressure on the main economic activities and livelihoods of the people in the continent. For instance, projections indicate that the population at risk of increased water stress in Africa will be between 75-250 million and 350-600 million people by the 2020s and 2050s, respectively (IPCC, 2007). In addition, climate change is predicted to reduce the area of land suitable for rainfed agriculture by an average of 6%, and reduce total agricultural GDP in Africa by 2 to 9% (TerrAfrica, 2009).

Like many other developing countries of the world, Ethiopia is also experiencing climate change and its impacts. Model predictions for Ethiopia indicate not only a substantial increase in mean temperatures and an increase in rainfall variability but also a higher frequency of extreme events such as flooding and drought. The country's geographical location within the tropics and extremes of topography in combination with the low adaptive capacity of the people and their resources result in a high degree of vulnerability to the adverse impacts of climate change. A strong link has been observed between climate variations and the overall performance of the country's economy, mainly due to the direct impacts of unreliable weather on agriculture and the links to other sectors of the economy.

1.2 Key concepts and terminologies

This section attempts to describe some of the key concepts and terminologies often used in climate science.

Weather: Weather describes the conditions of the atmosphere at a certain place and time with reference to temperature, pressure, humidity, wind, and other key parameters (meteorological elements); the presence of clouds, precipitation; and the occurrence of special phenomena, such as thunderstorms, dust storms, tornadoes and others (Cubasch, 2013).

Climate: Climate is usually defined in a narrow sense as the average weather, or more rigorously, as the statistical description in terms of the mean and variability of relevant quantities over a period of time ranging from months to thousands or millions of years (Cubasch, 2013).

Greenhouse Gases (GHG): A greenhouse gas is any gaseous compound in the atmosphere that is capable of absorbing infrared radiation, thereby trapping and holding heat in the atmosphere. The most significant greenhouse gases include carbon dioxide (CO_2), methane (CH_4), nitrous oxide (N_2O) and water vapor (H_2O). Greenhouse gases increase the heat in the atmosphere and cause the greenhouse effect, which leads to global warming.

Greenhouse Effect: The greenhouse effect is a process whereby the earth's atmosphere traps thermal radiation from a planetary surface due to the presence of greenhouse gases that allow incoming sunlight to pass through but absorb heat radiated back from the earth's surface.

Global warming: Global warming refers to an increased in average global temperatures which are believed to be caused primarily by increasing in greenhouse gases such as carbon dioxide and other greenhouse gases (John 1997; Anup S. 2006).

Land use: *Land use* is commonly defined as a series of operations on land, carried out by humans, with the intention to obtain products and/or benefits through using land resources.

Land cover: *Land cover* is defined as the vegetation (natural or planted) or man-made constructions (buildings, etc.) which occur on the earth surface. It is the observed physical and biological cover of the earth's land, as vegetation or man-made features. Water, ice, bare rock, sand and similar surfaces also count as land cover.

Albedo: The fraction of solar radiation reflected by a surface or object, often expressed as a percentage. Snow-covered surfaces have a high albedo, the surface albedo of soils ranges from high to low, and vegetation-covered surfaces and oceans have a low albedo. The Earth's planetary albedo varies mainly through varying cloudiness, snow, ice, leaf area and land cover changes (IPCC, 2013)

2. Observations of Atmosphere and land surface

2.1. Changes in Atmospheric Composition/Radiation Budget

Anthropogenic influence on climate occurs primarily through perturbations of the components of the Earth's radiation budget. The radiation budget of the Earth is a central element of the climate system. On average, radiative processes warm the surface and cool the atmosphere, which is balanced by the hydrological cycle and sensible heating. Spatial and temporal energy imbalances due to radiation and latent heating produce the general circulation of the atmosphere and oceans. The major landmark in this direction has been the detection of an increasing trend of downward thermal radiation, based on data from observatories.

The major causes for this increasing trend in the downward thermal radiation were finally identified through various studies to be the increase in the green house gases emitted to the atmosphere. Recent modeling studies based on observations indicate an increase of 2.6 Wm^{-2} per decade over the 1990s, in line with model projections and the expectations of an increasing greenhouse effect (Wild et al., 2008). Thermal radiation, also known as long wave, terrestrial or far-IR radiation is sensitive to changes in atmospheric GHGs, temperature and humidity.

The 1750 globally averaged abundance of atmospheric CO_2 based on measurements of air extracted from ice cores was 278 ± 2 ppm (Etheridge et al., 1996). The current level of CO_2 400 ppm, which is 1.4 times the amount recorded in the pre-industrial time.

Both the fifth assessment and the fourth assessment reports of the IPCC indicate that increasing atmospheric burdens of well-mixed GHGs resulted in a 9% increase in RF from 1998 to 2005 and in a 7.5% increase in RF from 2005 to 2011, with carbon dioxide (CO_2) contributing 80% of these amounts. Thus, the global warming observed in the 20th and in the 21st century is intrinsically connected with the radiative forcing of the green house gases. This connection has been well captured in the climate model outputs. However, it is important to note that aerosols would have the opposing tendency of affecting the radiation budget, dimming the solar radiation reaching the surface of the earth. The level of aerosols in the atmosphere over Ethiopia is basically

dependent on the level of dust activity and biomass burning that occur over the country in addition to transport of aerosols from nearby regions (e.g., anthropogenic aerosol haze over the north Indian Ocean, due to atmospheric circulation). Moreover, volcanic activity over the Afar depression may also have some contribution. In this regard, it is important to realize that aerosol from anthropogenic sources (i.e., fossil and biofuel burning) are confined mainly to populated regions in the Northern Hemisphere (NH), whereas aerosol from natural sources, such as desert dust, sea salt, volcanoes and the biosphere, are important in both hemispheres and likely dependent on climate and land use change (Carslaw et al., 2010). Aerosols levels over Ethiopia due to dust activity is greatly characterized by seasonality, where the maximum dust activity occurs in May–July. Though there are evidences from observations that show increase in aerosols over the country, it is clear that the state of the aerosols over Ethiopia can be considered as very insignificant as compared with the state of aerosols observed over South Asia. However the likelihood impact of the transport of aerosols from the South Asia region to the region including Ethiopia is addressed in Chapter 4. It is important to note here that it has not yet been established how much the seasonally varying aerosols affect the surface radiation balance over Ethiopia, though there are various eye witness reports of sudden cooling during intense dust storms over north-eastern and northwestern lowlands of the country.

2.2. Changes in Land Use, Land Cover and Albedo

Land use and land cover change in relation to natural resources management over Ethiopia is perhaps one of the topics investigated extensively. Knowledge on land use and land cover changes, both on a local scale and large scale, is essential as these changes cause great environmental concerns to local and regional climate change. Several papers have been published which monitored land use and land cover changes over the past several decades in the different parts of Ethiopia. However, most of these studies cover smaller areas, and there is no a comprehensive study which covers the entire country yet. Available studies focused mostly on the highlands than the lowlands of the country.
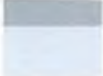
In northern Ethiopia, Nyseen et al (2009) investigated land use and land cover change using a matched pair of photographs that date back to 1868 to assess

the changes over the last 140 years. They found out that the landscape has already been in a severe state of degradation with limited vegetation cover in 1868. Until the recent massive plantations, the northern highlands in general and Tigray in particular have been devoid of vegetation cover. A watershed scale investigation by Aynekulu et al (2006) indicated that 75% of the forest land had been converted into arable land over a period of 50 years. Studies carried out in the north-western highlands of Ethiopia indicate a considerable decline in the natural forest cover and expansion of cultivated land (Zeleke and Hurni, 2001; Beweket, 2002; Gebrehiwot et al., 2010).

In the north-eastern part of Ethiopia, land use and land cover change over the past several decades has been considerable. Evidences indicate that there has been massive deforestation that probably contributed to the prevalence of severe droughts. Based on analysis of matched pairs of photographs from 1937 and 1997, Crummey (1998) found out that the land cover in Tahuladare area in Wollo is marked by more trees. Whereas in Kalu district, Tekle and Hedlund (2000) found reduction of shrub lands by 51% and forests by 31% between 1958 and 1986. Similarly, there has been a decline in land area covered with shrubs by 58% between 1957 and 1986 in the Derekolli catchment of South Wollo (Tegene, 2002).

A study in the Chemoga watershed of the north-western highlands of Ethiopia shows a remarkable decrease of woodlands (by 46%) and shrublands (by 41%), and an expansion of cultivated land (by 13%) between 1957 and 1982 (Beweket, 2002). Zeleke and Hurni (2001) also reported a similar trend of land use and land cover change: a decline of the natural forest cover from 27% in 1957 to 2% in 1982 with an increase of cultivated land from 39% in 1957 to 70% in 1982, which is a 78% increment of cultivated land within only two and a half decades. According to Gebrehiwot et al (2010), the forest cover has declined by about 86% and cultivated land expanded by 40% between 1957 and 1986 in the Koga watershed at the headwaters of the Blue Nile Basin.

Using travellers' accounts, MacCann (1995) found out that much of the central highlands has been devoid of trees and wood fuel for at least 150 years due to deforestation. Based on analysis of remote sensing data in Beressa watershed in North Shewa, Amsalu et al (2007) found a reduction of the natural forest cover and plantations by 55% and 35%, respectively,

between 1957 and 1984. In Debre Sina area, on the other hand, an increase in woody plant cover, from 4.4% in 1957 to 9.2% in 1986, has been observed mainly due to government afforestation and land rehabilitation programs during the early 1980's (Wøien, 1995).

Significant loss of forest cover has been observed by Dessie and Christiansson (2008) in parts of the south central Rift Valley region. A similar study by Muzein (2006) in the Zeway-Awassa basin found a substantial loss of vegetation cover at the expense of cultivated land expansion: about 27% of the woodland cover is lost between 1973 and 1986, and cultivated land expanded by 113% during the same period. Furthermore, Dessie and Kleman (2007) in Awassa watershed, Garedew et al. (2009) in Arsi Negele area, Moges and Holden (2009) in Umbulo catchment of the southern Ethiopian highlands, and Mengistu (2009) in the Abaya-Chamo sub-basin of the southern Ethiopian Rift valley area revealed a considerable decline in forest cover mainly due to farmland expansion. In Western Ethiopia, Tefera and Sterk (2008) studied land use and land cover changes in Fincha watershed and found out that forest cover declined by 51.6% between 1957 and 1980 with a corresponding expansion of cropland by 18.7% and decreased grazing land by 50.8%.

2.3. Greenhouse gases (GHG)

Climate change is mainly caused by the build-up of greenhouse gases in the atmosphere which has led to an enhancement of the natural greenhouse effect. Hence, the increasing concentration of greenhouse gases (such as CO_2, CH_4, and N_2O) in the atmosphere as a result of human activities and its possible consequence of global warming and climate change has become a serious international concern. GHG emissions have increased since the beginning of the industrial era and accelerated worldwide, particularly since 1945. The dominant causes of increase in emissions over the last 250 years mainly include fossil fuel use, agriculture and land use (IPCC, 2007). However, the extent of emissions varies across countries and economic sectors. Developed countries are generally regarded for causing significant contributions to the global greenhouse gas emissions.

Global trends

According to the fifth assessment report (IPCC, 2014), the atmospheric concentrations of major GHG such as carbon dioxide, methane, and nitrous oxide have increased to levels unprecedented in at least the last 800,000 years. In particular, carbon dioxide concentrations have increased by 40% since pre-industrial times, primarily from fossil fuel emissions and secondarily from net land use change emissions. However, though negligible, other natural events can also contribute to an increase in global GHG emissions and average global temperature. In 2011, the concentrations of carbon dioxide, methane, and nitrous oxide were 391 ppm, 1803 ppb, and 324 ppb, and exceeded the pre-industrial levels by about 40%, 150%, and 20%, respectively. On the other hand, global estimates indicate that deforestation can account for 5 billion metric tons of CO_2 emissions, or about 16% of emissions from fossil fuel sources. Tropical deforestation in Africa, Asia, and South America are thought to be the largest contributors to emissions from land use change globally.
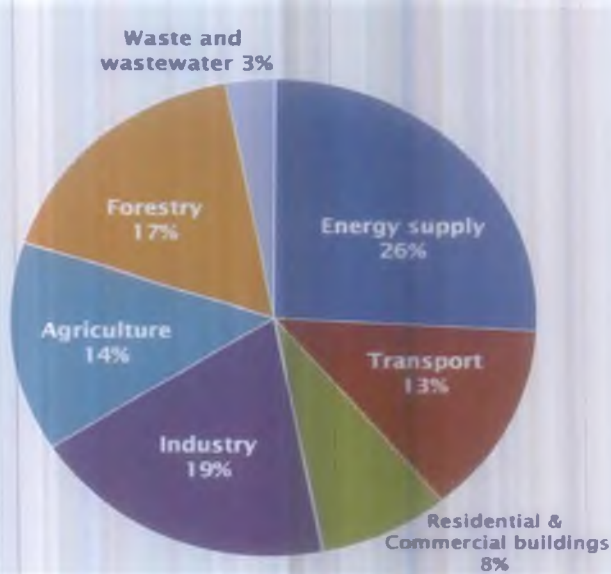

Figure 1. Global GHG emissions by source (Source: IPCC, 2007).

As shown in Fig. 1, the energy sector is relatively the biggest contributor of greenhouse gas emission. Most of the emissions result from the combustion of fossil fuels mainly for transport and industrial activities. Of all the GHGs,

the global trend of carbon emissions indicates a significant increase since the 1950's. Remarkable trends were seen in the top 3 emitting countries/ regions, which accounted for 56% of total global CO_2 emissions: China (29%), the United States (16%), and the European Union (11%) (PBL, 2013).
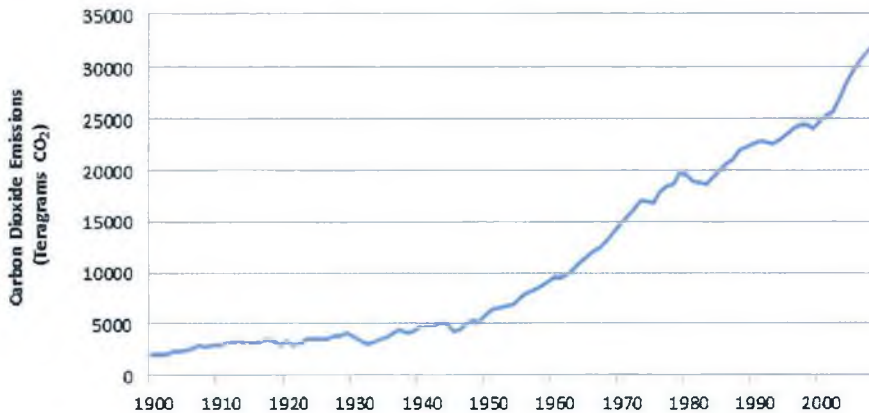

Figure 2. Global carbon dioxide emission (Source: US EPA).

There has been a growing controversy over the extent of Africa's contribution to global greenhouse gas emissions. Many argue that Africa's contribution is generally insignificant. According to UNEP, when comparing the greenhouse gas emissions per capita in the typical African country with the typical European country, the Europeans emit roughly 50-100 times more, while the Americans emit 100-200 times more (UNEP, u.d). Although deforestation, land use changes and wildfires contribute to greenhouse gas emissions in Africa, there is a considerable potential to absorb carbon from the atmosphere.

Emissions profile of Ethiopia

Ethiopia's contribution to global greenhouse gas emissions is low with per capita emission below the sub-Sahara Africa average. Ethiopia has started to conduct a national greenhouse gas inventory in 2001. It has submitted four national climate change related reports to the UNFCCC, of which two of these reports have made an assessment of greenhouse gas emission from the country. The Initial Communication to the UNFCCC (2001) provides emission estimates for 1994 and the Climate Change Technology Needs Assessment Report (2007) provides estimates for 2004.

In general, the contribution of Ethiopia to the global GHGs emission is negligible. According to the first National Communication total greenhouse gas emission across four key economic sectors (energy, agriculture, industry, waste) indicates national emissions of 48 million tons CO_2-equivalent, excluding CO_2 emissions/removals from the Land Use, Land Use Change and Forestry (LULUCF) sector. Agriculture, mainly the livestock sub-sector, accounted for 80% of total emissions ($38MtCO_2e$), energy 15% of the total emissions ($7.2MtCO_2e$) and the balance was emitted from waste, land use change and industrial processes. The Climate Change Technology Needs Assessment Report estimated greenhouse gas emissions from petroleum combustion to have increased to $4.7MtCO_2e$ by 2004, an increase of 63% compared to 1994. The total greenhouse gas emissions is estimated to have increased to nearly $100MtCO_2e$, i.e., twice that of 1994, and per capita emission was $0.9tCO_2e$ in 1994 and reached to $1.2tCO_2e$ in 2010. Generally, there were increasing trends of greenhouse gas emissions in the country in the period from 1990 to 1995. The relative comparisons of increase indicated that, CO_2 have increased by 24% while emission of CH_4 and N_2O increased by 1% and 119%, respectively. Aggregate greenhouse gases emissions in terms of CO_2 equivalents have increased by 12% (NMSA 2001).

Although, it was planned to undertake a GHG emissions inventory for all sources/sectors recommended by IPCC, only emissions from the following sources/sectors are considered. These are:

- Energy consumption, either traditional or modern ;
- Agricultural practices: livestock, burning of agricultural residues, and savanna;
- Natural forests (special attention given to emission from on site burning) ;
- Waste emissions from landfills, municipal, and industrial liquid waste; and
- Industrial processes (for instance, emissions from cement factories).

These sources/sectors are believed to be the most significant based on Ethiopia's economic level of development. Ethiopia's emission profile is dominated by emissions from energy and agriculture sectors, contributing about 90% of the total emissions. The greenhouse gas emission from energy sector is an important contributor to the total national emission. According

to the 2004 inventory, it was accounted for more than 50% of the total GHGs emission and was twice of the 1994 values. The combustion of fossil fuels mainly in the transportation sector was responsible for 88% of the total CO_2 in 1994 (B and M Development Consultants, 2006). Emissions from these sectors and for five types of greenhouse gases (CO_2, CO, CH_4, N_2O, and N_2O) is summarized as follows:

- Emissions from agriculture account for 80% to 85% of the total emissions (38Mt CO_2e 84Mt CO_2e in 1994 and 2010 respectively). The main greenhouse gases emitted from the agriculture sector are methane, N_2O emissions from fertilizer, and methane and other greenhouse gases from animal waste.;
- The energy sector constitutes 14% of the total emissions. Emissions from the sector are due to CO_2 released during the combustion of fossil fuels and methane released during the combustion of biomass fuels;
- Greenhouse gas emission from Industrial processes (not from energy consumed in industry) in Ethiopia is mainly due to cement and lime production (calcining of limestone to form clinker generates CO_2, as a result of chemical transformation of limestone); other industrial processes with GHG emission include production of iron and steel, aluminum, magnesium, and nitric acid;
- Land use change and forestry contribute to greenhouse gas emissions due to deforestation and burning of forests, woodlands and grasslands. Emissions from land use change are estimated to amount to 656ktCO2e in 2010; and
- Emission from waste (mainly solid and liquid waste from humans) is due to emission of methane in anaerobic decomposition. A significant and increasing amount of waste is generated in the main cities in open waste dump sites and landfills and from waste water. Emissions are expected to increase rapidly due to increased urbanization, increased affluence of the population in cities and increased waste collection.

2.4 The Climate System over Ethiopia

The climate of Ethiopia is tropical modified by the topography of the country and is dominated by convective precipitation associated with the seasonal

migration of the Inter tropical Convergence Zone (ITCZ). Moreover, dynamic convergence systems such as the Tropical Easterly jet stream also do play an important role associated with the East west overturning Walker circulation system during the northern hemisphere summer, locally known as Kiremt season. The major topographies that affect the Climate system of Ethiopia include the major mountain chains, the highland plateaus, the low lying plains, the Great Rift Valley and river valleys associated with the major river basins of the country. Thus, temperature is greatly determined by altitude over Ethiopia where various attempts have been successful to develop a relation between the mean annual average temperature of a place and its altitude.

Rainfall in Ethiopia is characterized by high spatial and temporal variability as a result of the topographic variation and geographical location. Topgraphic highs play a major role in releasing the conditional thermodynamic instabilities of the moist incoming air into the country strengthening convective developments, where as precipitation patterns over topographic lows greatly depend on the strength of large scale rainfall producing systems, such as the ITCZ, the Tropical Easterly Jet, the creation of convergence zones and local convective systems. When the windward side of the mountains is characterized with a rising moist air, the leeward side of the mountains is characterized with a descending warm dry air. Thus, rainfall activity on locations with the same altitude can differ depending on whether they are found over the windward or on the leeward side. As a result, one can observe great difference in the rainfall between the western lowlands of the country which are on the windward direction as compared with the lowlands of the eastern parts of the country, which are usually on the leeward side.

2.4.1 Seasons and seasonal classification over Ethiopia

In high and mid-latitudes, seasons are classified as winter, spring, summer and autumn, while in low latitudes they are categorized as wet and dry seasons. In the case of Ethiopia, air mass analysis of seasonality over the country indicates that there are three major seasons over the country, which include the Belg Season (Feb-May), Kiremt season (June-September) and Bega Season (October-January). This seasonality is basically the result of the seasonal migration of the Inter tropical Convergence Zone (ITCZ) and

the seasonal distribution of the atmospheric pressure systems (both over land and over the near by Oceans) and the quasi stationary sub tropical anticyclones over the Indian Ocean and the Atlantic Ocean (Endalew, 2007).

The major rainfall regimes of the country include four cases where group A of the rainfall regime corresponds with areas having a distinct wet and a distinct dry season, group B corresponds with areas having two wet and two dry seasons, and group C corresponds with two wet and one dry season in between (Fig. 3).
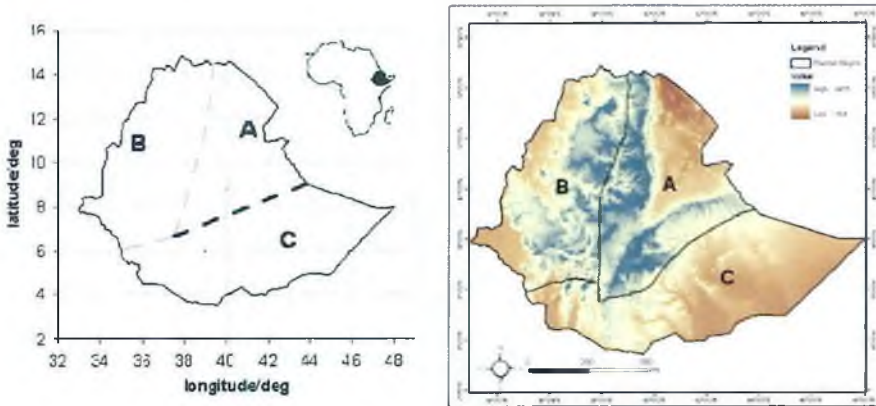

Figure 3. Rainfall Regimes (left) and topography map (right) of the Country.

The main moisture source during the Belg (Spring season) and the Bega (October-January) can be considered as the Indian Ocean where as the Ethiopian summer rains occur as air masses carrying moisture from the Indian Ocean, the Gulf of Guinea and the region to the north of Ethiopia, converge above the Ethiopian highlands (Hurk et al. 2005; Korecha and Barnston 2007; Segele, 2009; Lamb et al. 2009; Viste and Sorteberg 2011). Recent studies (Mengistu Tsidu, 2012a) based on high resolution gridded rainfall shows presence of more rainfall regimes within the three broad categories (see Fig. 4).
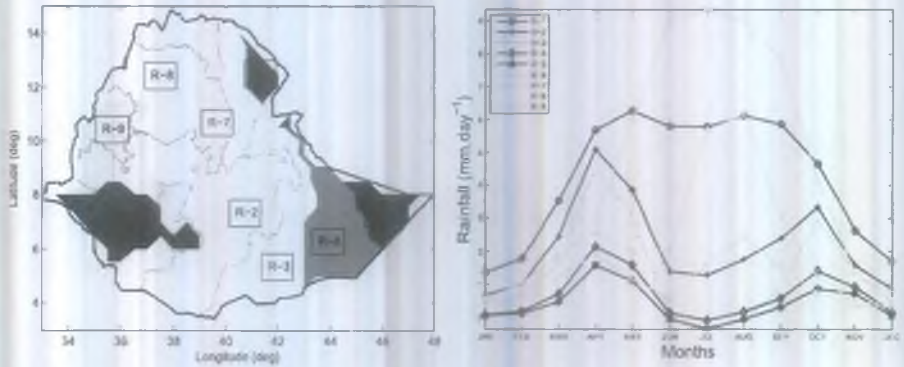
Figure 4. (left) The homogeneous rainfall regimes determined from the new gridded gauge rainfall data based on the self-organizing map and (right) their seasonal rainfall variation (Source: Mengistu Tsidu, 2012a).

The major basic reasons for the division of the country, in to the given rainfall regimes can be ascribed to the combined effect of the major topographies of the country with the associated orientation of the moisture bearing winds and the North-South meridional movement of the ITCZ.

2.4.2 Weather systems affecting Ethiopia

Seasonal and annual rainfall variations in Ethiopia as well as the neighboring areas of the region are associated with the macro-scale pressure systems and monsoon flows (Tesfaye 1986, 1987; Hastenrath, 1991). Bekuretsion (1987a) has indicated that the weather and climate of Ethiopia arises from the influence of tropical weather systems, like the Intertropical Convergence Zone (ITCZ), the monsoon, easterly waves, etc., and quasi-stationary subtropical anticyclones of both northern and southern hemisphere. The interactions between the tropical and extratropical weather systems produce major active weather over the country, especially during the months of February to May (Northern Hemisphere Spring). The main weather bearing systems for the Bega, Belg and Kiremt seasons, respectively are discussed below

2.4.2.1 Weather Systems during the Bega season

During Bega (October to January) the country predominantly falls under the influence of warm and cool northeasterly winds. These dry air masses originate either from the Saharan anticyclone or from the ridge of high

pressure extending into Arabia from the large high over central Asia (Siberia). However, occasionally the northeasterly winds are interrupted when migrating low pressure systems originating in the Mediterranean area move southwards and interact with the tropical systems resulting in unseasonal rains over central and northern Ethiopia. Occasionally the development of the red Sea Convergence Zone (RSCZ) also produces rains over northeastern Ethiopia (Pedgley, 1966). Moreover the southward migration of the ITCZ produces rains over the southern and southeastern lowlands of the country, where October-November constitutes their short rainy season with moisture incursion from the Indian Ocean.

Figure 5. The ITCZ and the quasi stationary subtropical anticyclones during the Bega season.

2.4.2.2. Weather Systems during the Belg season

During Belg (the small rainy season) which is from March to May, the Arabian high moves towards the northern Arabian Sea. When it is pushed over the water body, it causes a moist southeasterly air current to flow towards Ethiopia (NMSA 1996; Camberlin et al, 2002). Occasionally, there are also frontal lows that either originate from the Mediterranean area or originate within the Atlantic Ocean and are swept through from west to east. These occur in association with a cold front, the intensity of which depends on the temperature contrast ahead and behind the front. As it reaches east

of Mediterranean Sea, the surface front is split into two: one front over the Arabian lowland and the other over the Sudan lowland (Gizaw, 1968). Once the surface fronts reach over the high grounds, they interact with the equatorial systems and produce abundant rains over the northern, northeastern, central parts of Ethiopia and the escarpments. Sometimes when the low-level westerly trough penetrates along the Rift Valley, the rainfall activity could linger for some days.

The meridional arm of the ITCZ also contributes for the rainfall activity over East Africa. Hence, it produces rainfall during February/March over south west of Ethiopia (Kassahun, 1987a). The formation of intense and frequent tropical disturbances over the southeast Indian Ocean occurs simultaneously with Belg and Kiremt rainfall deficiency in Ethiopia (Bekele, 1992).

Figure 6. The ITCZ and the quasi stationary subtropical anticyclones during the Belg season.

2.4.2.3 Weather systems during the Kiremt season

During Kiremt season, the low-level air circulation over the western half of the Indian Ocean is dominated by the southwest monsoon winds over the Arabian Sea, a strong cross-equatorial flow along the East African coast and over the adjacent ocean, and southeasterly trade winds in the Southern Hemisphere (SH). The high topography of the African coast diverts the main

monsoon flow northwards and eastwards. This means that, in Ethiopia, rain during the boreal summer is associated with the migration of the ITCZ rather than the southwest monsoon winds. The major regional features during the Kiremt (June to September) include, in addition to the ITCZ, the macro-scale pressure systems and monsoon flows (Tesfaye 1986, 1987; Hastenrath, 1991). The northward propagation of ITCZ as well as the formation of heat lows over the Sahara and Arabian landmasses (Korecha et al, 2007). ITCZ attains a peak position of 15°N and 15°S during July and January, respectively (Asnani, 2005). The airflow is dominated by zones of convergence in the low pressure systems accompanied by the oscillatory ITCZ extending from West Africa through Ethiopia towards India (NMSA, 1996). There is convergence between the air stream of African southwest monsoons diverted from the south Atlantic southeast trades and the Indian southwest monsoon on the Ethiopian highlands, especially on the western, central and eastern high grounds, resulting in heavy rainfall over the region (Gizaw, 1968).

The position and strength of subtropical high pressure systems over the Azores, St. Helena, and Mascarene, especially the St. Helena and Mascarene, influence the moisture flux and the rainfall over Ethiopia (Kassahun, 1987b). A boundary zone defined by the confluence of Atlantic/Congo and Indian Ocean air streams extends northwards along western part of Ethiopia. The rainfall activity decreases significantly in Ethiopia when the St. Helena High is weak or the boundary is displaced westwards (Kassahun, 1987a,b).

The East African Low Level Jet (EALLJ) induces abundant moist air from the Southern Indian Ocean towards the high grounds of Ethiopia. Besides, there is southwesterly moisture flow from the equatorial Atlantic and Congo Basin area. Tropical Easterly Jet (TEJ), which is located at the boundary of the southern and northern Hadley Cells at around 200 mb, is among the systems that are most influential to the circulations in Africa (Camberlin 1997) and its formation enhances the rainfall over Ethiopia (Kassahun, 1987a,b). Besides, the dry spells over central Ethiopia are directly related to the strength of the TEJ (Segele and Lamb 2005). TEJ also facilitates the development of summer storm when low level conditions are fulfilled (Gissila et al, 2004).
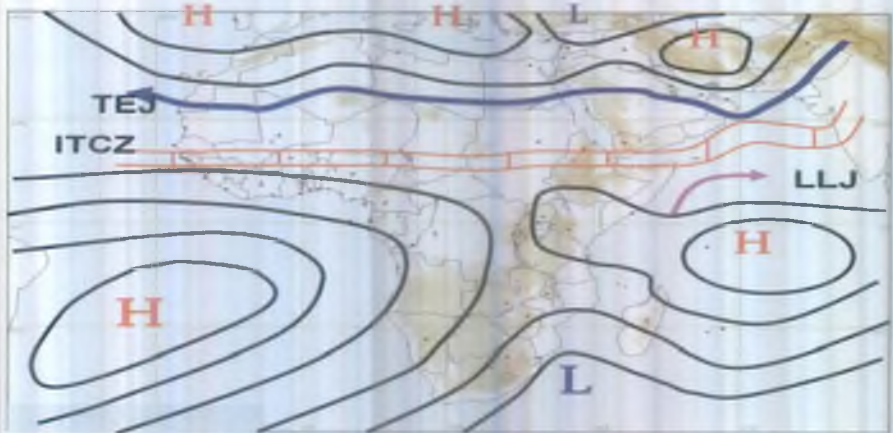
Figure 7. The ITCZ, the macro-scale pressure systems and the quasi stationary subtropical anticyclones during the Kiremt season.

2.5 Ethiopian rainfall and global teleconnection features

Various studies on the inter-annual rainfall variability over Ethiopia have shown the presence of a teleconnection between the rainfall variability over the country and patterns of large scale atmospheric circulations like the Walker circulation which have proved to be associated with variabilities related with large sea surface temperature anomaly over the Indian and the Pacific Ocean (Nicholls, 1993; Ininda et al., 1987; Tadesse, 1994; Camberlin, 1995; Gissila et al., 2004; Shanko, 2000; Endalew, 2007).

The major result of these studies is the association between strong El Nino–southern oscillation (ENSO) events and regional climate anomalies over Ethiopia. The first person to indicate indirectly the presence of a link between the southern oscillation and rainfall variability in parts of Ethiopia was Sir Gilbert Walker. In his calculations of the southern oscillation, one of the variables he used was the Nile flood level, whose major water source is the Ethiopian Highlands (Walker and Bliss, 1932). Later on , Quinn (1992) confirmed this, demonstrating that the variability between high and low flood levels of the River Nile is related to the ENSO cycle. El Nino's role in Ethiopian drought was explored by Nicholls (1993). That study associated the severe drought and famine of 1888–89 in Ethiopia with the 1888 strong El Nino warming. Ininda et al. (1987), Tadesse (1994) and Camberlin (1995) have also

described the close association between El Nino events and drought over Ethiopia.

June-September rainfall over the Ethiopian highlands is positively correlated to the equatorial East Pacific sea level pressure and the southern oscillation index, and negatively correlated to SST over the tropical eastern pacific Ocean as expected, confirming again that ENSO episodes are associated with below-average June-September rainfall over the Ethiopian Highlands (Seleshi and Zanke, 2004). Various studies have revealed the relationship between ENSO and Ethiopian rainfall and atmospheric systems (Bekele, 1993). The principal cause of drought is asserted to be the fluctuation of the global atmospheric circulation, which is triggered by the SST anomalies occurring during ENSO events. These phenomena have significant impact on the displacement and weakening of the rain-producing mechanisms in Ethiopia (Haile, 1988). A comparative study of a drought year (1972) and a normal rainfall year (1967) over the global tropics for the boreal summer months revealed that for a drought year we have (1) a weaker TEJ, (2) a weaker Tibetan high, and (3) a southeastward shift of the major circulation patterns as well as of several dynamic parameters (Krishnamurti and Kanamitsu, 1981). Similarly, the major rain-producing mechanism in Ethiopia and its vicinity - the ITCZ - was found to be weak, shallow, and shifted southeastward in drought years (Kruzhkova, 1981; Lamb, 1978). The findings of a case study of seasonal forecasts in Ethiopia are also consistent with the above mentioned results (Haile, 1987). These and other findings confirm that the fluctuations of atmospheric circulation, which are sometimes triggered by SST anomalies in the equatorial Pacific have significant impacts on the position, magnitude, and intensity of the rain-bearing systems in Ethiopia The above-mentioned changes of the rain-bearing systems frequently caused meteorological, agricultural, and hydrological drought. However, the 1982-83 El Niño, which was by far the most intense one, did not produce a very dry Kiremt (Ward and Yeshanew, 1990).

The ENSO events may not be the only cause of meteorological drought in Ethiopia. A growing body of evidence suggests that Indian Ocean processes also play an important role in controlling African rainfall (e.g. Goddard and Graham, 1999; Latif et al., 1999; Black et al., 2003). Although all three of these studies focus on equatorial coastal regions, rather than on Ethiopia,

studies of the dynamics of the Indian Ocean basin as a whole suggest that Indian Ocean processes affect Ethiopian climate. For example, Cadet and Diehl (1984) identified the warming over the western Indian Ocean in the area of the Somali Current and the southwestern Indian Ocean as important characteristics of the year 1972, a drought year in Ethiopia. The relationship between the Ethiopian rainfall during Belg and the tropical cyclones over the southwest Indian Ocean indicates that low/high frequency of the cyclones resulted in excess/deficit rainfall (Shanko et al, 1998).

Furthermore, in Ethiopia and Eritrea, Belg rainfalls have been shown to be associated with the Northern Hemispherical subtropical westerly jet (Habtemichael and Pedgley, 1974). The bega and belg seasons are overwhelmed by the north east continental cool air- stream from the Sahara and progression of the ITCZ in its south- north migration (Camberlin and Philippon, 2002; Conway 2000; Sileshi and Zanke, 2004). The belg season also coincide with the development of a thermal low (Cyclone) over southern Sudan, and winds blowing from the Gulf of Aden and the Indian Ocean highs (Sileshi and Zanke, 2004).

The variability of African rainfall is statistically related to both Pacific and Indian oceans, but the variability in the two oceans is also related. While the SST variability of the tropical Pacific exerts some influence over the African region, it is the atmospheric response to the Indian Ocean variability that is essential for simulating the correct rainfall response over eastern, central, and southern Africa. Analysis of the dynamical response(s) seen in the numerical experiments and in the observations indicate that the Pacific and Indian Ocean have a competing influence over the Indian Ocean/African region. This competition is related to the influence of the two oceans on the Walker circulation and the consequences of that variability on low-level fluxes of moisture over central and southern Africa (Hastenrath and Polzin, 2003).

Comparison of the wind anomalies that develop during extreme Indian Ocean dipole or Zonal mode (IOZM) events with those that develop during weaker (moderate) events shows that strong easterly anomalies in the northern-central Indian ocean are a persistent feature of extreme, but not of moderate, IOZM years. It is suggested that these anomalies weaken the westerly flow that normally transports moisture away from the African continent, out over

the Indian Ocean. Thus, during extreme IOZM years, rainfall is enhanced over east Africa and reduced in the central and eastern Indian Ocean basin (Emily and Julia, 2002; Bahaga et al., 2015).

2.6 Observations over Indian, Atlantic and Pacific Ocean and their implication

Global warming impacts over the Indian and the Pacific Ocean as well as the Atlantic Ocean are expected to have an influence on the general pattern of the regional circulation which thus can affect the hydrological cycle over our region. According to the fifth IPCC assessment report, the observed trends over the Indian Ocean include a decrease of Sea level pressure and an increase of sea surface temperature over the tropical Indian Ocean. **Indian Ocean Basin Mode (IOBM) is SST averaged over the Indian Ocean covering 40°-110°E, 20°S-20°N** (Yang et a, 2007). The Indian Ocean Basin Mode (IOBM) has been shown to have exhibited a strong warming trend (significant at 1% since the middle of the 20th century). This phenomenon is well-known (Du and Xie, 2008) and its consequences for the regional climate are subject of active research (Du et al., 2009; Xie et al., 2009).
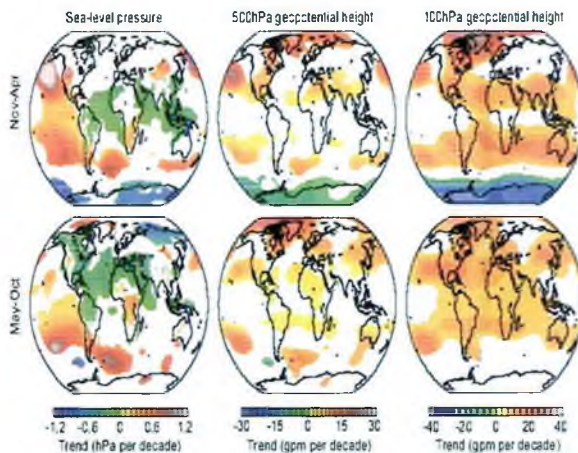

Figure 8. Trends in (left) sea level pressure (SLP), (middle) 500 hPa geopotential height (GPH) and (right) 100 hPa GPH in (top) November to April 1979/1980 to 2011/2012 and (bottom) May to October 1979 to 2011 from ERA-Interim data. Trends are shown only if significant (i.e., a trend of zero lies outside the 90% confidence interval).

This warming has been estimated to be greater than 1K, which can affect the large scale circulation over the region (Sperber et al. 2000). Normally the impact of the warming over the Indian Ocean over the circulation systems over Ethiopia is greatly determined on the time of the year or the season and also on which part of the Indian Ocean is this warming significant. For example an increase in the warming of the northern Indian Ocean on the Arabian sea during the months of October-November can lead to the formation of more depressions that can move to the horn of Africa and bring rain (which is usually called unseasonal rainfall over the central and the northern parts of Ethiopia), where as in combination with other dynamical systems can lead to more rain to the short rain season of the southern and southeastern lowlands of Ethiopia. In contrast, a warming over the South West Indian Ocean and also the western Indian Ocean during the months of February/March to May season can lead to the formation of tropical cyclones resulting in much drier condition over Ethiopia including other parts of East Africa, where most of moisture bearing winds from the Indian Ocean will be directed towards the south-eastern parts of Africa, resulting in more wetter condition over Mozambique and neighboring areas.

SST anomalies in the Indian and Pacific Oceans have a fundamental influence on Sahel rainfall and have been associated with Nile flows (Folland et al. 1986). These variations in the Indian and Pacific oceans are affiliated with rainfall changes in Ethiopia and East Africa (Beltrando and Camberlain, 1993; Sileshi et al., 1995; Conway, 2000). It has also been suggested that positive SST anomalies in the southwestern Indian Ocean (SWIO) may increase oceanic precipitation and decrease rainfall over eastern Africa, especially during March-May (Funk et al. 2005). It is believed that the low pressure systems associated with the storms of April 1984 in the SWIO accounted for the severe and widespread drought in the horn (Macodras et al., 1989).

ENSO has been shown to strongly interact with climate dynamics in the Indian Ocean where during most El Niño events, anomalies are observed in the Indian Ocean (Cadet 1985; Reveredin et al 1986; Beltrando and Camberlin 1993). There exist a strong coupling between the short rainy season in the neighboring East African countries, and both the ENSO and the east – west circulation over the Indian Ocean (Beltrando and Cambrlin 1993). However, other studies have contradicted similar findings. Ogallo et al. (1988) observed

a 'see-saw' pattern between the eastern Pacific Ocean and the Indonesia region which coincides with positive anomalies over the coast of Eastern Africa indicating a relationship between rainfall variability in the region and ENSO phenomena. Nicholson and Entekhabi (1986) also identified significant Teleconnection between the southern oscillation and seasonal rainfall over part of East Africa. Coupling between the East African long rains and ENSO, however did not show any significant correlations (Ogallo 1988, Hastenrath et al. 1993; Rowell et al. 1994; Philipps and McIntyre 2000). These findings are at odds with several other studies that noted a relationship between Nino-3 SST and rainfall across the season (Nicholson 1996; Nicholson and Kim 1997; Indeje et al. 2000).

On the other hand, warming in the Indian Ocean which has been linked to anthropogenic causes (Funk et al. 2005, 2008) have had major impacts on eastern African rainfall from March to June (Belg, Funk et al. 2008, Funk and Williams, 2010). It was suggested that long established interannual teleconnections between large scale climate variability and long rains precipitation are being altered due to warming with in the south central Indian Ocean. Reduced rainfall across eastern Africa, thus, is linked to deep atmospheric convention over the Indian Ocean due to warming near tropical Pacific-Indian Ocean (Funk et al, 2008; Funk and Williams 2010). Consistent weakening and pole ward expansion due to reduced upward Convective mass flux as diagnosed in climate change simulations imply reduced subsidence in the tropics (Held and Soden 2006; Lu et al. 2007).

The weakening of the atmospheric overturning is driven by changes in the atmospheric hydrologic cycle (Held and Soden 2006) and is primarily evident as a reduction in the zonally asymmetric overturning of air (i.e., the Walker circulation) rather than in the zonal-mean overturning, the Hadley circulation (Vecchi and Soden 2007). A projected weakened walker circulation as a result, resembles a more "El Nino like" climate with withered subsidence over eastern tropical Pacific and eastern tropical Africa (Vecchi and Soden 2007).

Consecutive occurrences of several tropical depressions over the SWIO coincide with the drought years of Ethiopia (Shanko and Camberlin 1998). In contrast, years of low frequency tropical cyclones are associated with

heavy rainfall in Ethiopia. Shanko and Camberlin (1998) have shown that Belg rainfall is influenced much more by the cyclonic activity than Kiremt rainfall, which occurs outside the cyclonic season of the SWIO. Ogallo (1988) presented cases from further south in East Africa where rainfall is influenced directly and indirectly by tropical storms that originate from SWIO and the Arabian Sea.

Shanko and Camberlin (1998) quoted four well documented cases of cyclones which have hit the East African coast in April 1872, April 1952, May 1966 and April 1974. Inter annual variability of rainfall is remarkably coherent with in Eastern Africa implying major large scale influences (Nicholson, 1996). Camberlin (1996) further investigated the Teleconnection between Nile floods and the Indian monsoon, and found a close relationship between summer (July – September) sea level pressure (SLP) in India and concurrent interannual rainfall variations over the horn of Africa. He also noted a direct link between monsoon variations in these two regions suggesting that ENSO plays a prominent part in the India–East Africa co-variability of rainfall.

2.6.1 The Walker Circulation

There have been various attempts to investigate the nature and cause of the Indian Ocean warming and its impact on the regional circulation. Since the approach is based on the impact of the Walker Circulation We will have a brief review of the importance of Walker circulation. The term Walker Circulation was first introduced in 1969 by Professor Jacob Bjerknes, referring to the large-scale atmospheric circulation along the longitude–height plane over the equatorial Pacific Ocean. The Walker Circulation features low-level winds blowing from east to west across the central Pacific, rising motion over the warm water of the western Pacific, returning flow from west to east in the upper troposphere, and sinking motion over the cold water of the eastern Pacific. Since Bjerknes's introduction of the Walker Circulation, there have been reports of similar east–west circulation cells spanning different longitudinal sectors along the Equator. Today, the Walker Circulation generally refers to the totality of the circulation cells as shown in Fig. 9 over the Pacific, the Indian and the Atlantic Ocean. Ethiopia also happens to be affected greatly by the characteristics of the strength and orientation of the Global Walker Circulation, where the surface processes can be important

over the neighboring Indian Ocean, which is expected to affect the strength of the local East-west circulation cell.
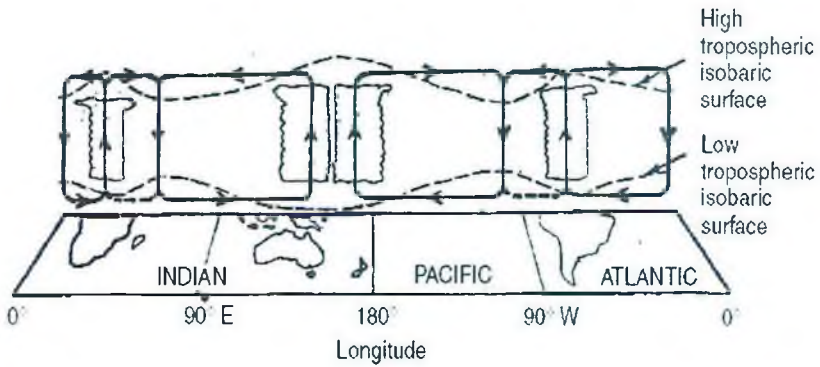

Figure 9. Schematic view of the east–west atmospheric circulation along the longitude–height plane over the Equator.
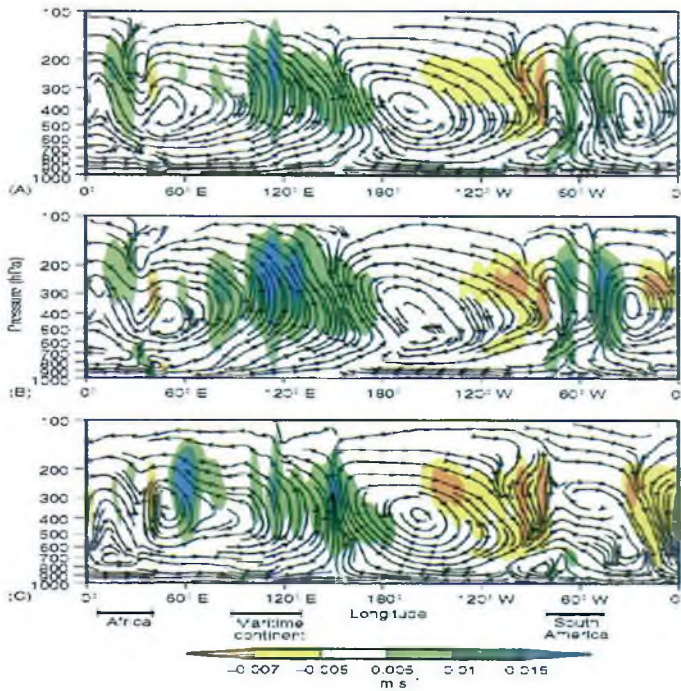

Figure 10. The equatorial east–west atmospheric circulation calculated from the

reanalysis of data from the US National Centers for Environmental Prediction and National Center for Atmospheric Research. Shown are the climatologies of all months (top panel), January (middle panel), and July (bottom panel) for the period 1949–99. The streamlines where vertical motions have been multiplied by 30 times are constructed from the divergent components of winds. Areas of strong upward and downward motions (in meters per second) are shaded.

As is evident from Fig. 10, the Walker Circulation also includes secondary circulation cells whose rising motions appear over the land regions of South American and Africa, with compensating subsidence over the Atlantic and the Indian Ocean.

The Walker circulation affects convection and precipitation patterns, the easterly trade winds, oceanic upwelling and ocean biological productivity; hence, changes in this circulation can have far-reaching consequences. The Warm Pool has extended westward into the Indian Ocean, causing the western, convective branch of the Walker Circulation to extend to the west as well. As evaporation, convection, and precipitation have increased over the Indian Ocean, circulation has been altered in surrounding areas including the Horn of Africa. The physical explanation is that the Tropical Warm Pool: where the eastern tropical Pacific Ocean meets the western tropical Indian Ocean, in the region of the Indonesian and Malaysian Islands. The ocean's surface is warmer here than anywhere else on earth. The fact that the ocean's surface is very warm has two very important impacts within the Warm Pool region. One, water evaporates from the Warm Pool's surface very rapidly, causing the air above the Warm Pool to be very humid. Two, warm air rises, and where warm, humid air rises, you get heavy rain. When the humid air condenses into liquid water high above the Warm Pool, a massive amount of energy is released into the atmosphere. This energy causes wind to flow in all directions away from the area where the storm clouds are produced. While the ocean's surface is very warm within the Warm Pool region, it is much cooler to the east and west, in the central Pacific Ocean and the central/western Indian Ocean, respectively.

The work of *Williams and Funk (2011)* shows a connection between warming in the Indian Ocean and the expansion of the warm pool over the Equatorial Pacific. The physical explanation is that the Tropical Warm Pool: where the

eastern tropical Pacific Ocean meets the western tropical Indian Ocean, in the region of the Indonesian and Malaysian Islands has extended westward into the Indian Ocean, causing the western, convective branch of the Walker Circulation to extend to the west as well. As the globe has warmed over the last century, the Warm Pool region has warmed as well. As it has warmed, it has expanded. On its western side, the Warm Pool has expanded by about 4,000 km into the central Indian Ocean. This westward expansion of the Warm Pool has caused surface waters in central Indian Ocean to warm about one-and-a-half times faster than the global average temperature, and about three times faster than the cooler tropical waters of the central Pacific Ocean. Westward expansion of the Warm Pool has led to increased humidity, upward movement of air, and storm activity over the central and western Indian Ocean. As the region of warm water, convection, and storminess has expanded to the west, the western sinking branch of the circulation system has also moved to the west During the March-June rains season in Kenya and Ethiopia, the rate at which dry air sinks over northern Africa has substantially increased, in step with storminess over the central Indian Ocean. When this dry air returns to the surface over northern Africa, much of it flows east, back to the Indian Ocean, and travels through the Horn of Africa on the way. Numerous researchers have tried to connect the more frequent occurrences of drought during the March to May rainfall season in East Africa to this factor (Du et al., 2009; Xie et al., 2009, Vincent et al, 2011b , Funk et al., 2008; Williams and Funk, 2011, Lyon and DeWitt, 2012 , Jury et al., 2013). There may be a need for more research regarding the impact of this westward extension of the warm pool to the Indian Ocean on the Summer rainfall season of June/July to September over the Ethiopian highlands.

The investigation of whether the Walker Circulation over the Equatorial Pacific has strengthened or weakened due to global warming is still a debatable topic where the major implication for Ethiopia is its impact on the hydrological cycle during the main northern hemisphere summer rainfall season. Major proponents of a weakened or a slowed down Walker Circulation are using two major hypothesis. The first hypothesis, for example Vichy et al, 2012, attributes the Walker circulation slowdown to a decrease in convective mass flux under global warming that balances a slower increase in global mean precipitation than can be expected from the increase in atmospheric water

vapor, due to Clausius-Clapeyron equation, prediction of a strong increase of boundary layer water vapor content with temperature (about 7% per degree of warming). It is important to note here that the Clausius Clapeyron equation is also cited to explain cases of extremely heavy rainfall events due to the capacity of the atmosphere to contain more moisture due to global warming. The second hypothesis is changes in zonal SST gradient across the Equatorial West and East Pacific Ocean. This mechanism is dominant for ENSO, but the effort to test its role in the long-term weakening of the Walker circulation has been hampered by uncertainty in observed SST warming. Thus a more exhaustive research both observational trend analysis and modeling are very important to make an assessment on the impact regarding the hydrological cycle over our region for the northern hemisphere summer rainfall season. Moreover various findings indicating the pole ward extension of the Hadley Cell circulation system due to global warming also needs further research on assessing its implication for the Hydrological Cycle over Ethiopia and the neighborhood.

3. Observed Changes in extremes

According to the forth assessment report of the Intergovernmental Panel on Climate Change (IPCC), not only the mean climate but also the variability of climate and the occurrence of extreme events are changing and will likely continue to change, due to human influences on the weather (IPCC, 2007).

The occurrence of extreme events in air temperature and precipitation is typically evaluated based on the analysis of a set of indicators defining variation and extreme conditions. For example, the Climate Variability and Predictability (CLIVAR) Expert Team on Climate Change Detection and Indices (ETCCDI), has developed a set of indices on moderate extremes (Peterson et al., 2001) that represents a common guideline for regional analysis of climate.

Table 1. Definition of extreme indices used in this report

Indices	Name	Definition	Units
CDD	Consecutive dry days	Maximum number of consecutive days with RR<1 mm	days
CWD	Consecutive wet days	Maximum number of consecutive days with RR>=1 mm	days
PRTOT	Annual total wet-day precipitation	Annual total PRCP in wet days (RR>=1 mm)	mm
R10	Number of heavy precipitation days	Annual count of days when PRCP>=10 mm	days
R20	Number of very heavy precipitation days	Annual count of days when PRCP>=20 mm	days
SDII	Simple daily intensity index	Annual total precipitation divided by the number of wet days	mm
R95pTOT	Precipitation on very wet days	Annual total PRCP when RR>95th %	mm
R99pTOT	Precipitation on extremely wet days	Annual total PRCP when RR>99th %	mm
RX1day	Max 1-day precipitation amount	Maximum 1-day precipitation	mm
RX5day	Max 5-day precipitation amount	Maximum 5-day precipitation	mm
TN10P	Cold nights	Percentage of days when TN<10th %	days
TN90P	Warm nights	Percentage of days when TN>90th %	days
TX10P	Cold days	Percentage of days when TX<10th %	days
TX90P	Warm days	Percentage of days when TX>90th %	days
TNn	Coldest nights	Monthly minimum value of daily TN	°C
TNx	Warmest night	Monthly maximum value of daily TN	°C
TXn	Coldest days	Monthly minimum value of daily TX	°C
TXx	Warmest days	Monthly maximum value of daily TX	°C
DTR	Diurnal temperature range	Monthly mean difference between TX and TN	°C
WSDI	Warm spell duration indicator	Annual count of days with at least 6 consecutive days when TX>90th percentile	days
CSDI	Cold spell duration indicator	Annual count of days with at least 6 consecutive days when TN<10th percentile	days
SU25	Summer days	Annual count when TX>25°C	days
TR20	Tropical nights	Annual count when TN>20°C	days

Takele et al (2012) have generated and analyzed the temporal trends of the indices shown in Table 1 for selected meteorological stations in Ethiopia based on 30 years period (1981–2010) rainfall, minimum and maximum temperature data. Mengistu Tsidu et al. (2015) have also determined the changes in the precipitation and temperature extremes over East Africa from analysis of Climate Hazards Group Infrared Precipitation with Stations (CHIRPS) rainfall and ERA-Interim maximum and minimum temperature at a horizontal resolution of 0.25°. The findings in this report on the climate extremes are mainly compiled from the two studies.

3.1 Extreme precipitation events

According to Takele et al (2012), higher percentage of stations located in Ethiopia showed an increasing trend in most of the precipitation indices with the exception of extreme ends of precipitation distribution (i.e., R95TOT and R99TOT, where almost equal percentage of stations showed increasing and decreasing trend), and continuous dry days (i.e., CDD index where 70% of stations showed a decreasing trend) (Fig.11).
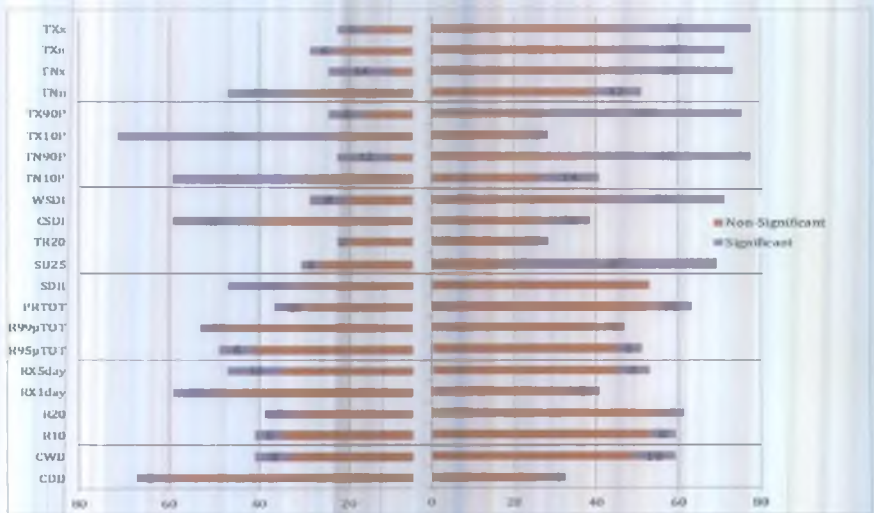

Figure 11. Proportion of stations for positive (on the right side of zero i.e., increasing towards right) and negative (on the left side of zero i.e., increasing towards left) trends. Proportion and number of stations with significant extreme climate indices are shown in purple color.

3.2 Extreme Temperatures events

For the temperature extremes, the majority of stations showed a consistent upward trend in warm weather indicators. For example, 75% and 76% of the stations showed an upward trend in the 90th minimum and maximum temperature percentiles (i.e., TN90P, TX90P), of which 42% and 48% exhibit statistically significant trend respectively.
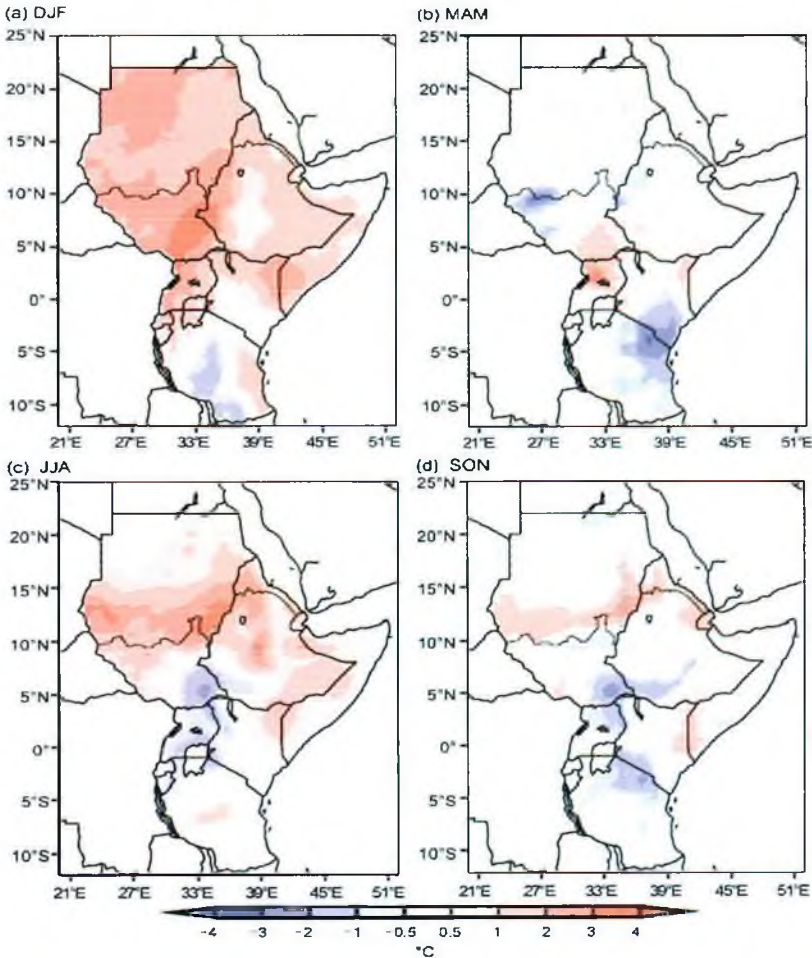

Figure 12. Eastern Africa seasonal anomalies of the maximum temperature 90th percentiles (°C) in 2014 with respect the 1981–2010 90th percentile mean.

Since the changes in climate extremes differ from one season to the other, it is important to investigate climate extremes of each season separately. For example in a recent report for state of climate in 2014 over Eastern Africa, significant differences between seasons were observed (Mengistu Tsidu et al. , 2015). The authors found that during December to February (DJF), there were warm anomalies in the extreme ends of maximum temperature exceeding 90th percentiles over most of the country except over south-central Ethiopia, which were normal in 2014 with respect to the 1981-2010 base period (Fig. 12a). The June-August (JJA) season 90th percentile maximum temperatures were also above average over most parts of Ethiopia in 2014 (Fig. 12c). Observations during SON were similar to JJA, specifically over northern Ethiopia (Fig. 12d) (Mengistu Tsidu et al. , 2015) .
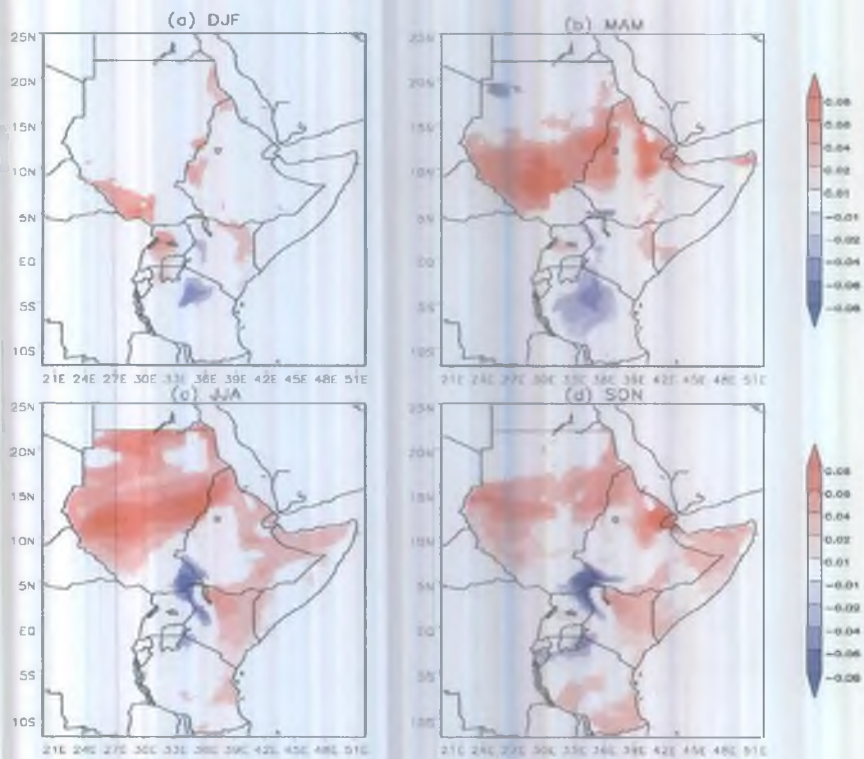
Figure 13 The 90th percentiles minimum temperature trend (°C/year) during the 1981–2014 period.

In case of cold weather indicators, majority of stations showed a decreasing trend in the 10th minimum and maximum percentiles with 30% and 48% of stations showing significant trend. Furthermore, consistent pattern of changes were detected for the majority of temperature extreme indices (Fig. 11). Moreover, the 90th percentile minimum temperature trend also shows increasing trend over western, northern and eastern Ethiopia in spring, summer and autumn seasons whereas central Ethiopia and southwestern Ethiopia exhibit normal to decreasing trend. However, during winter (DJF), the 90th percentile minimum temperature does not show any trend during the last 3 decades (Fig. 13).

The observed increasing changes in warm extremes are consistent with the already happening global warming. The heterogeneous behavior identified in most precipitation extreme indicators might be attributed to the high variations in local geographical features.

4. Changes in hydrological cycle

Both the AR4 and AR5 concluded that precipitation has generally increased over land north of 30°N over the period 1900–2005, which is noted as statistically significant. However it has also been indicated that longer term trends in large scale precipitation pattern for the years 1901–2008 in the tropics has been reported as non significant. Further more, the fifth assessment report suggests that precipitation over tropical land areas (30°S to 30°N) has increased over the last decade (2000-2010), reversing the drying trend that occurred from the mid-1970s to mid-1990s. The mechanism for a change in the hydrological cycle over Ethiopia and the neighborhood due to global warming stems from two major aspects and these are the impact of the global warming over the sea surface temperature of the neighborhood oceans and thus the resulting impact on the distribution of the pressure systems and the circulation patterns and the other impact is on the characteristics profile of surface and troposphere humidity. The characteristics of the profile of surface and troposphere humidity are largely determined apart from the level of the presence of moisture on the land surface temperature (for near surface humidity) and tropospheric temperature (for tropospheric humidity). The most important factor usually cited here is the Clausius Clapeyron equation, where an increase of 1 degree Celsius is responsible for an increase

in the moisture holding capacity of the atmosphere by 7%. This condition is usually associated with enhancing the occurrences of extreme weather events.

4.1 Surface humidity

There have been reports of widespread increases in surface air moisture content since 1976, along with near-constant relative humidity over large scales though with some significant changes specific to region, time of day or season. In good agreement with previous analysis from Dai (2006), Willett et al (2008) show widespread increasing specific humidity across the globe from the homogenized gridded monthly mean anomaly product Had-CRUH (1973–2003). Since 2000 surface specific humidity over land has remained largely unchanged, whereas land areas have on average warmed slightly implying a reduction in land region relative humidity. This may be linked to the greater warming of the land surface relative to the ocean surface (Joshi et al., 2008). The marine specific humidity (Berry and Kent, 2009), like that over land, shows widespread increases that correlate strongly with SST. In summary, it is very likely that global near surface air specific humidity has increased since the 1970s. However, during recent years the near surface moistening over land has abated (medium confidence). As a result, fairly widespread decreases in relative humidity near the surface are observed over the land in recent years.

4.2 Troposphere humidity

Observations from radiosonde and GPS measurements over land and satellite measurements over ocean indicate increases in tropospheric water vapour at near-global spatial scales which are consistent with the observed increase in atmospheric temperature over the last several decades. In each analysis, the rate of increase in the free troposphere is concluded to be largely consistent with that expected from the Clausius– Clapeyron relation (about 7% per degree Celsius). Jin et al. (2007) found an average column integrated water vapor trend of about 2 $kg.m^{-2}$ per decade during 1994-2006 for 150 (primarily land-based) stations over the globe, with positive trends at most NH stations and negative trends in the SH. There is a need to make an assessment of near surface relative humidity and specific humidity trend over Ethiopia to understand more the impact on the hydrological cycle over the country.

4.3 Evapotranspiration including Pan Evaporation

On a global scale, evapotranspiration over land increased from the early 1980s up to the late 1990s (Wild et al., 2008; Jung et al., 2010; Wang et al., 2010) and Wang et al. (2010) found that global evapotranspiration increased at a rate of 0.6 W.m^{-2} per decade for the period 1982–2002. After 1998, a lack of moisture availability in SH land areas, particularly decreasing soil moisture, has acted as a constraint to further increase of global evapotranspiration (Jung et al., 2010). In semiarid and arid regions, trends in evapotranspiration largely follow trends in precipitation (Jung et al., 2010).

Over the last 50 or so years, pan evaporation has been carefully monitored. For decades, nobody took much notice of the pan evaporation measurements[1]. But in the 1990s in Europe, Israel, and North America, scientists spotted something that at the time was considered very strange: the rate of evaporation was falling although they had expected it to increase due to global warming. The same trend has been observed in China over a similar period. A decrease in solar irradiance is cited as the driving force. However, unlike in other areas of the world, in China the decrease in solar irradiance was not always accompanied by an increase in cloud cover and precipitation. It is believed that aerosols may play a critical role in the decrease of solar irradiance in China. Thus, it is important to note that decreasing trends in Pan Evaporation was detected over some areas of the world, where aerosol emission has shown a large increase over countries especially over the South Asia region. Other factors that can be responsible for a decrease of pan evaporation include decreased surface solar radiation due to aerosols, decrease in sunshine duration due to increased specific humidity and increase in cloud cover. It is important to note here that pan evaporation depends on some additional factors besides net radiation from the sun. The other two major factors are vapor pressure deficit and wind speed, where the ambient temperature could tern out to be a negligible factor. Though research literature is very few over Ethiopia, it is expected that there has been a general increase in the pan evaporation due to the warming of the atmosphere. However, it is important to note seasonal peculiarities where increase in cloud cover and volcanic ash may induce a decrease in pan evaporation.

4.4 Clouds and aerosols

The general review of the status of aerosol trend over Ethiopia and the neighborhood is important for the assessment of possible impact over the climate system of Ethiopia for two major reasons. The first reason is that of the recent detection of the aerosol haze observed over the north Indian Ocean due to the transport of anthropogenic emissions carried over from the South Asia region by the prevailing wind system in the atmospheric circulation system especially during the months of November to May. This aerosol mix substantially absorbs solar radiation, and recent modeling studies have proposed that the resulting atmospheric heating reduces daytime cloud cover. (Norris, 2001)

Thus, though the level of aerosols in the atmosphere over Ethiopia is basically dependent on the level of dust activity and biomass burning that occurs over the country, there can result a transport of aerosols from nearby regions associated with the anthropogenic aerosol haze over the north Indian Ocean, due to atmospheric circulation. The second reason is that of the problem of land degradation over our region that is usually associated with natural types of aerosols. Moreover volcanic activity over the Afar depression may also have some contribution.

The main aerosol types occurring over Africa are desert dust and biomass burning aerosols, which are UV-absorbing. Widespread biomass burning over Africa is identified by satellites especially south of 15°N from about October to March.

Though the contribution of the local industrial emitted particulate matter is minimal for the aerosols over Ethiopia and the neighborhood, the status of particulate matter over big urban centers such as Addis Ababa requires close monitoring.

According to Gebeyehu and Mengistu (2012), there is seasonal variation of stratospheric Carbonyl Sulfide aerosol distribution over Ethiopia. The total column stratospheric aerosol also shows seasonal variation with maximum value attained during Spring and minimum during Summer. The annual mean value of total column AOD is observed to be steadily increasing from 1984 to 2005, which revealed the increasing trend of stratospheric aerosols of both fine and course mode particles.

Aerosols levels over Ethiopia due to dust activity is greatly characterized by seasonality. During maximum dust activity in May–July, high AAI values extend from the western flanks of the Ethiopian highlands west to the plateaus of western Sudan roughly between 15° and 22°N. Dust activity over the Ethiopian Rify Valley peaks in June and July. Dust distributions are sharply defined by the mountains to the west and to the south in Ethiopia and to the east, across the Red Sea and the Gulf of Aden, the mountains in Yemen. Total Ozone Monitoring Satellite (TOMS) shows a maximum at 14°N, 42°E, slightly to the east of the Danakil Depression and Kobar Sink in the Rift Valley of northern Ethiopia. Almost all major sources are located in arid regions and are centered over topographical lows or on lands adjacent to strong topographical highs.

AOD is a measure of the integrated columnar aerosols load and is an important parameter for evaluating aerosol–radiation interactions. A multi-regional analysis for 1973– 2007 (Wang and Liang, 2009) shows positive AOD trends over Africa. Seasonal average AOD trends at 0.55 μm for 1998–2010 using SeaWiFS data (Hsu et al., 2012) indicates that there is a strong positive AOD trend over our region in the Arabian Peninsula and also including northeastern and northwestern lowlands of Ethiopia (Fig. 14) occurring mainly during spring (MAM) and summer (JJA), during times of dust transport, and is also visible in MODIS data.

-0.04 -0.03 -0.02 -0.01   0   0.01 0.02 0.03 0.04

Aerosol Optical Depth Trend (per year)
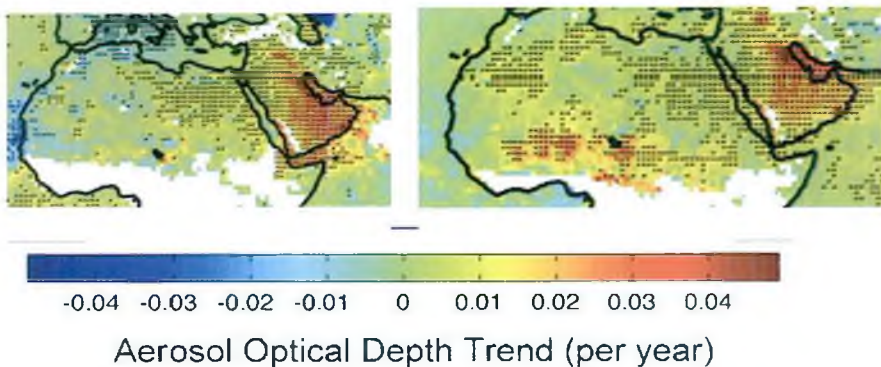
Figure 14. Seasonal average AOD trends at 0.55 μm for 1998–2010 using SeaWiFS data (Hsu et al., 2012) for MAM (left) and JJA (right). White areas indicate incomplete or missing data. Black dots indicate significant trends

Annual average aerosol optical depth (AOD) trends at 0.55 μm for 2000–2009, based on deseasonalized, conservatively cloud-screened MODIS aerosol data over oceans (Zhang and Reid, 2010) clearly identifies the northern Indian Ocean as one area of increasing trend of aerosols.
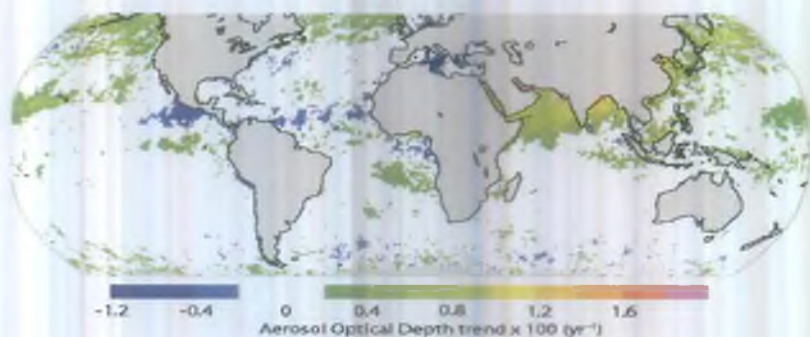

Figure 15. Annual average aerosol optical depth (AOD) trends at 0.55 μm for 2000–2009, based on deseasonalized, conservatively cloud-screened MODIS aerosol data over oceans (Zhang and Reid, 2010).

4.4.1 The Aerosol Haze over the Northern Indian Ocean

The recent Indian Ocean Experiment (INDOEX) observed high aerosol concentrations over much of the northern Indian Ocean resulting from transportation of polluted air from south and southeast Asia during the dry monsoon season (Rajeev et al., 2000; Lelieveld et al., 2001). This aerosol mix substantially absorbs solar radiation, and recent modeling studies have proposed that the resulting atmospheric heating reduces daytime cloud cover. Anthropogenic emissions over the Asian region have grown rapidly with increase in population and industrialization. Air pollutants from this region lead to a brownish haze over most of the North Indian Ocean and South Asia during winter and spring. The haze, with as much as 10–15% of black carbon (by mass), is known to reduce the surface solar insolation by about 10% (15 Wm^{-2}) and nearly double the lower atmospheric solar heating. Each year, during the winter and spring months, anthropogenic haze spreads over most of North Indian Ocean, South and Southeast Asia (Ramanathan et al., 2001a). This is a unique region for studying the climate response to radiative forcing by absorbing aerosols. Firstly, the percentage

contribution to global anthropogenic emissions from the South and East Asian countries has increased considerably over the last few decades (Smith Steven et al., 2001). Every dry season from November to May, anthropogenic haze spreads over most of the northern Indian Ocean and Southeast Asia. INDOEX documented this Indo-Asian haze at various scales during 1995-2001. The observed high aerosol concentrations over much of the northern Indian Ocean have been shown to be the result of transportation of polluted air from south and Southeast Asia during the dry monsoon season (Rajeev et al., 2000; Lelieveld et al., 2001). It is estimated that anthropogenic sources contributed as much as 75% ($\pm$10%). This haze, about the size of USA, extends from the south Asian continent to the Arabian Sea, and from the Bay of Bengal to the Indian Ocean ITCZ. The reason why this anthropogenic haze appears over the north Indian Ocean during Months of November to May is due to the direction of the prevailing wind system from the Indian Sub continent towards the Arabian Sea and the associated subsidence during this season. There is also a need to address whether the transport of these anthropogenic air pollutants can reach Ethiopia during these months. It is important to note that this anthropogenic aerosol haze over the northern Indian Ocean could have an important impact on the climate system of Ethiopia by modifying the sea surface temperature pattern over this region. The haze layer can reduce the net solar flux at the surface by as much as 20 to 40 Wm^{-2} on a monthly mean basis and can heat the lowest 3 km atmosphere by as much as 0.4 to 0.8 K/day, which would enhance the solar heating. Moreover, Soot was a sizable fraction of the aerosol mix and caused substantial absorption of solar radiation. Satheesh and Ramanathan (2000) infer from satellite and surface measurements that aerosol heating in the lower atmosphere over the northern Indian Ocean at local noon is 1-3 K/day, an increase of 50-100% over aerosol-free solar heating.
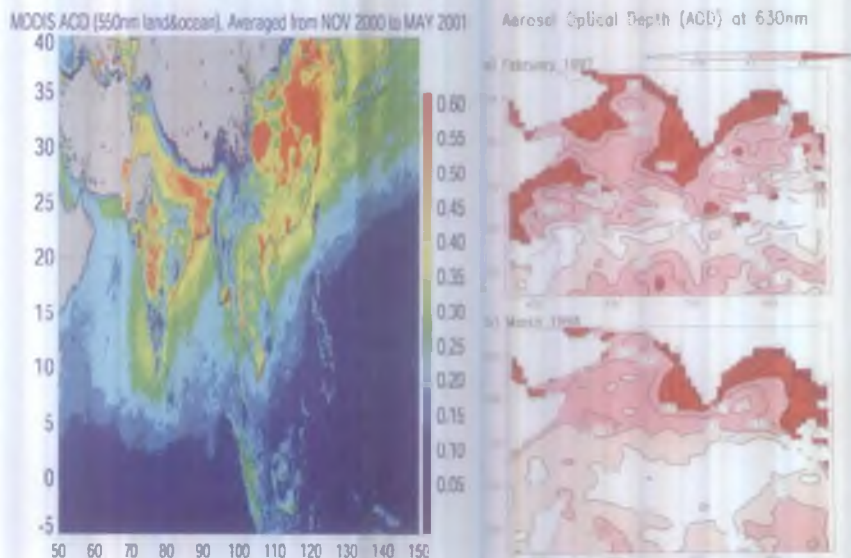
Fig 16 Left: Aerosol Optical Depths (AOD) at 550 nm derived from Moderate Resolution Imaging Spectrometer (MODIS) instrument onboard the TRRRA satellite. **Right:** Monthly mean AOD at 630 nm over the Indian Ocean (a)February 1997 and (b) March 1998.

Fig. 16 (left) shows, the brownish hazy layer covering the Asian regions extensively, and is now called the "Asian Brown Cloud (ABC)". In view of the widespread extent and the brownishness, the climatic effects must be large and significant. It is very important to note that the haze stabilizes the boundary layer, because the stabilization will trap the pollutions longer, thus making the pollution removal harder. As a result of the stabilization, the sensible heat flux from the surface decreases sensible heat flux from the surface decreases and this decrease balances most of the solar flux reduction in surface energy budget. The remaining balance of the surface solar radiation reduction is compensated by decreased surface evaporation (by about 6 Wm^{-2} and a decrease in net (up minus down) long wave radiation. Suppressed evaporation indicates a slowed down hydrological cycle in this area.

Fig. 16 (right) Monthly mean AOD at 630 nm over the Indian Ocean (a) February 1997 and (b) March 1998. Both months had a widespread presence of haze, and yet the southward extent varied substantially from one year to another. In February 1997, the haze reached as far as 10°S over the coasts

of the horn of Africa but in March 1998 it stayed north of the equator. The aerosol climate forcing over this area is one order of magnitude greater than the green house gas forcing. Furthermore, the haze is regionally concentrated diminishing towards the ITCZ. Modeling studies have indicated the impact of the aerosol haze over the sea surface temperature pattern over the Indian Ocean as can be exhibited in Fig. 17.
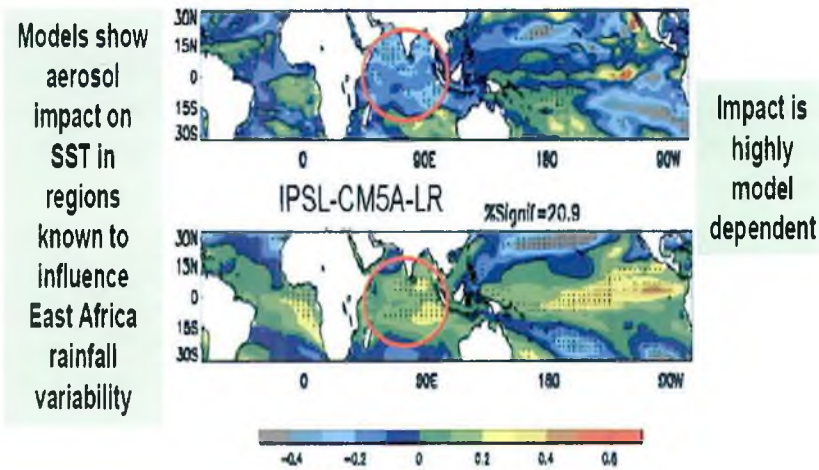
Figure 17. Modeled impacts of the aerosol haze over the North Indian Ocean on the sea surface temperature pattern.

One major impact of the aerosol haze over the Indian Ocean then would be the modification of the meridional SST gradient over the Indian Ocean, which can have negative impact on the circulation pattern over the region. The sea surface temperature pattern over the northern Indian Ocean has both a direct and an indirect link with the weather systems over Ethiopia. The aerosol haze phenomena over the north Indian Ocean has also been identified as one major reason for the so called the East Africa Climate paradox of contrast between the observed drying of the March to May rainfall season over East Africa during the recent decades and the CMIP5 wetting projection of the March to May seasonal rainfall over East Africa. Thus, there is a need to address this impact on the climate system of Ethiopia.

5. Climate Impact on Agriculture

5.1 Onset, Cessation, and Length of Growing Season

The onset, cessation, and length of growing Season were determined from graphical representations of rainfall amount and reference evapotranspiration (ETo) relationship, after the reference evapotranspiration was estimated using the Hargreaves' equation (FAO, 1998).

Mean decadal rainfall amounts were determined and plotted against their corresponding 0.5 ETo values for each year. The first point of intersection of the rainfall-0.5 ETo graphs indicates the onset decade of the growing season and the second point of intersection gives the cessation decade of the growing season (Mawunya et al., 2011). The method is applied to Ethiopian situation and the following discussions are based on the results from such analysis by the authors.

5.2 Onset of the growing season

Generally, the mean onset of the growing season gradually advances north-eastward from south-western regions, which is consistent with the previous work by Segele and Lamb (2005). The early onset is in mid-to-late March over southwestern Ethiopia and progress northward to cover much of western Ethiopia on the last decade of May. In contrary, the northeastern part of the country has late onset in July as shown in Fig. 18
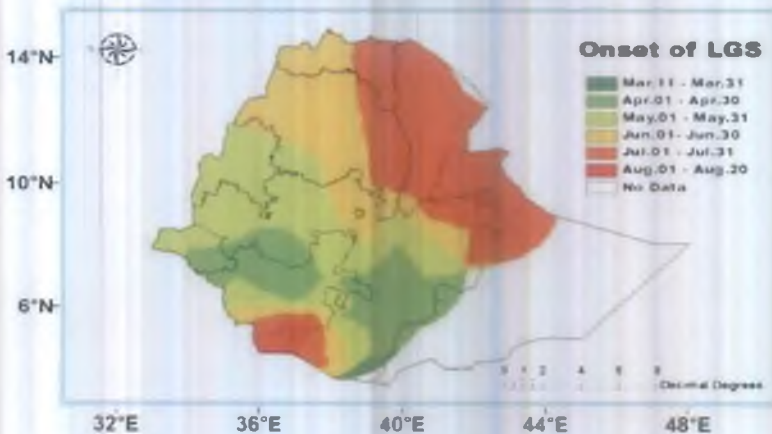
Figure 18. Mean onset of the growing season.

Fig. 19 shows the annual variability of the mean onset of the growing season. It is highly variable, with standard deviation across the country ranging from 9 to 47 days. South-western regions have the highest onset variability with standard deviation of 34 to 48 days, whereas north-eastern regions have the lowest onset variability with standard deviations from 9 to 15 days.
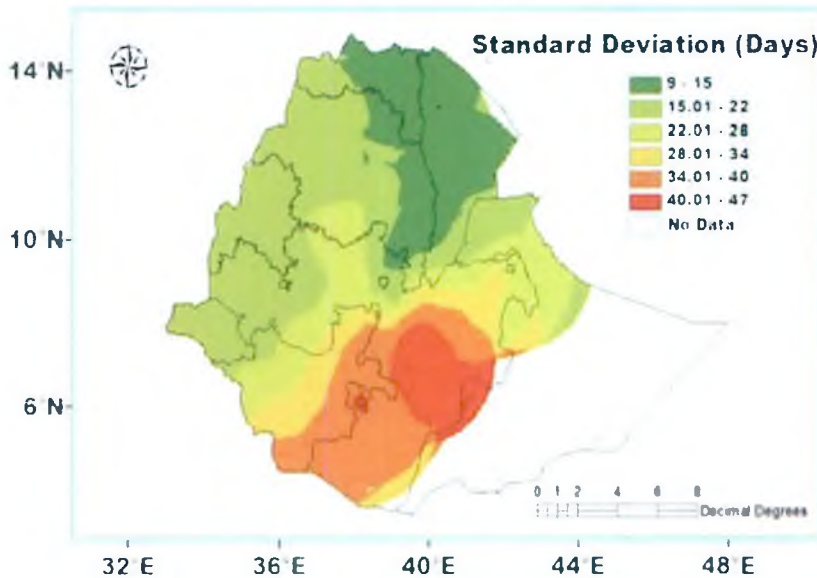

Figure 19. The standard deviation of the mean onset of the growing season.

5.3 Cessation of the growing season

The mean cessation of the growing season advances south-westward from northeastern part of Ethiopia (Fig. 20). North-eastern Ethiopia has the earliest cessation on the first decade of September, followed by central and northern Ethiopia, which have cessation in October. South-western regions have late cessation in early-to-mid December.
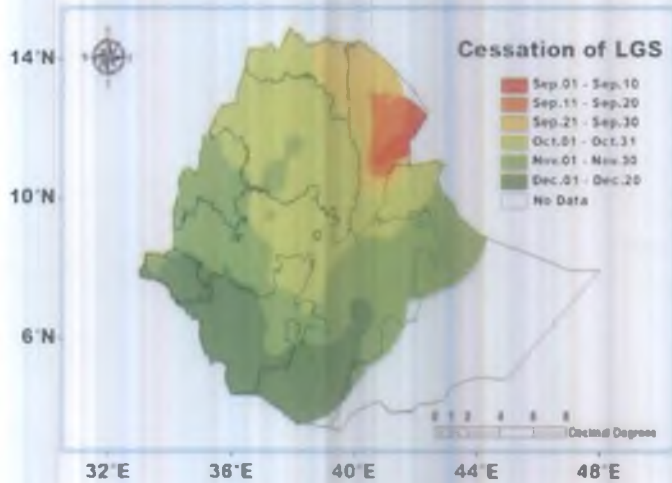
Figure 20. The mean cessation of the growing season.

The mean cessation of the growing season is less variable temporally than the mean onset, with standard deviation of 10 to 32 days (Fig. 21). The highest variability of the mean cessation occurs over southern, south-eastern Ethiopia which have standard deviation of 26 to 32 days, while the lowest variability is over north-eastern and north-western regions, where the standard deviation ranges from 10 to 18 days.
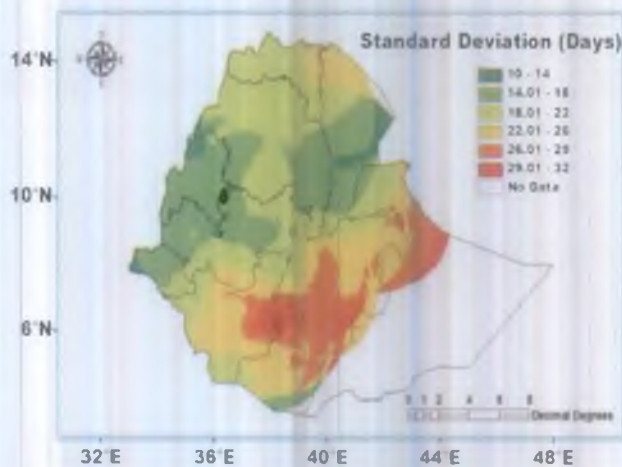

Figure 21. The standard deviation of the mean cessation of the growing season.

5.4 Length of the growing season

In general, the mean length of the growing season decrease as we move northeastward from south-western regions of Ethiopia (Fig. 22), following the spatial pattern of the mean onset (Fig. 18). It has high special variability with values ranging from 40 to 260 days. Southern and south-western parts of Ethiopia have the longest mean growing season from 180 to 260 days, followed by central and north-western regions (121 to 180 days). North-eastern Ethiopia has the shortest mean growing season (from 40 to 60 days).
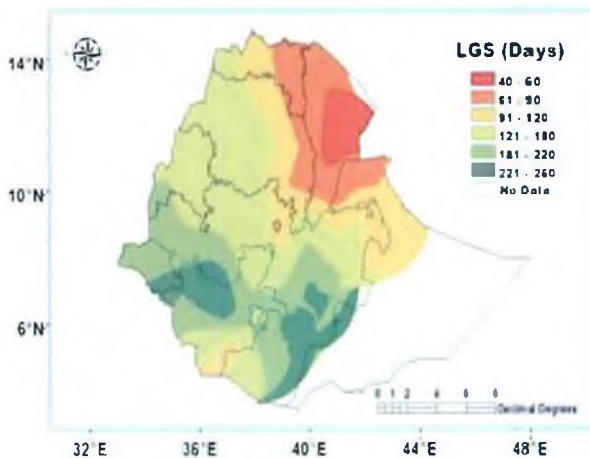
Figure 22. The mean length of the growing season.

The annual variability of the mean length of the growing season is shown in Fig. 23.. Its standard deviation ranges from 8 to 55 days. North-eastern and small portion of western Ethiopia have the lowest variability with standard deviation of 8 to 24 days, whereas southern and south-western regions have the highest variability (standard deviations of 32 to 55 days).
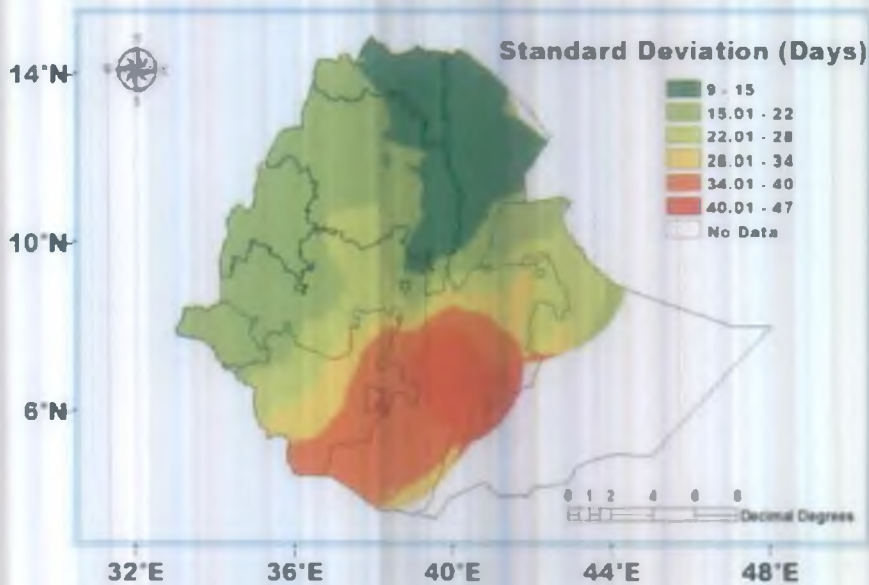
Figure 23. The standard deviation of the mean length of the growing season.

6. CLIMATE MODELS AND THEIR CHARACTERISTICS

6.1 Introduction

Our understanding of how climate will change over the next century is largely based on the projections of the global coupled climate models used in the fifth IPCC assessment report on climate change (IPCC, 2013). In order to have confidence in the projections of climate models it is essential that they can simulate the present day climate. On global scales, climate models have already shown they can make credible simulations of the temperature record of the 20th century (IPCC, 2007) and of the response of global temperatures to major climatic events, such as the Mount Pinatubo eruption and the El Nino phenomenon in the Tropical Pacific. However, one of the key challenges for climate models and climate science is that they should be capable of not only making predictions at the global scale, but that their predictions should also be relevant at the local scale. Central to this is understanding and predicting how climate will change at regional and country scales (e.g., rainfall, temperature).

6.2 Characteristics of Climate Models

Climate models use quantitative methods to simulate the interactions of the atmosphere, hydrosphere, lithosphere, cryosphere and and biosphere. They are used for a variety of purposes from study of the dynamics of the weather and climate system to projections of future climate. Climate models are systems of differential equations based on the basic laws of physics, fluid motion, and chemistry. To apply a climate model, scientists divide the planet into a 3-dimensional grid, apply the basic equations, and evaluate the results. Atmospheric models calculate winds, heat transfer, radiation, relative humidity, and surface hydrology within each grid and evaluate interactions with neighboring points. Due to the large number of calculations involved, climate models currently use bigger grid spacing and longer time steps so that they can be run further ahead in time for a given amount of computer time.

Without more powerful computers, simulation of the climate with the same detail as in weather forecasts would take far too long, especially if we want to explore many different scenarios of the future. Nevertheless, there is increasing convergence between weather forecasting and climate models, especially for predictions in the range out to months and seasons.

There have been major advances in the development and use of models over the last 20 years and the current models give us a reliable guide to the direction of future climate change. Computer models cannot predict the future exactly, due to the large number of uncertainties involved. The models are based mainly on the laws of physics, but also empirical techniques which use, for example, studies of detailed processes involved in cloud formation. The most sophisticated computer models simulate the entire climate system. By linking the atmosphere and ocean, they also capture the interactions between the various elements, such as ice and land.
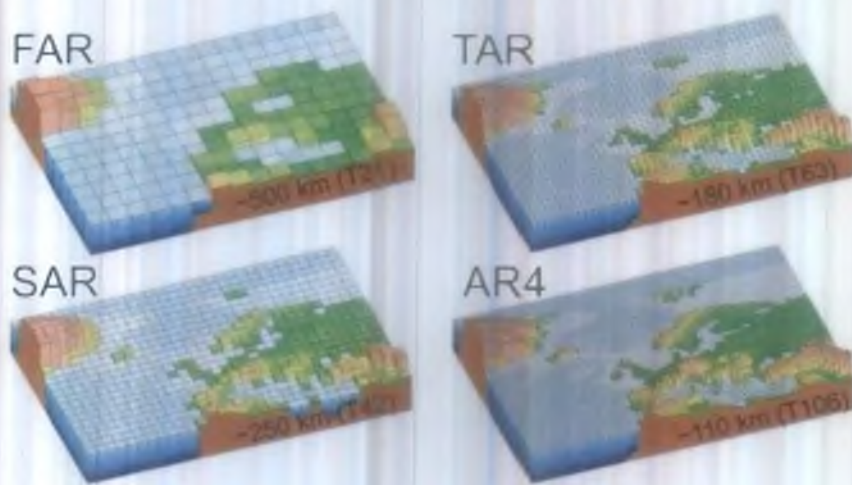
Figure 24. Improvement of climate model resolution over the four IPCC reports.

Climate models have been used successfully to reproduce the main features of the current climate; the temperature changes over the last hundred years, and the main features of the Holocene (6,000 years ago) and last glacial maximum (21,000) years ago. Current models enable us to attribute the causes of past climate change, and predict the main features of the future climate, with a high degree of confidence.

The most talked-about models of recent years have been those relating temperature to emissions of carbon dioxide (and other greenhouse gases). These models project an upward trend in the surface temperature record, as well as a more rapid increase in temperature at higher altitudes.

6.3 Global climate models (GCMs)

Weather forecasting models must handle the properties of the atmosphere in three dimensions, and work with current analyses of the ocean surface temperatures and at least some basic land surface processes. These models have come to be known as atmospheric general circulation models (GCMs). In parallel, studies of the oceans can concentrate on three-dimensional properties of the oceans and are generally known as ocean GCMs.

Assessments of vulnerability are informed by estimates of the impacts of

climate change, which in turn are often based on scenarios of future climate. These scenarios are generally derived from projections of climate change undertaken by Global Climate Models (GCMs).

These GCM projections may be adequate up to a few hundred kilometres or so, however they do not capture the local detail often needed for impact assessments at a regional level. One widely applicable method for adding this detail to global projections is to use a regional climate model (RCM). Other techniques include the use of higher resolution atmospheric GCMs and statistical techniques linking climate information at GCM resolution with that at higher resolution or at point locations.

6.3.1 Coupled model systems

When it comes to simulating the general behavior of the climate system over lengthy periods, however, it is essential to use models that represent, and where necessary conserve, the important properties of the atmosphere, land surface and the oceans in three dimensions. At the interfaces, the atmosphere is coupled to the land and oceans through exchanges of heat, moisture and momentum. These models of the climate system are usually known as coupled GCMs.

Coupling the ocean processes to atmospheric GCMs is a major challenge. The thermal capacity of the oceans is massive compared to the atmosphere and can provide to, or extract from, the atmosphere, massive amounts of latent and thermal heat. Representing their heat storage, and the absorption of greenhouse gases by the oceans, in long-term simulations of climate requires a full three-dimensional ocean model, which simulates even the deep currents. Changes in the intensity and location of deep-water currents can ultimately have profound effects on the atmosphere. In the past, changes in the circulation of the oceans have produced major atmospheric responses.

The models must also be able to handle shorter-term fluctuations such as those associated with ENSO. Recent developments in climate modeling, which take into account not only surface processes at the ocean-atmosphere interface but also those acting at depth, have produced considerable improvement to the quality of climate model results. An oceanic GCM typically requires very high spatial resolution to capture eddy processes associated with the major

currents, bottom topography and basin geometry. High-resolution ocean models are therefore at least as costly in computer time as are atmospheric GCMs. Further coupling of other climate system component models, especially the cryosphere and the biosphere, are also necessary to obtain more realistic simulations of climate on decadal and longer timescales.

6.3.2 Parameterization

There are certain physical processes that act at a scale much smaller than the characteristic grid interval (e.g., clouds and turbulence). And if the complete physics of these processes, for example, clouds, were to be computed explicitly at each time step and at every grid-point, the huge amount of data produced would swamp the computer. These processes cannot be eliminated, so simplifying equations are developed to represent the gross effect of the many small-scale processes within a grid cell as accurately as possible. This approach is called parameterization. There is a lot of research going on to devise better and more efficient ways for incorporating these small scale processes into climate models.

6.3.3 Regional Climate Models (RCMs)

Simulating climate change at the regional and national levels is essential for policymaking. Only by assessing what the real impact will be on different countries will it be possible to justify difficult social and economic policies to avert a dangerous deterioration in the global climate. Furthermore, understanding processes on the regional scale is a crucial part of global research. Processes acting on local or regional scales, such as mountain range blocking air flow or dust clouds interacting with radiation will ultimately have impacts at the global level.
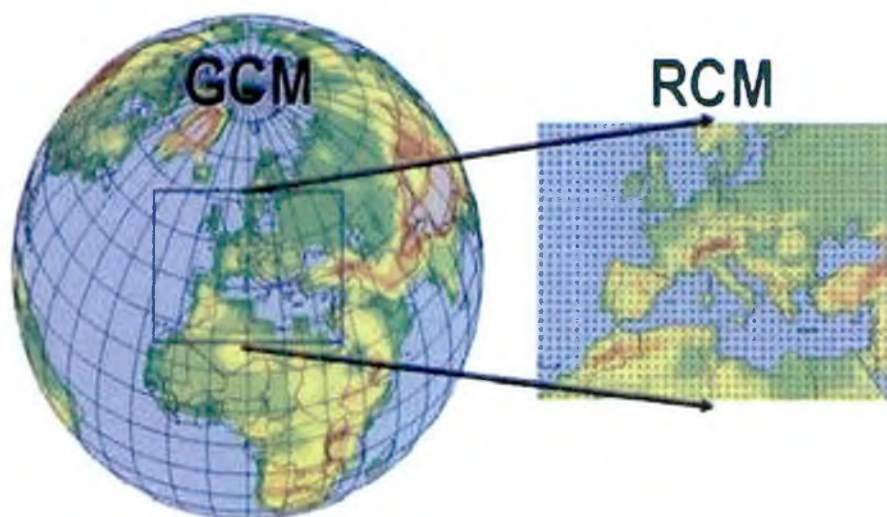
Figure 25. Regional climate model nesting approach.

One technique used to overcome the coarse spatial resolution of coupled GCMs is that of nested modeling, depicted in the image above. This involves the linking of models of different scales within a global model to provide increasingly detailed analysis of local conditions while using the general analysis of the global output as a driving force for the higher resolution model. Results for a particular region from a coupled GCM are used as initial and boundary conditions for the RCM, which operates at much higher resolution and often, with more detailed topography and physical parameterizations. This enables the RCM to be used to enhance the detailed regional model climatology and this downscaling can be extended to even finer detail in local models. This procedure is particularly attractive for mountain regions and coastal zones, as their complexity is unresolved by the coarse structure of a coupled GCM grid.

The provision of a flexible Regional Climate Model (RCM) is thus part of an integrated package of methods, which would also include a range of GCM projections for assisting countries to generate climate change scenarios and hence to inform adaptation decisions. It must be stressed that the RCM does not replace GCMs, but it is a powerful tool to be used together with the GCMs in order to add fine-scale detail to their broad-scale projections.

6.4 Downscaling techniques and Simulation of Regional-Scale Climate

The climate change information required for many impact studies is of a spatial scale much finer than that provided by global or regional climate models. The ensuring problem of impact assessment have been recognized for a long time (Kim et al., 1984; Gates, 1985; Robinson and Finkelstein, 1989; Lamb, 1987; Smith and Tirpak, 1989; Cohen, 1990).

Global climate models (GCMs) have resolution of hundreds of kilometers whilst regional climate models (RCMs) may be as fine as tens of kilometers. However, many impact application require the equivalent of point climate observations and highly sensitive to fine-scale climate variations that parameterized in coarse-scale models. This especially true for regions of complex topography, coastal or island locations, and in regions of highly heterogeneous land-cover.

The most straightforward means of obtaining higher spatial resolution scenarios is to apply coarse-scale climate change projections to a high resolution observed climate baseline-the change factor methods. This method is often used when RCM output are unavailable, for sensitivity studies, or whenever rapid assessments of multiple climate change scenarios (and/or GCM experiments) are required. Fine resolution climate change information for use in impact studies can also obtained via more sophisticated statistical downscaling (SD) methods but such studies have to date, largely restricted themselves to the use of a single driving GCM.

6.4.1 Climate Scenarios developed from Statistical Downscaling

Statistical downscaling is based on the view that the regional climate is conditioned by two factors; the large scale climate state and regional/local physiographic featured (e.g. topography, land-sea distribution and land use; (Von Storch, 1995, 1999). From this perspective, regional or local climate information is derived by first determining a statistical model which relates large-scale climate variable (or "predictors") to regional and local variable (or "predict ands"). Then the large-scale output of a GCM simulation is fed into this statistical model to estimate the corresponding local and regional climate characteristics. One of the primary advantages of these techniques

is that they are computationally inexpensive, and thus can be easily applied to output from different GCM experiments. Another advantage is that they can be used to provide site-specific information, which can critical for many climate change impact studies. The major theoretical weakness of a SD methods is that their basic assumption is not verifiable, i.e., that the statistical relationship develop for the present day climate also hold under the different forcing conditions of possible future climates – a limitation that also applies to the physical parameterizations of dynamic models.

6.4.2 Dynamical downscaling for development of climate scenario

In recent years, Regional Climate Models (RCMs) are one of the fundamental techniques used to downscale global (large-scale) climate processes for regional applications. Several studies have demonstrated the capability of RCMs in representing details of regional climate variability when such models are driven by initial and lateral boundary conditions taken from the analyses of observations or the Global Circulation Models (GCMs) output.

The RCMs have also become suitable tools for regional climate processes, seasonal climate variability, regional climate change and impact studies that are not well represented by coarse resolution GCMs. In RCMs the influence of local climatic forcing superimposed on large-scale climate variability are resolved than using GCMs.

6.4.3 The Case of Ethiopia: Regional-Scale Simulation using RegCM (Dynamical)

Ethiopia presents a particularly difficult test for climate models. The central part of Ethiopia is dominated by the East African Highlands, which split the country climatically.

To the south and east the land is semi-arid and the rains fall in two short spells either side of the dry season of Kirmet (June to August). To the north and west, the vegetation is lusher, and Kirmet is the major rainy season. This split in the geographical distribution of rainfall, and the different seasonal cycles in different regions of Ethiopia, make the task of simulating Ethiopian rainfall extremely challenging. This was noted in recent work by Mengistu Tsidu (2012a) which has shown that there is large wet bias over highlands and

dry bias over lowlands of Ethiopia in ECMWF reanalysis rainfall. Furthermore, climate models need to be able to capture the processes that influence the year-to-year (interannual) variability of Ethiopian rainfall. Variations of El Nino, the Indian Monsoon and the position of the African Easterly Jet all impact the rainfall over Ethiopia.

Disentangling these remote influences on the climate of Ethiopia, and correctly simulating them in a climate model is an exceptionally difficult task. One of the most challenging and uncertain aspects of present-day climate research is associated with the prediction of a regional response to a global forcing. Evaluations of the GCMs show that they still have significant systematic errors in and around Africa, with excessive rainfall in the south, a spurious southward displacement of the Atlantic inter-tropical convergence zone (ITCZ), and insufficient upwelling in the seas off the western coast. These conditions are exacerbated over Ethiopia due to its complex topography as we have discussed before.

Mengistu et al (2012b) used the latest version of the International Center for Theoretical Physics (ICTP) Regional climate model version 4 (RegCM4) to study the climate variability of Ethiopia. The model was configured to a spatial resolution of 50 km and model performance evaluations were made for the known three Ethiopian seasons which are JJAS (June, July, August and September), ONDJ (October, November, December and January) and FMAM (February, March, April and May).

According to Mengistu et al (2012b), RegCM4 was able to capture the structure of the dominant atmospheric circulation patterns which are associated with precipitation over Africa north of the Equator especially over complex orography like Ethiopian highlands.

The model simulated well the depth and northward extent of the low level jet (LLJ) ; the strength, location and depth of the upper troposphere Tropical Easterly Jet (TEJ) ; the location (both in latitude and height) of the African Easterly Jet (AEJ). The main model deficiency being the underestimation of the mid-tropospheric easterlies in both seasons over the southern equatorial regions and the overestimations of TEJ and LLJ.

Mengistu et al (2012b) also conclude that RegCM4 reproduces well the spatial

pattern of the mean temperature climatology of the three seasons although there is slight deference locally resulting in mixed bias. Generally, the model was found to have moderate warm and cold biases over low and highlands of Ethiopia respectively.

Although the performance of RegCM4 in simulating precipitation varies with the selection of convective parametrization scheme, Mengistu et al (2012b) reported that RegCM4 reproduced the major features of precipitation in all seasons. The model able to reproduce the observed intrannual cycle peaks, although it tends to over-predict their magnitude except some cases. The RegCM4 rainfall climatology also shows some deficiencies in reproducing the intensities and phase of the observed rainfall. They suggested that this deficiency might be due to the fact that the limitations of RegCM4 in reproducing the observed rainfall climatology of those climate Eco-regions of Ethiopia which is characterized by complex topographical features, land cover and mesoscale circulations that might be difficult to capture with 50 km horizontal resolution. However, the above study is mainly based on simulations for the current climate and one of the AR4 emission scenarios. While the study can in principle be replicated under RCP scenarios, this is not the case for this report. Therefore, the results on both current and future climate model projections are based on data interpolated to finer spatial resolution from coarse-resolution coupled climate models shown in Table A.2 of the annex of this report. Moreover, the errors that could arise from the interpolation procedure is not included in the overall uncertainty budget of the ensemble mean from the GCMs.

7. FUTURE CLIMATE CHANGE

7.1 Introduction

Projections of changes in the climate system are made using a hierarchy of climate models ranging from simple climate models, to models of intermediate complexity, to comprehensive climate models, and Earth System Models. These models simulate changes based on a set of scenarios of anthropogenic forcings. A new set of scenarios, the Representative Concentration Pathways (RCPs), was used for the new climate model simulations carried out under the framework of the Coupled Model Intercomparison Project Phase 5 (CMIP5) of the World Climate Research Program. In all RCPs, atmospheric CO_2 concentrations are higher in 2100 relative to present day as a result of

a further increase of cumulative emissions of CO_2 to the atmosphere during the 21st century (IPCC, 2013).

7.2 CMIP5 model ensemble based historical changes in rainfall and temperature

Figs. 26-27 show the CMIP5 model ensemble-based historical annual mean precipitation and temperature trends with their significance. Although there is no significant change in simulated mean annual precipitation, there is a tendency of a decrease over the central and an increase over the rest of the country.

The change is pronounced when seasonal precipitation is considered. For the Belg rains, the decrease in rainfall ranges from -150 to -50 mm across the south-central and eastern parts of the country, and will be associated with lower Belg harvests and poorer pastoral rangelands during the summer and early fall. For the Kiremt rains, the decline in rainfall ranges also from -150 to -50 mm across the western and southern parts of Ethiopia. The combined Belg and Kiremt rainfall reductions results in a total loss of more than 150 mm of rainfall per year in the most densely populated (Fig. 26) long cycle crop growing area of the country. During the past 11 or 12 years, average rainfall conditions have been poor in most areas, more than 0.4 standard deviations below average.
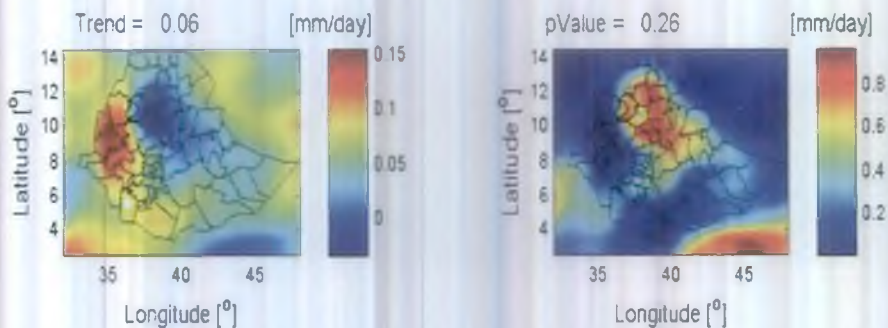
Figure 26. Trend (left) and significance (right) of historical ensemble mean annual precipitation from 1975 to 2005 from fourteen CMIP5 models. The rainfall trends are determined by linear regression from each model data with 95% confidence.

There is significant trend in mean annual surface temperature during 1975-2005 period. The annual mean surface temperature increases within a range of 0.6 to 0.8 0C from place to place over the country.
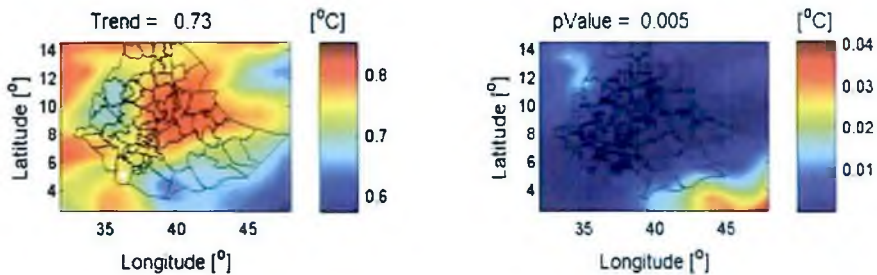
Figure 27. Trend (left) and significance (right) of historical ensemble mean surface temperature 1975 to 2005 from fourteen CMIP5 models in the same manner as in Fig. 26.

7.3 CMIP5 model ensemble based projected changes in rainfall

Fig. 28 shows the CMIP5 model-based historical and projected annual mean precipitation. The single line represents the historical (1975-2005) ensemble model simulations, whereas RCP2.6, RCP4.5 and RCP8.5 ensembles mean precipitation are indicated with the solid lines. The shaded areas represent the standard errors of each RCP as determined from the scatter among the models in the ensemble.
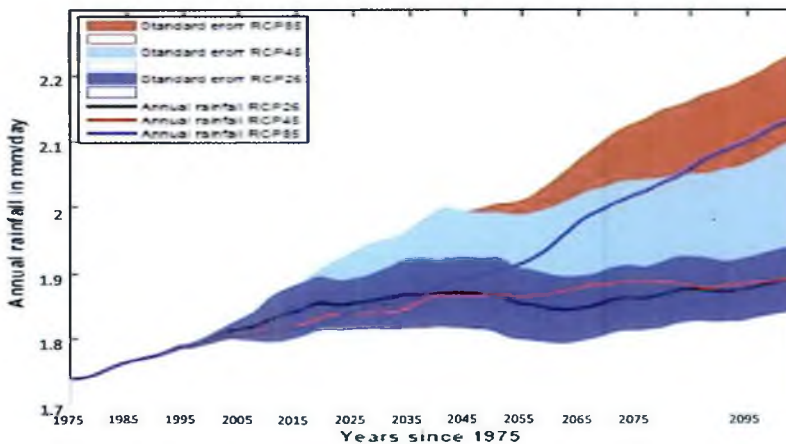
Figure 28. Mean annual rainfall over Ethiopia from 1975-2099.

Mean precipitation projections have larger uncertainties as evident from the large spread of the precipitation projections in the figure, which ranges from 1.8 to 2.2 mm/day towards the end of the century. The RCPs diverge from each other while there is also an increase in the uncertainty with time as expected (see Table A.1 for the definition of RCPs). RCP8.5 project the lowest and highest precipitation values during the near term and the last two terms respectively.

Fig. 29 shows the CMIP5 model ensemble-based average percentage change of rainfall over Ethiopia for the near-term (2006-2036, left column), for the mid-term (2037-2067, middle column) and for the end-term (2068-2099, right column) relative to the baseline period (1975-2005) mean for the RCP2.6 (top row), RCP4.5 (middle row) and RCP8.5 (bottom row)..
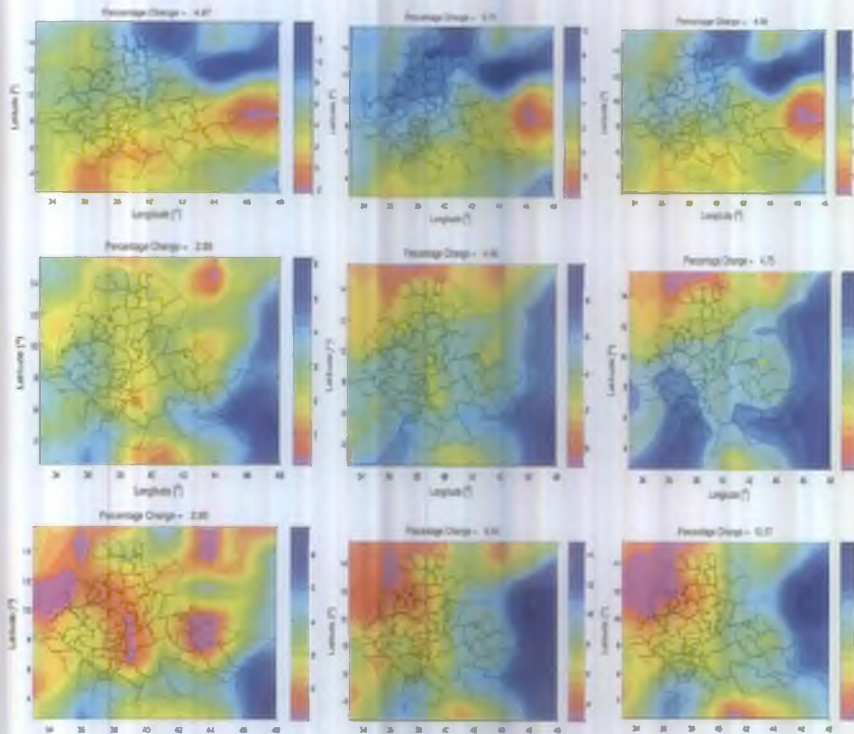
Fig. 29. Percentage change of rainfall under RCP2.6 (upper), RCP4.5 (middle) and RCP8.5 (bottom) scenarios over Ethiopia with respect to the historical period (1975-2005) mean.

An increased precipitation over Ethiopia is projected during the 21st century, except the negative to no change projections of the RCP2.6 over the eastern part of the country. The ensemble-mean annual precipitation for all RCPs increase by 4% to 12% by 2100 compared to the 1975– 2005 baseline.

The response of different parts of the country to different RCPs is slightly different. The percentage increase is high over northern part of Ethiopia under RCP2.6 scenario and over southern and east-southern part of the country under RCP4.5 and RCP8.5 scenarios.

According to Cline (2007), projections from different models indicate that there will be an increasing of annual rainfall in the short rainfall season in southern Ethiopia. However, the larger proportion of the country will see mixed result showing slight increase in south east and decrease over the north.

7.4 CMIP5 model ensemble based projected changes in tempera ture

Fig. 30 shows the CMIP5 model-based historical and projected annual mean temperature. The solid line represent RCP2.6, RCP4.5 and RCP8.5 ensembles mean temperatures, whereas the shaded areas represent the standard errors of each RCP.
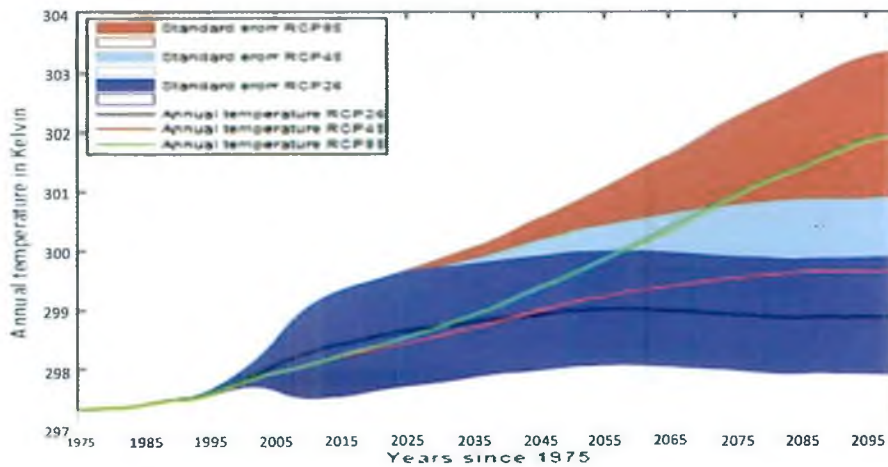
Figure 30. Historical and projection period mean annual temperature over Ethiopia (1975-2099).

Although there is a slight spatial difference among the three RCPs in mean temperature projections of the 2020s, the difference increases with time. The range of annual temperature increase for all the RCPs by 2100 relative to the 1975-2005 baseline period mean ranges from -0.5° to 6°C. From Fig. 31, one can see that under RCP2.6 the mean temperature increases by approximately 1°C at the end of the century relative to the baseline period, and 5°C in RCP8.5. For RCP 4.5, which represents the moderate scenario, the projected increase in temperature is around 2°C.
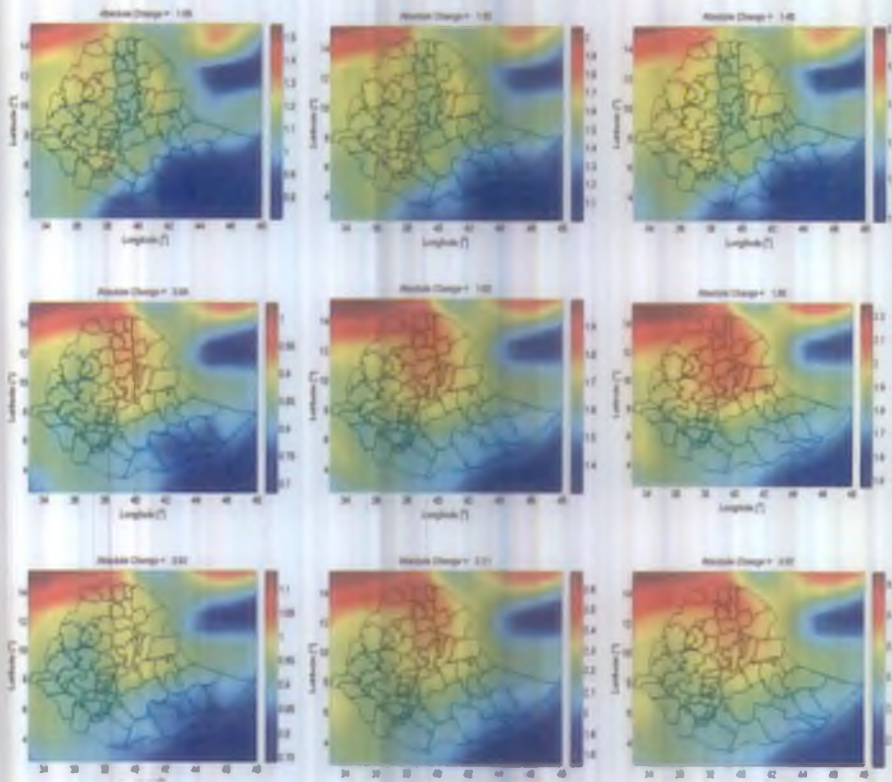
Figure 31. Change in annual mean temperature under RCP2.6 (upper), RCP4.5 (middle) and RCP8.5 (bottom) scenarios over Ethiopia from the historical period (1975-2005) mean.

The mean surface temperature change for the near-term relative to the baseline will likely be in the range of 0.84°C to 1.08°C. Relative to natural internal variability, near-term increases in seasonal mean and annual mean

temperatures are expected to be larger in the tropics and subtropics than in mid-latitudes. Increase of mean surface temperatures for the end-term relative to 1975–2005 is projected to likely be in the range of 0.8°C to 1.1°C (RCP2.6), 1.8°C to 2.6°C (RCP4.5), 2.6°C to 3.6°C (RCP8.5).

This is in agreement with the report by (World Bank, 2008) which report that the average temperature in Ethiopia has been projected to increase from 23.08°C during 1961-1990 to 26.92°C in 2070-2099. However, Temesgen et al, (2007) also reported that, there will be significant temperature difference among different parts of the country. While highlands in the Central North of the country will be as cold as -0.5°C, the Southeast low lands will be as warm as 37°C. These extreme temperatures constrain crop production by limiting water availability and growth of many plants.

Table 2. Summary of projected change in mean surface air temperature and percentage change of rainfall over Ethiopia for the near, mid- and late 21st century relative to the reference period (1975–2005) mean.

	Scenario	Near	Mid	End
Mean Surface Temperature (°C)	RCP2.6	1.08	1.50	1.45
	RCP4.5	0.84	1.65	1.89
	RCP8.5	0.92	2.21	3.07
Percentage change of Rainfall (%)	RCP2.6	4.67	3.75	4.69
	RCP4.5	2.93	4.46	4.75
	RCP8.5	2.95	8.49	12.27

References

Amsalu, A., Stroosnijder, L. and Graaff, J. (2007) Long-term dynamics in land resource use and   the driving forces in the Beressa watershed, highlands of Ethiopia. Journal of Environmental Management, 83, 448–459.

Aynekulu, E., Wubneh, W., Birhane, E. and Begashaw, N. (2006) Monitoring and Evaluating Land Use/Land Cover Change Using Participatory Geographic Information System (PGIS) Tools: A Case Study of Begasheka Watershed, Tigray, Ethiopia. The Electronic Journal of Information Systems in Developing Countries, 25, 1–10.

Asnani, G. (2005). Tropical Meteorology, Volume 1. Praveen Printing Press, revised edition.

Bahaga, T. K., Mengistu Tsidu, G., Kucharski, F. and Diro, G. T. (2015), Potential predictability of the sea-surface temperature forced equatorial East African short rains interannual variability in the 20th century. Q.J.R. Meteorol. Soc., 141:16–26. doi:10.1002/qj.2338

Bekele, F. (1997), Ethiopian use of ENSO information in its seasonal forecasts, Internet J. Afr. Studies, No. 2. [Available at http://www.ccb.ucar.edu/ijas/ijasno2/bekele.html.]

Beltrando, G., and P. Camberlin, (1993): Interannual variability of rainfall in the eastern Horn of Africa and indicators of atmospheric circulation. Int. J. Climatol., 13, 533–546.

Bewket, W. (2002) Land cover dynamics since the 1950s in Chemoga watershed, Blue Nile basin, Ethiopia. Mountain Research and Development, 22, 263–269.

Boko, M., I. Niang, A. Nyong, C. Vogel, A. Githeko, M. Medany, B. Osman-Elasha, R. Tabo and P. Yanda (2007) Africa. Climate Change 2007: Impacts, Adaptation and Vulnerability. Contribution of Working Group II to the Fourth Assessment Report of the Intergovernmental Panel on Climate Change, M.L. Parry, O.F. Canziani, J.P. Palutikof, P.J. van der Linden and C.E. Hanson, Eds., Cambridge University Press,Cambridge UK, 433-467.

Cadet DL, Diehl BC. (1984) Interannual variability of surface fields over the

Indian- Ocean during recent decades. Monthly Weather Review 112: 1921–1935.

Camberlin P., (1997) Rainfall anomalies in the source region of the Nile and their connection with the Indian summer monsoon. J. Climate, 10, 1380–1392.

Camberlin P., and Philippon,N. (2002) The East African March-May Rainy season: Associated Atmospheric dynamics and predictability over the 1968-97 period. J. Climate, 15, 1002-1019.

Carslaw et al, (2010): A review of natural aerosol interactions and feedbacks within the Earth system. Atmos. Chem. Phys., 10, 1701–1737.

Cline, W.R. (2007). *Global warming and agriculture: impact estimates by country*. Center for Global Development. Preferred estimates based on World Bank Ricardian model and a crop model.

Conway D , (2000): Some aspects of climate variability in the northeast Ethiopian highlands-Wollo and Tigray. SINET: Ethiopian J. Sci. 23(2):139-161.

Conway, D., Mould, C., & Bewket, W., (2004): Over one century of rainfall and temperature observations in Addis Ababa, Ethiopia. International Journal of Climatology, 24(1), 77-91.

Conway, G. (2009) The science of climate change in Africa: impacts and adaptation. Discussion paper No 1. Grantham Institute for Climate Change. London.

Crummey, D. (1998) Deforestation in Wollo: Process or illusion? Journal of Ethiopian Studies, 31, 1–42.

Cubasch, U., D. Wuebbles, D. Chen, M.C. Facchini, D. Frame, N. Mahowald, and J.-G. Winther (2013) Introduction. In: Climate Change 2013: The Physical Science Basis. Contribution of Working Group I to the Fifth Assessment Report of the Intergovernmental Panel on Climate Change [Stocker, T.F., D. Qin, G.-K. Plattner, M. Tignor, S.K. Allen, J. Boschung, A. Nauels, Y. Xia, V. Bex and P.M. Midgley (eds.)]. Cambridge University Press, Cambridge, United Kingdom and New York, NY, USA.

Degefu, W. (1987) Some aspects of meteorological drought in Ethiopia, in

Drought and Hunger in Africa: Denying Famine a Future, edited by M. H. Glantz, pp. 23–36, Cambridge Univ. Press, , Cambridge, U. K.

Dessie, G. & Kleman, J. (2007) Pattern and magnitude of deforestation in the South Central Rift Valley region of Ethiopia. Mountain research and development, 27, 162–168.

Dessie, G. & Christiansson, C. (2008) Forest decline and its causes in the south-central Rift Valley of Ethiopia: Human impact over a one hundred year perspective. Ambio, 37, 263–271.

Endalew, Gebru J. (2007) Changes in the frequency and intensity of extremes over Northeast Africa. KNMI scientific report = wetenschappelijk rapport ; WR 2007-02.

Etheridge et al, (1996): Natural and anthropogenic changes in atmospheric CO_2 over the last 1000 years in Antarctic ice and firn. J. geophys. Res. Atmos., 4115-4128

FAO, (1998): Crop Evapotranspiration, Irrigation and Drainage, paper 56.FAO, Rome, pp. 15-86.

Funk C, Senay G, Asfaw A et al (2005) Recent drought tendencies in Ethiopia and equatorial-subtropical eastern Africa. US Agency for International Development, Washington

Funk, C., Senay, G., Asfaw, A., Verdin, J., Rowland, J., Korecha, D., Eilerts, G., Michaelsen, J., Amer, S., and Choularton, R., (2005): Recent drought tendencies in Ethiopia and equatorial-subtropical eastern Africa: Washington, D.C., U.S. Agency for International Development.

Funk, C., Dettinger, M.D., Michaelsen, J.C., Verdin, J.P., Brown, M.E., Barlow, M., and Hoell, A., (2008) Warming of the Indian Ocean threatens eastern and southern African food security but could be mitigated by agricultural development: Proceedings of the National Academy of Sciences of the United States of America, v. 105, no. 32, p. 11,081–11,086. (Also available online at ftp://chg.geog.ucsb.edu/pub/pubs/PNAS_2008.pdf.)

Funk, C., Dettinger, M.D., Michaelsen, J.C., Verdin, J.P., Brown, M.E., Barlow, M., and Hoell, A., (2008): Warming of the Indian Ocean threatens eastern and southern African food security but could be mitigated by agricultural

development: Proceedings of the National Academy of Sciences of the United States of America, v. 105, no. 32, p. 11,081–11,086.

Garedew, E., Sandewall, M., Söderberg, U. & Campbell, B. M. (2009) Land-use and land-cover dynamics in the Central Rift Valley of Ethiopia. Environmental Management, 44, 683–694.

Gebrehiwot, S., Taye, A. & Bishop, K. (2010) Forest cover and stream flow in a headwater of the Blue Nile: Complementing observational data analysis with community perception. Ambio, 39, 284–294.

Gebeyehu M. and G. Mengistu (2012) Stratospheric Aerosol and Its Main Deriver Over Equatorial Africa, LAP Lambert Academic Publishing, ISBN-10: 3659129356.

Gissila, T., E. Black, D. I. F. Grimes, and J. M. Slingo (2004) Seasonal forecasting of the Ethiopian summer rains, Int. J. Climatol., 24, 1345–1358.

Gizaw Attlee (1968) weather and climate at Addis Ababa, Asmara(1964), Diredawa and Jimma. Met. Serv. Ethiopia, Addis Ababa.

Goddard L, Graham NE. (1999) Importance of the Indian Ocean for simulating rainfall anomalies over eastern and southern Africa. Journal of Geophysical Research–Atmospheres 104: 19 099–19 116.

Habtemichael, A., and D. E. Pedgley, (1974): Synoptic case-study of spring rains in Eritrea. Meteor. Atmos. Phys., 23, 285–296.

Haile, T., (1987) A case study of seasonal forecasts in Ethiopia. In: WMO RAI (Africa) Seminar on Modern Weather Forecasting (Part II), 30 November-4 December 1987. Addis Ababa, Ethiopia.

Haile, T., (1988): Causes and characteristics of drought in Ethiopia. Ethiopian. Journal of Agricultural Science, 10, 85-97.

Hastenrath, S. (1991) Climate Dynamics of the Tropics. Norwell Massachusetts: Kluwer Academic Publishers. 488 pp.

Hastenrath S. and Polzin D., (2003): Dynamics of the surface wind field over the equatorial Indian Ocean. Q. J. R. Meteorol. Soc. (2004), 130, pp. 503–517.

Held, I., and B. J. Soden, (2006): Robust responses of the hydrological cycle to global warming. J. Climate, 19, 5686–5699.

IPCC, (2007): Climate Change 2007: Synthesis Report. Contribution of Working Groups I, II and III to the Fourth Assessment Report of the Intergovernmental Panel on Climate Change [Core Writing Team, Pachauri, R.K and Reisinger, A. (eds.)]. IPCC, Geneva, Switzerland, 104 pp.

IPCC (2013) Summary for Policymakers. In: Climate Change 2013: The Physical Science Basis. Contribution of Working Group I to the Fifth Assessment Report of the Intergovernmental Panel on Climate Change [Stocker, T.F., D. Qin, G.-K. Plattner, M. Tignor, S.K. Allen, J. Boschung, A. Nauels, Y. Xia, V. Bex and P.M. Midgley (eds.)]. Cambridge University Press, Cambridge, United Kingdom and New York, NY, USA.

Ininda J, Desalgne B, Befekadu A. (1987) The characteristics of rainfall in Ethiopia and its relationship to the El Nino southern oscillation. In First Technical Conference on Meteorological Research in Eastern and Southern Africa, Nairobi, Kenya, Kenya Meteorological Department; 133–135.

Jury M. R. and C. Funk (2013) Climate change over Ethiopia: regional signals and drivers, International Journal of Climatology, in press.

Kassahun, B (1987a) Large Scale Features Associated with Kiremt Rainfall Anomaly. African Climate and Climate Change: Physical Social and Political perspectives: Charles J. R. Williams, Dominic R. Kniveton.

Kassahun, B. (1987b) Weather systems over Ethiopia, paper presented at the first international Technical Conference on Meteorological Research in Eastern and Southern Africa, pp. 53–57, Nairobi, Kenya, UCAR

Korecha D. and Barnston A. G., (2007) Predictability of June–September Rainfall in Ethiopia. Amer. Meteor. Soc., 135, 625-650.

Krishnamurti, T.N., and M. Kanamitsu, (1981): Northern summer planetary-scale monsoons during drought and normal rainfall months. Monsoon Dynamics, 19-48.

Kruzhkova, T.S., (1981): On certain features of the atmospheric circulation in periods of drought. In: R.P. Pearce (Ed.), Tropical Droughts, Meteorological Aspects and Implication for Agriculture. Gidrometeostat: Moscow, 49-55.

Latif M, Dommenget D, Dima M, Grotzner A. (1999) The role of Indian Ocean

sea surface temperature in forcing East African rainfall anomalies during December–January 1997/98. Journal of Climate 12: 3497–3504.

Mawunya, F. D., S. G. K. Adiku, K. B. Laryea, M. Yangyuoru and E. Atika, (2011): Characterization of Seasonal Rainfall for Cropping Schedules, West African Journal of Applied Ecology, 19, pp. 107-118.

McCann, J. C. (1995): People of the plow: an agricultural history of Ethiopia 1800–1990. Madison: University of Wisconsin Press.

Mengistu, K. T. (2009) Watershed Hydrological Responses to Changes in Land Use and Land Cover, and Management Practices at Hare Watershed, Ethiopia. Dissertation, Universität Siegen Fakultät Bauingenieurwesen, Research Institute for water and Environment, Germany.

Mengistu Tsidu, G. (2012a) High-Resolution Monthly Rainfall Database for Ethiopia: Homogenization, Reconstruction, and Gridding. *J. Climate*, 25, 8422–8443. doi: http://dx.doi.org/10.1175/JCLI-D-12-00027.1

Mengistu Tsidu, G., Tamene Mekonnen, Robel Takele, Jemal Seid, Andualem Shimelis, Girma Mammo, (2012b): Dynamical and statistical downscaling of climate data for impact modeling over Ethiopia, unpublished report for Ethiopian Institute of Agricultural Research.

Mengistu Tsidu, G., W. Gitau, C. Oludhe, L. Ogailo, Z. Atheru, and P. Ambenje (2015): [Regional Climates] Eastern Africa [in "State of the Climate in 2014"]. *Bull. Amer. Meteor. Soc.* , P187-189.

Nicholls N. (1993) What are the potential contributions of El Nino southern oscillation research to early warning of potential acute food-deficit situations? Internet Journal of African Studies 2 http://www.brad.ac.ukresearch/ijas [May 2004].

NMSA, (1996) Climatic and agroclimatic resources of Ethiopia. National Meteorological Services Agency of Ethiopia, Meteorological Research Report Series, Vol. 1, No. 1, 1–137.

NMSA, (2001): Initial National Communication of Ethiopia to the United Nations Framework Convention on Climate Change. Federal Democratic Republic of Ethiopia, Ministry of Water and Energy, National Meteorological Agency, June 2001, Addis Ababa Ethiopia.

Nyssen, J., Poesen, J., Moeyersons, J., Deckers, J., Haile, M. & Lang, A. (2004) Human impact on the environment in the Ethiopian and Eritrean highlands – A state of the art. Earth-Science Reviews, 64, 273–320.

Nyssen, J., Haile, M., Naudts, J., Munro, N., Poesen, J., Moeyersons, J., Frankl, A., Deckers, J. & Pankhurst, R. (2009) Desertification? Northern Ethiopia re-photographed after 140 years. Science of the Total Environment, 407, 2749–2755.

PBL (2013) Trends in global CO2 emissions: 2013 Report. Bakgound studies. PBL Netherlands Environmental Assessment Agency. PBL publishers.

Pedgley, D. E. (1966) THE RED SEA CONVERGENCE ZONE. Weather, 21: 394–406. doi: 10.1002/j.1477-8696.1966.tb02788.x Desert Locust Control Organization for Eastern Africa on secondment from the British Meteorological Office.

Quinn WH. (1992) A study of the southern oscillation related climatic activity for AD 622–1990 incorporating Nile River flood data. In El Ni~no: Historical and Paleo Climatic Aspects of the Southern Oscillation, Diaz HF, Markgraf V (eds). Cambridge University Press.

Segele, Z. T. and P. J. Lamb, (2005): Characterization and variability of Kiremt rainy season over Ethiopia, Meteorol Atmos Phys, 89:153-180.

Segele, Z. T., P. Lamb, and L. Leslie (2009) Seasonal-to-Interannual variability of Ethiopia/Horn of Africa monsoon. part I: Associations of wavelet-filtered large-scale atmospheric circulation and global sea surface temperature, J. Clim., 22, 3396–3421.

Shanko D., and P. Camberlin, (1998) The effect of the southwest Indian Ocean tropical cyclones on Ethiopian drought. Int. J. Climatol., 18, 1373–1378.

Seleshi Y, Zanke U, (2004): Recent changes in rainfall and rainy days in Ethiopia. Int. J. Climatol. 24:973-983.

Seleshi Y, Camberlin P, (2006): Recent changes in dry spell and extreme rainfall events in Ethiopia. Theor. Appl. Climatol. 83(1-4):181-191.

Smith, J.B., and D. Tirpak, (1989): The Potential Effects of Climate Change on the United States, EPA-230-05-89-050, U.S. Environmental

Protection Agency, Washington, DC. World Bank, (2008): Ethiopia: A Country Study on the Economic Impacts of Climate Change. Environment and Natural Resource Management Report, no. 46946-ET. Washington, DC: World Bank, Sustainable Development Department, Africa Region.

Tadesse T. (1994) Summer monsoon seasonal rainfall of Ethiopia in ENSO episodic years. In WMO/TOGA International Conference on Monsoon Variability and Prediction, ICTP, Trieste, WMO; 48–55.

Tefera, B. & Sterk, G. (2008) Hydropower-induced land use change in Fincha watershed, western Ethiopia: Analysis and impacts. Mountain Research and Development, 28, 72–80.

Tegene, B. (2002) Land-cover/land-use changes in the Derekolli catchment of the South Welo zone of Amhara region, Ethiopia. Eastern Africa Social Science Research Review, 18, 1–20.

Takele R, Shimes A, Legesse G, Said J, Mekonen T, Gebre L, Tsega M, Girma Mamo, Tesfaye K. 2013. Analyzing Climate Risks and Exploring Options in Eastern and Southern Africa. Research Report. Addis Ababa: Ethiopian Institute of Agricultural Research (EIAR) and International Maize and Wheat Improvement Center (CIMMYT).

Tekle, K. & Hedlund, L. (2000): Land cover changes between 1958 and 1986 in Kalu District, southern Wello, Ethiopia, Mountain Research and Development, 20, 42-51.

Temesgen M, Rockstrom J, Savenije HHG, Hoogmoed WB (2007). Assessment of Strip Tillage Systems for Maize production in semi-arid Ethiopia: Effects on grain yield and water balance. UNESCO-IHE, Wageningen University, The Netherlands.

TerrAfrica, (2009) The role of sustainable land management for climate change adaptation and mitigation in sub-Saharan Africa. Issue Paper, TerrAfrica, Regional Sustainable Land Management. A TerrAfrica Partnership Publication

UNEP (u.d). Vital Climate Graphics Africa. A UNEP/GRID-Arendal publication. http://www.grida.no/publications/vg/africa

Viste, E., and A. Sorteberg (2011), Moisture transport into the Ethiopian highlands, Int. J. Climatol., 33, 249–263.

von Storch, H., (1995) Inconsistencies at the interface of climate impact studies and global climate research. -Meteor. Z. 4 NF, 72-80.

Von Storch, H., 1999: Misuses of statistical analysis in climate research. Analysis of Climate Variability: Applications of Statistical Techniques, 2nd edition [H. Von Storch and A. Navarra (eds.)]. Springer-Verlag, New York, and Heidelberg, Germany, pp. 11–26.

Walker GT, Bliss EW. (1932) World Weather V. Memoir of the Royal Meteorological Society 3: 81–95

Wang, K. C., and S. L. Liang, (2009) Global atmospheric downward long wave radiation over land surface under all-sky conditions from 1973 to 2008. J. Geophys. Res. Atmos., 114, D19101.

Wang et al, (2012): Recent change of the global monsoon precipitation (1979–2008). Clim. Dyn., 39, 1123–1135.

Wild, M., J. Grieser, and C. Schaer (2008) Combined surface solar brightening and increasing greenhouse effect support recent intensification of the global land-based hydrological cycle. Geophys. Res. Lett., 35, L17706.

William, A.P., and C. Funk; (2011) A westward extension of the warm pool leads to a westward extension of the Walker circulation, drying eastern Africa. Clim Dyn DOI 10.1007/s00382-010-0984-y.

Wøien, H. (1995) Deforestation, information and citations. GeoJournal 37, 501–511.

Zeleke, G. & Hurni, H. (2001) Implications of land use and land cover dynamics for mountain resource degradation in the northwestern Ethiopian highlands. Mountain Research and Development, 21, 184–191.

ANNEX: ATLAS OF CLIMATE PROJECTIONS FOR ETHIOPIA

This Annex presents a series of figures showing patterns of climate change over Ethiopia computed from twenty one global climate models output gathered as part of the Coupled Model Intercomparison Project Phase 5 (CMIP5; Taylor et al., 2012). Maps of surface air temperature change and relative precipitation change (i.e., change expressed as a percentage of mean precipitation) in different seasons are presented for Ethiopia and for eleven administrative regions in Ethiopia. Twenty-year average changes for the near term (2016–2035), for the mid term (2046–2065) and for the long term (2081–2100) are given, relative to a reference period of 1986–2005.

Maps are shown only for the RCP4.5 scenario; however, the time series presented show how the area-average response varies among the RCP2.6, RCP4.5 and RCP8.5 scenarios. Tables A.1 and A.2 give experiment description and the set of models used to produce the time series plots and the spatial maps. The 25th, 50th and 75th percentile of the distribution of ensemble members is presented in the spatial maps (different from similar plots in Chapter 4 and the time series which show the multi-model mean).

Table A.1 Short names for RCP scenario experiments used in this report and their descriptions.

Experiment Short Name	Experiment Description
Historical	Simulation of recent past (1850 to 2005). Impose changing conditions (consistent with observations).
RCP2.6	Future projection (2006-2100) forced by RCP2.6. RCP2.6 is a representative concentration pathway which approximately results in a radiative forcing of 2.6 W.m^{-2} at year 2100, relative to pre-industrial conditions.
RCP4.5	Future projection (2006-2100) forced by RCP4.5. RCP4.5 is a representative concentration pathway which approximately results in a radiative forcing of 4.5 W.m^{-2} at year 2100, relative to pre-industrial conditions. RCPs are time dependent, consistent projections of emissions and concentrations of radiatively active gases and particles.

RCP8.5	Future projection (2006-2100) forced by RCP8.5. RCP8.5 is a representative concentration pathway which a proximately results in a radiative forcing of 8.5 $W.m^{-2}$ at year 2100, relative to pre-industrial conditions. RCPs are time dependent, consistent projections of emissions and concentrations of radiatively active gases and particles.

Model	Institute	Link to model documentation
BCC-CSM1.1	Beijing Climate Center (BCC)	http://forecast.bcccsm.cma.gov.cn/web/c hannel-34.htm
BCC- CSM1.1(m)	Beijing Climate Center (BCC)	http://forecast.bcccsm.cma.gov.cn/web/c hannel-34.htm
CCSM4	National Center for Atmospheric Research (NCAR)	http://www2.cesm.ucar.edu/
CESM1 (BGC)	National Center for Atmospheric Research (NCAR)	http://www2.cesm.ucar.edu/
CESM1 (CAM5)	National Center for Atmospheric Research (NCAR)	http://www2.cesm.ucar.edu/
CESM1 (WACCM)	National Center for Atmospheric Research (NCAR)	http://www2.cesm.ucar.edu/errata
FGOALS-g2	Institute of Atmospheric Physics, Chinese Academy of Sciences	http://www.lasg.ac.cn/fgoals/index2.asp
GFDL-CM3	Geophysical Fluid Dynamics Laboratory (GFDL)	http://www.gfdl.noaa.gov/cmip
GFDL-ESM2G	Geophysical Fluid Dynamics Laboratory (GFDL)	http://journals.ametsoc.org/doi/abs/10.1 175/JCLI-D-11-00560.1
GFDL-ESM2M	Geophysical Fluid Dynamics Laboratory (GFDL)	http://journals.ametsoc.org/doi/abs/10.1 175/JCLI-D-11-00560.1
GISS-E2-R	NASA Goddard Institute for Space Studies (NASA-GISS)	http://data.giss.nasa.gov/modelE/ar5
HadGEM2-AO	National Institute of Meteorological Research,	http://dx.doi.org/10.1175/JCLI3712.1
HadGEM2-CC	Met Office Hadley Centre (MOHC)	http://dx.doi.org/10.1175/JCLI3712.1
HadGEM2-ES	**Met Office Hadley Centre (MOHC)**	http://dx.doi.org/10.1175/JCLI3712.1

Table A.2 The CMIP5 models used in this report for each of the historical and RCP scenario experiments. The data is a subset of the IPCC working group i AR5 snapshot of the 15th March 2013.
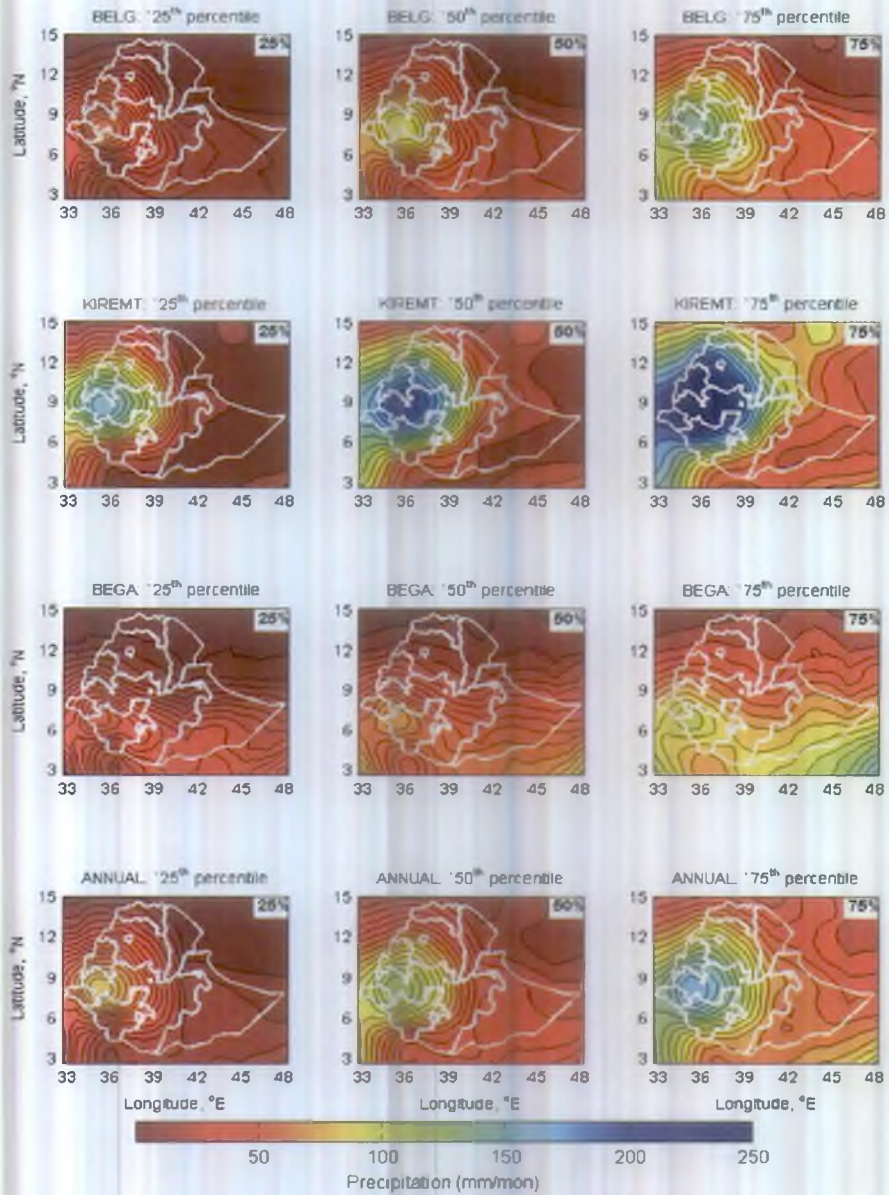
Figure A.1. Maps of seasonal and annual precipitation changes during 2016–2035 period with respect to 1986–2005 mean under the RCP4.5 scenario for the 25th, 50th and 75th percentiles of the distribution of the CMIP5 ensemble.
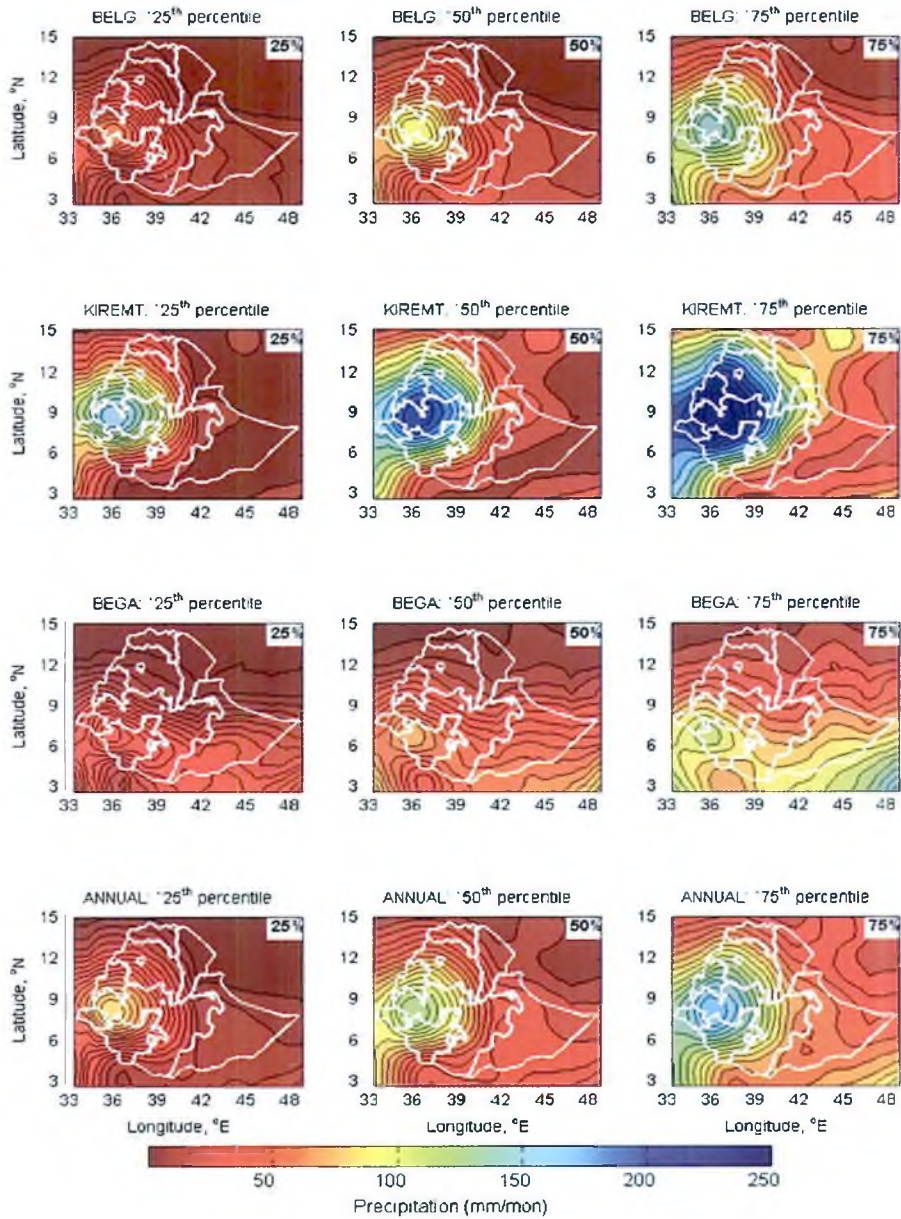
Figure A.2. Maps of seasonal and annual precipitation changes during 2046–2065 period with respect to 1986–2005 mean under the RCP4.5 scenario for the 25th, 50th and 75th percentiles of the distribution of the CMIP5 ensemble.
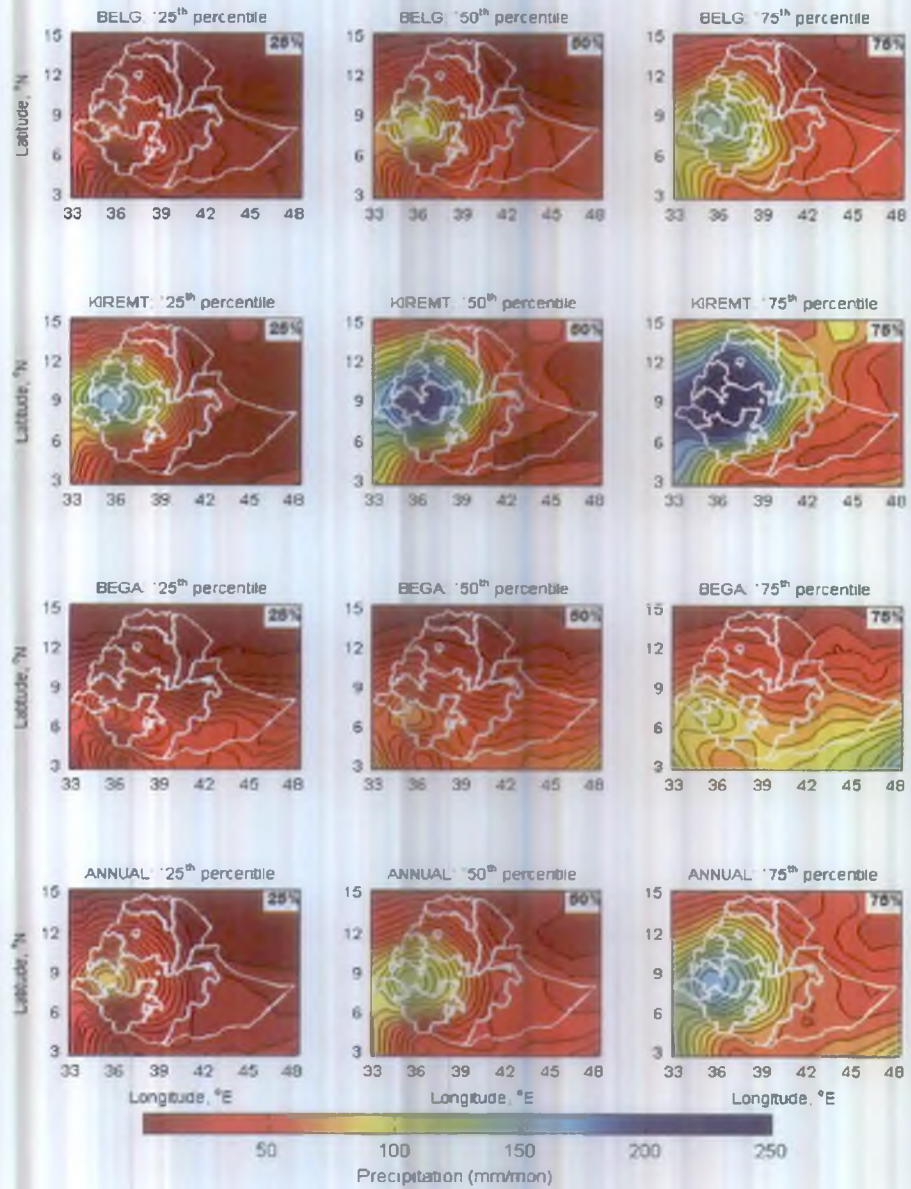
Figure A.3. Maps of seasonal and annual precipitation changes during 2081–2100 period with respect to 1986–2005 mean under the RCP4.5 scenario for the 25th, 50th and 75th percentiles of the distribution of the CMIP5 ensemble.
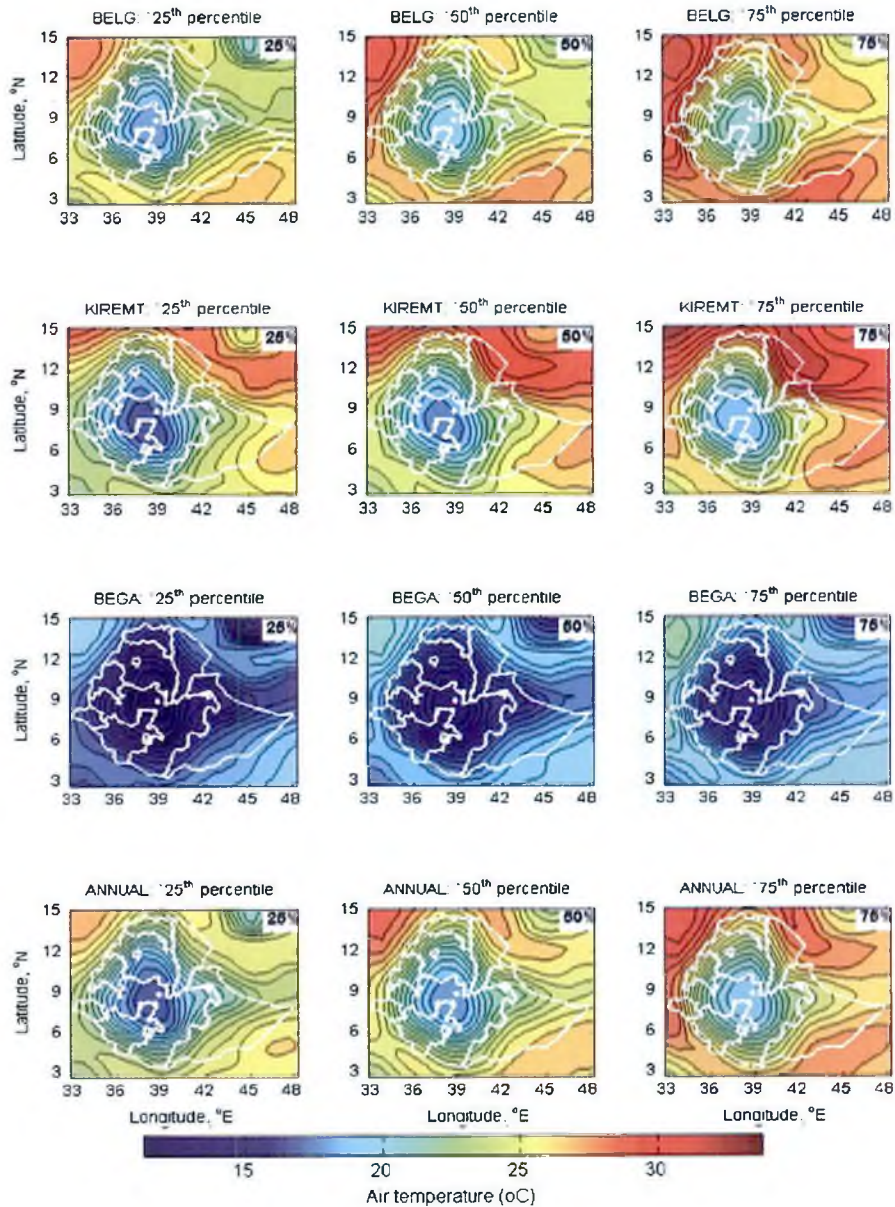
Figure A.4. Maps of seasonal and annual temperature changes during 2016–2035 period with respect to 1986–2005 mean under the RCP4.5 scenario for the 25th, 50th and 75th percentiles of the distribution of the CMIP5 ensemble.
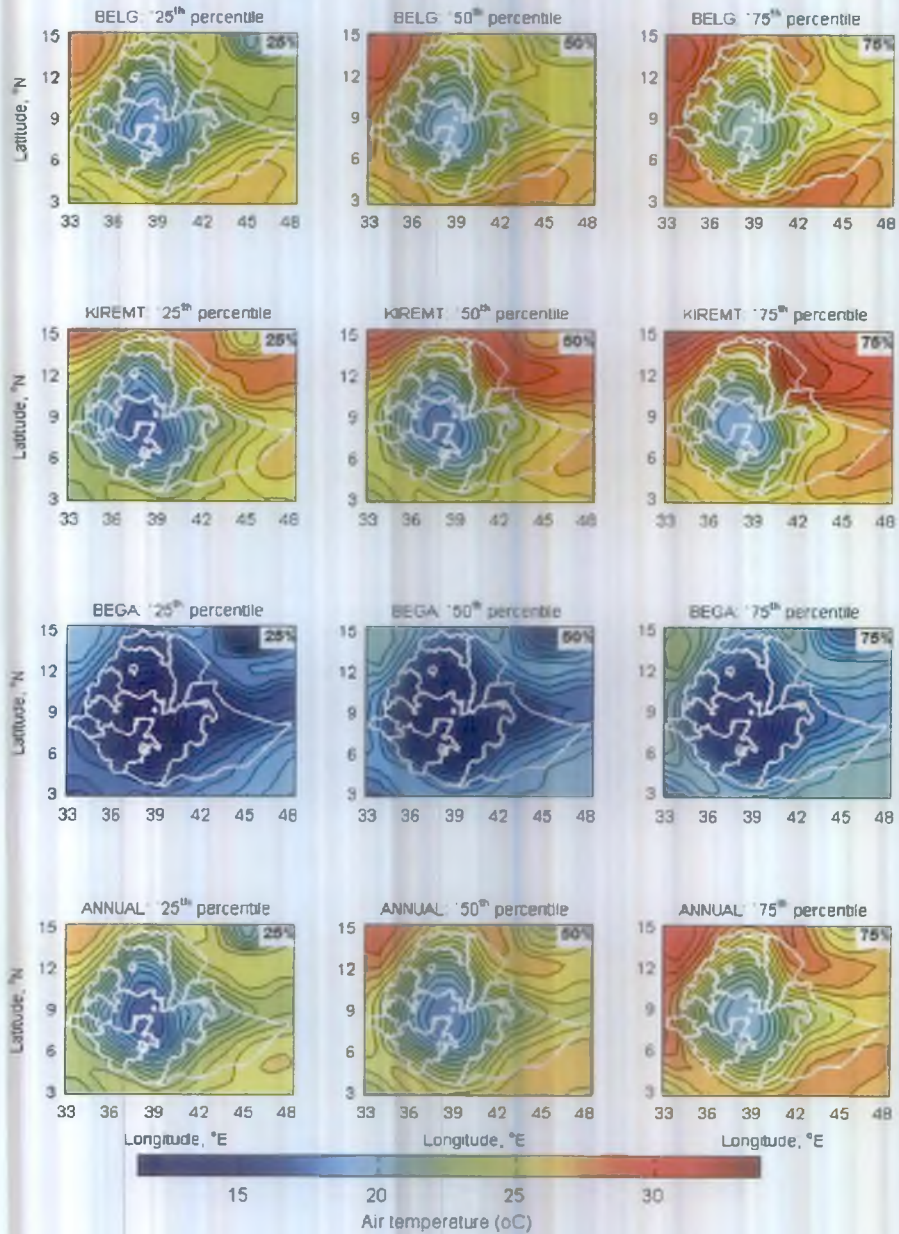
Figure A.5. Maps of seasonal and annual temperature changes during 2046–2065 period with respect to 1986–2005 mean under the RCP4.5 scenario for the 25th, 50th and 75th percentiles of the distribution of the CMIP5 ensemble.
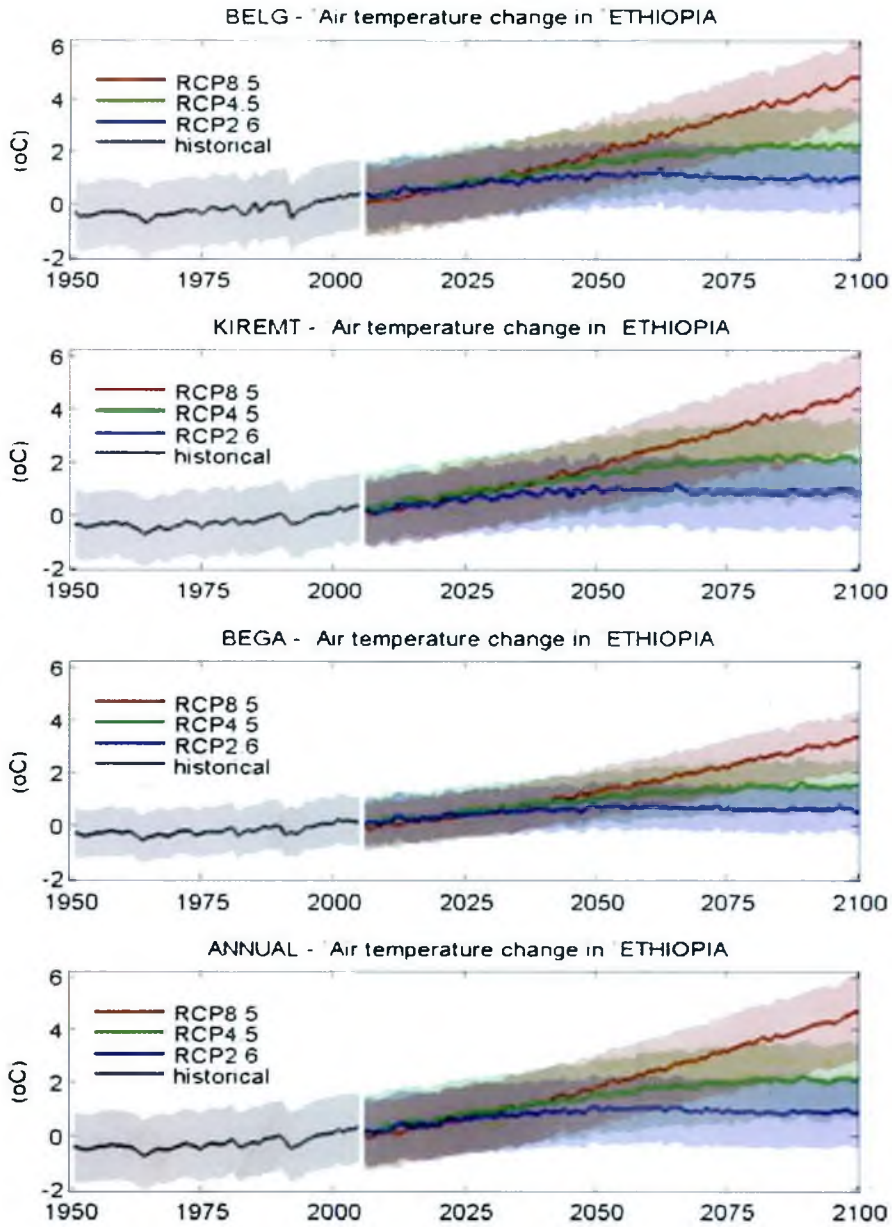
Figure A.8. Time series of seasonal and annual temperature change relative to 1986–2005 averaged over Ethiopia for the three RCP scenarios.
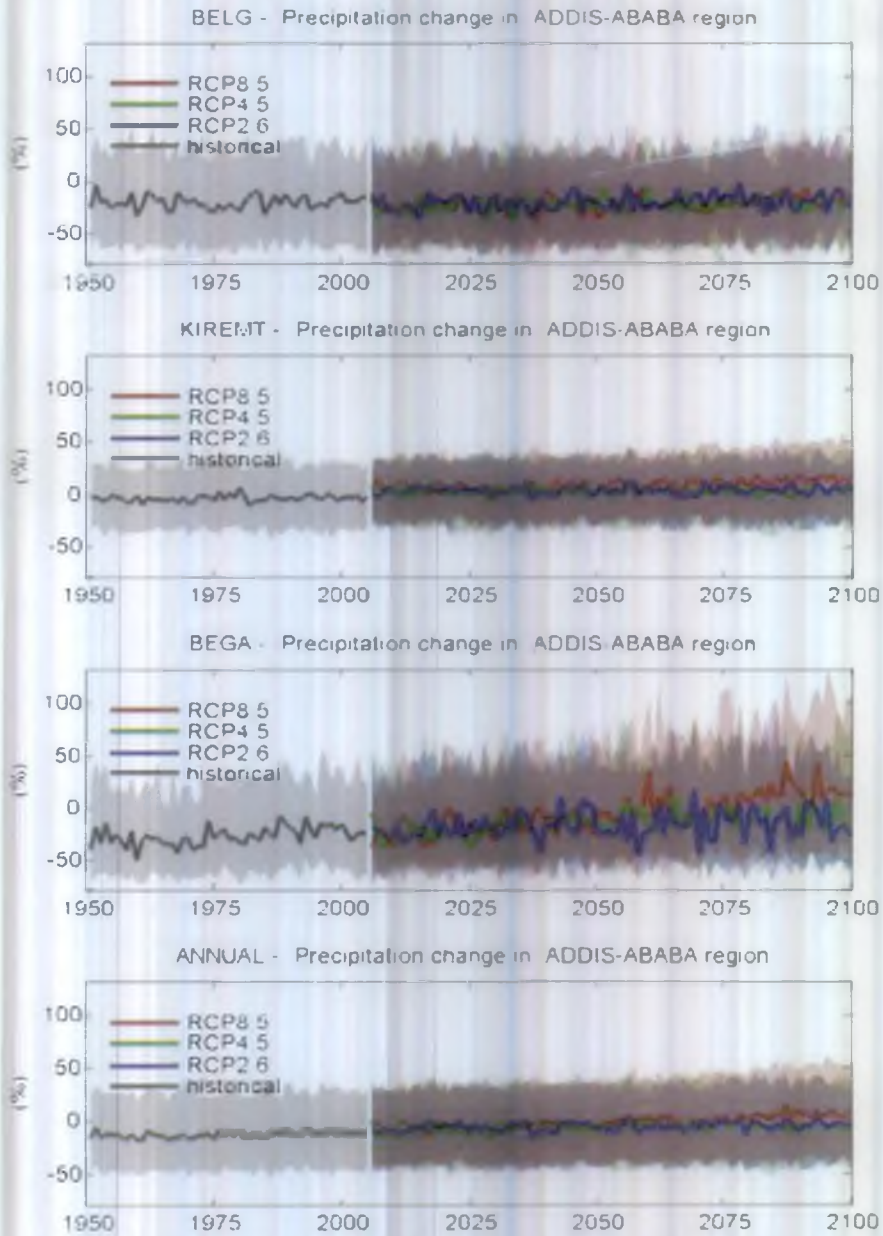
Figure A.9. Time series of relative change in seasonal and annual precipitation relative to 1986–2005 mean averaged over Addis Ababa region for the three RCP scenarios.
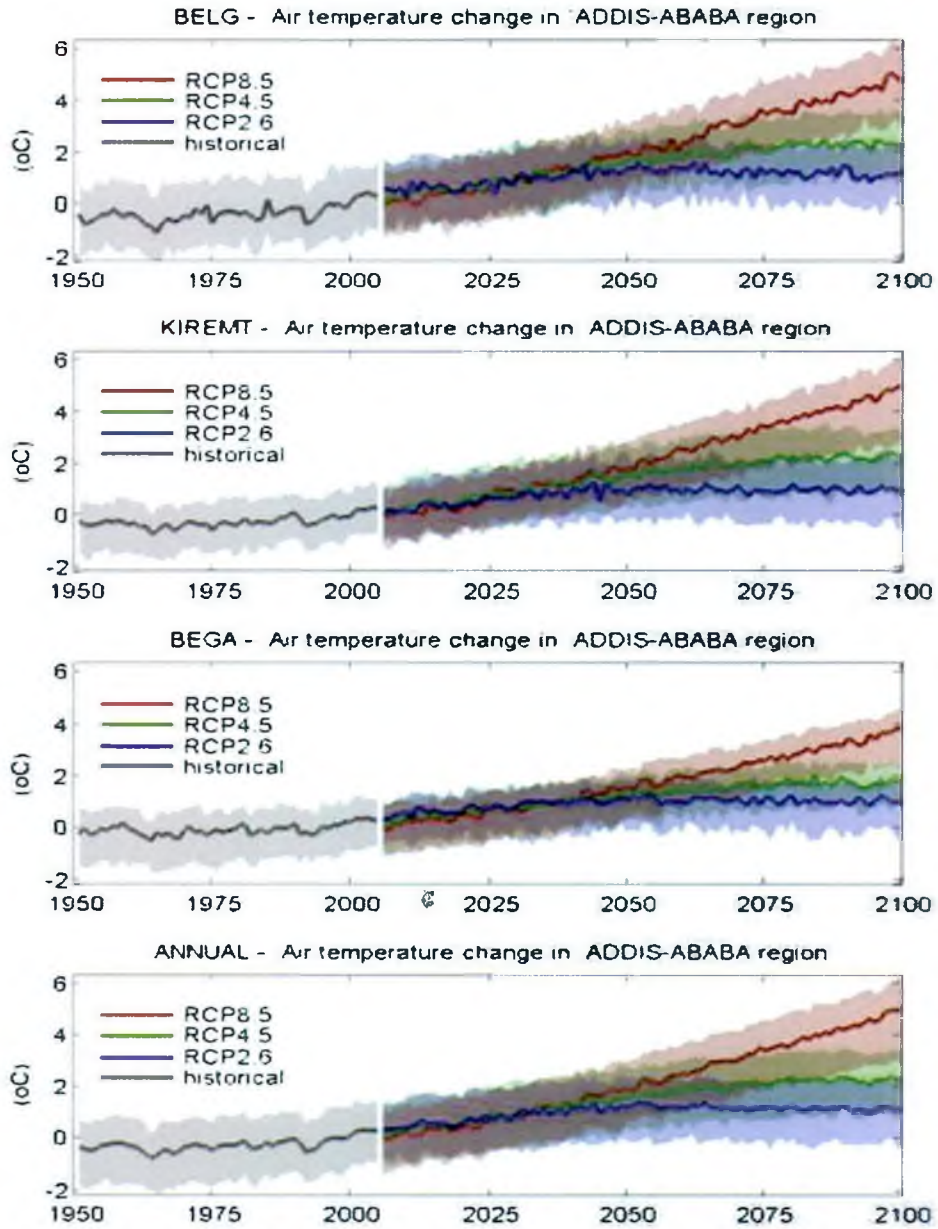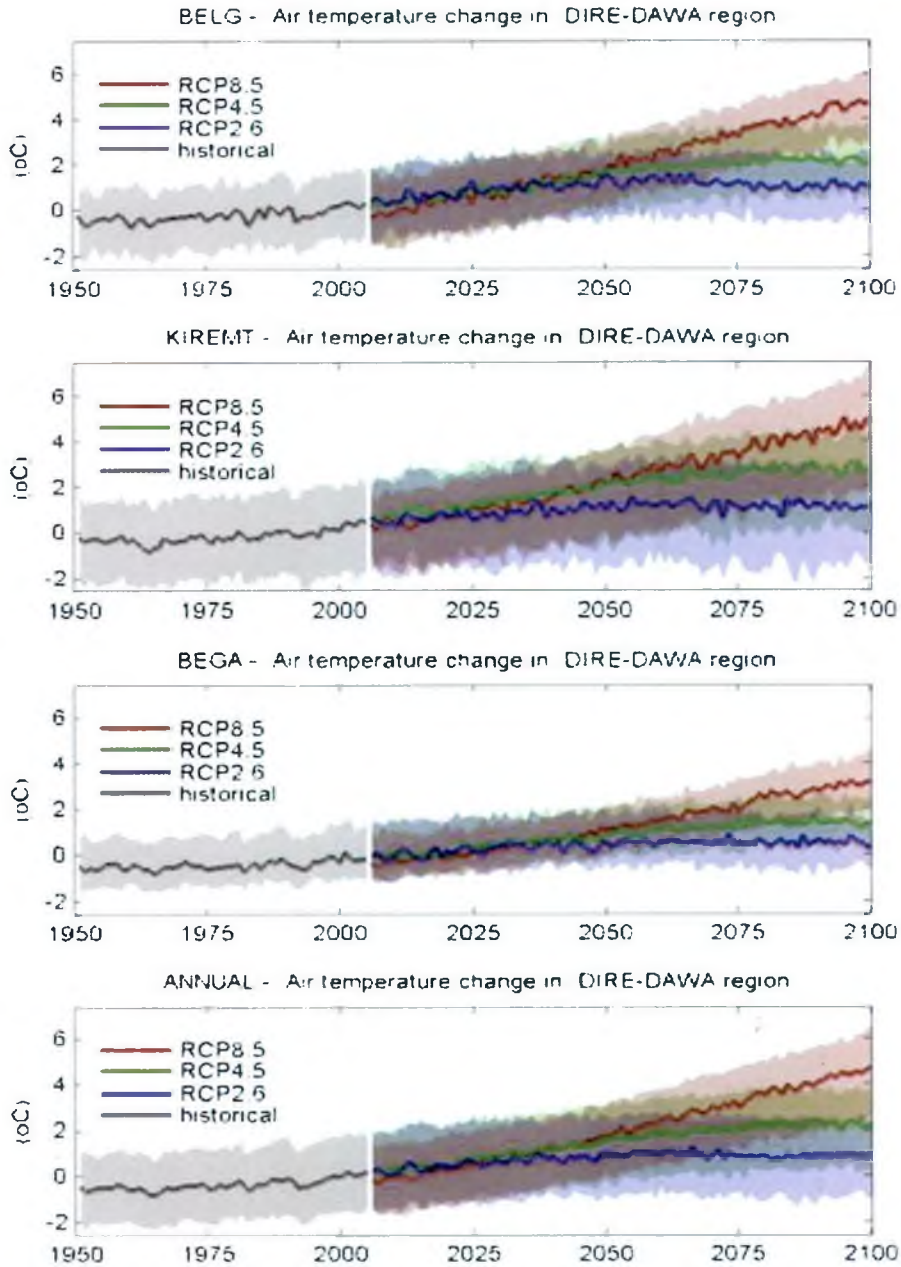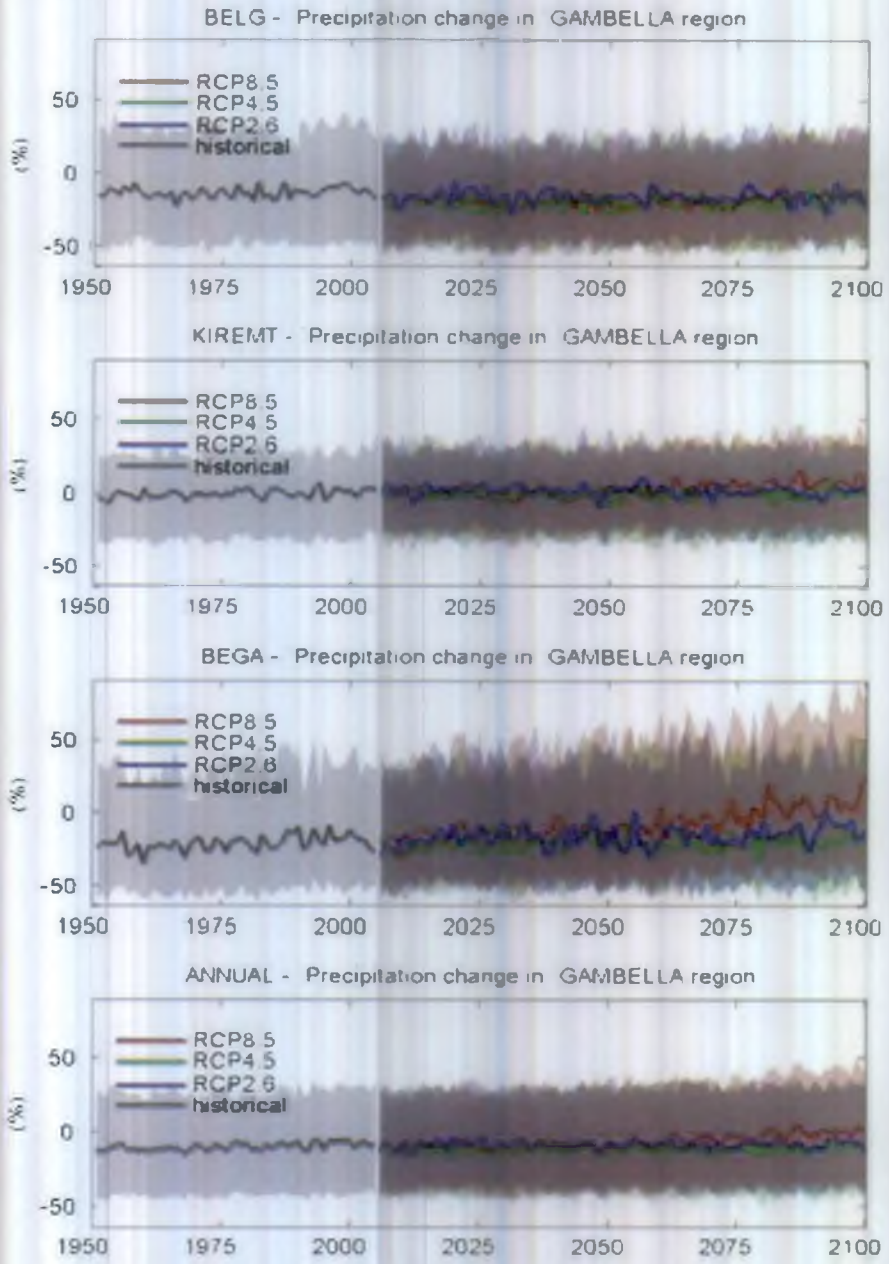
Figure A.10. Time series of seasonal and annual temperature change relative to 1986–2005 mean averaged over Addis Ababa region for the three RCP scenarios.
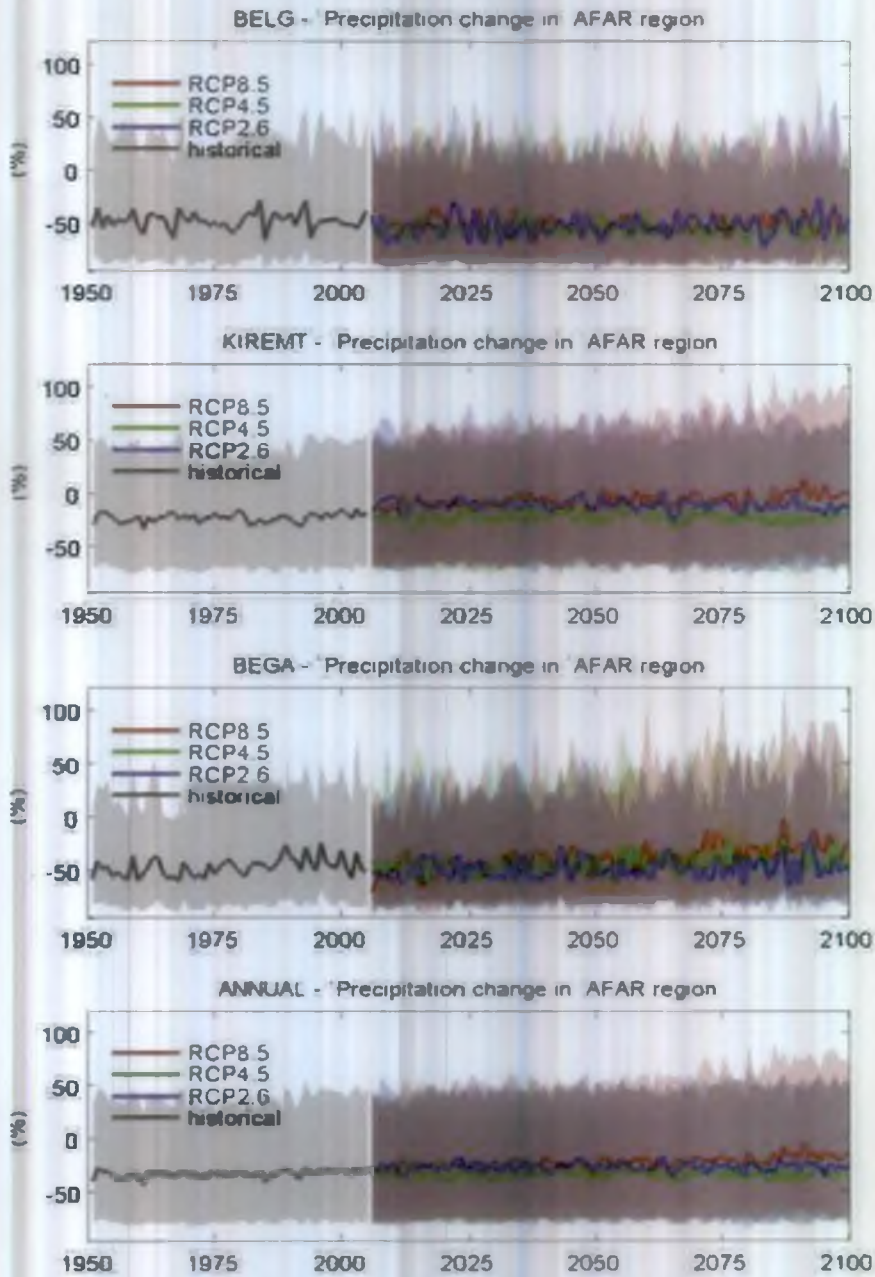
Figure A.11. Time series of relative change in seasonal and annual precipitation relative to 1986–2005 mean averaged over Afar region in the three RCP scenarios.
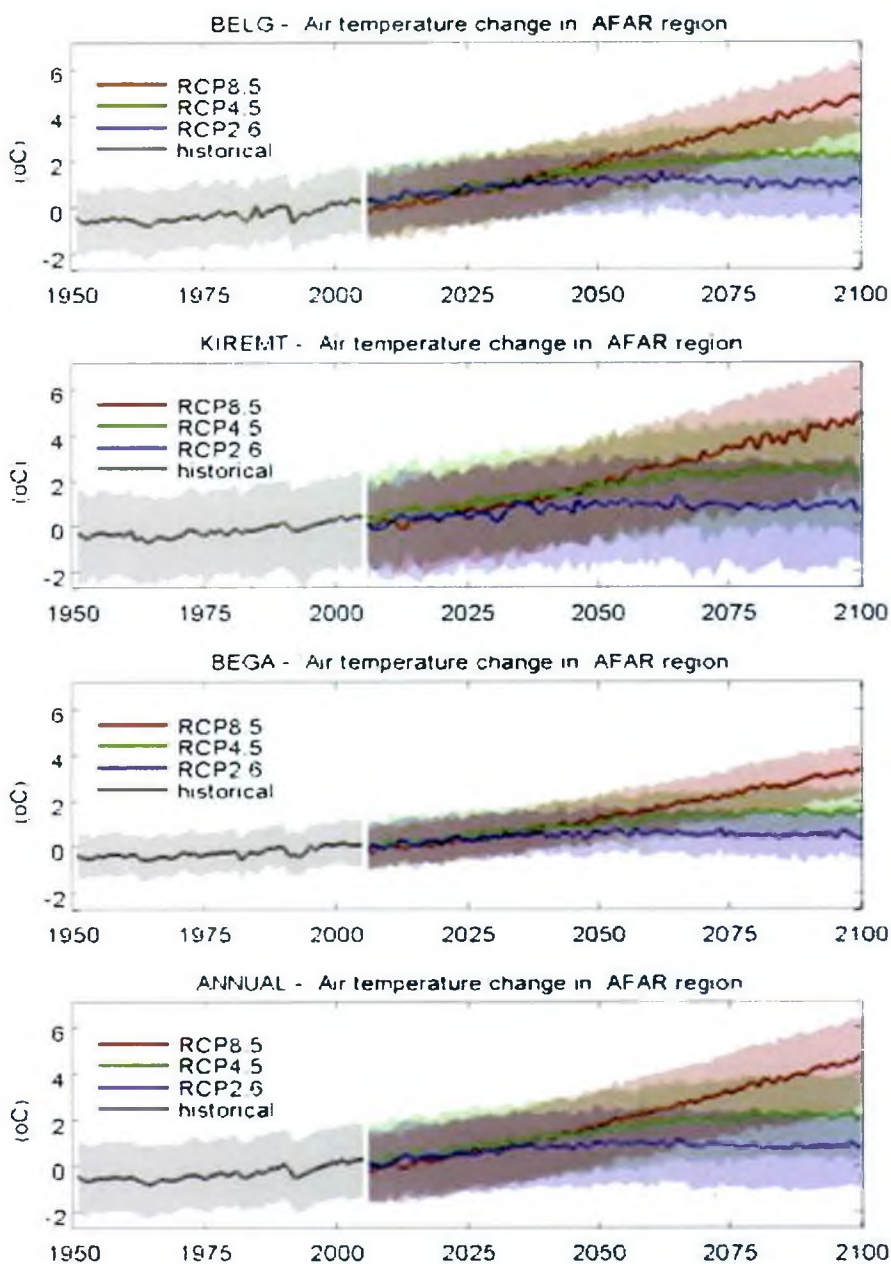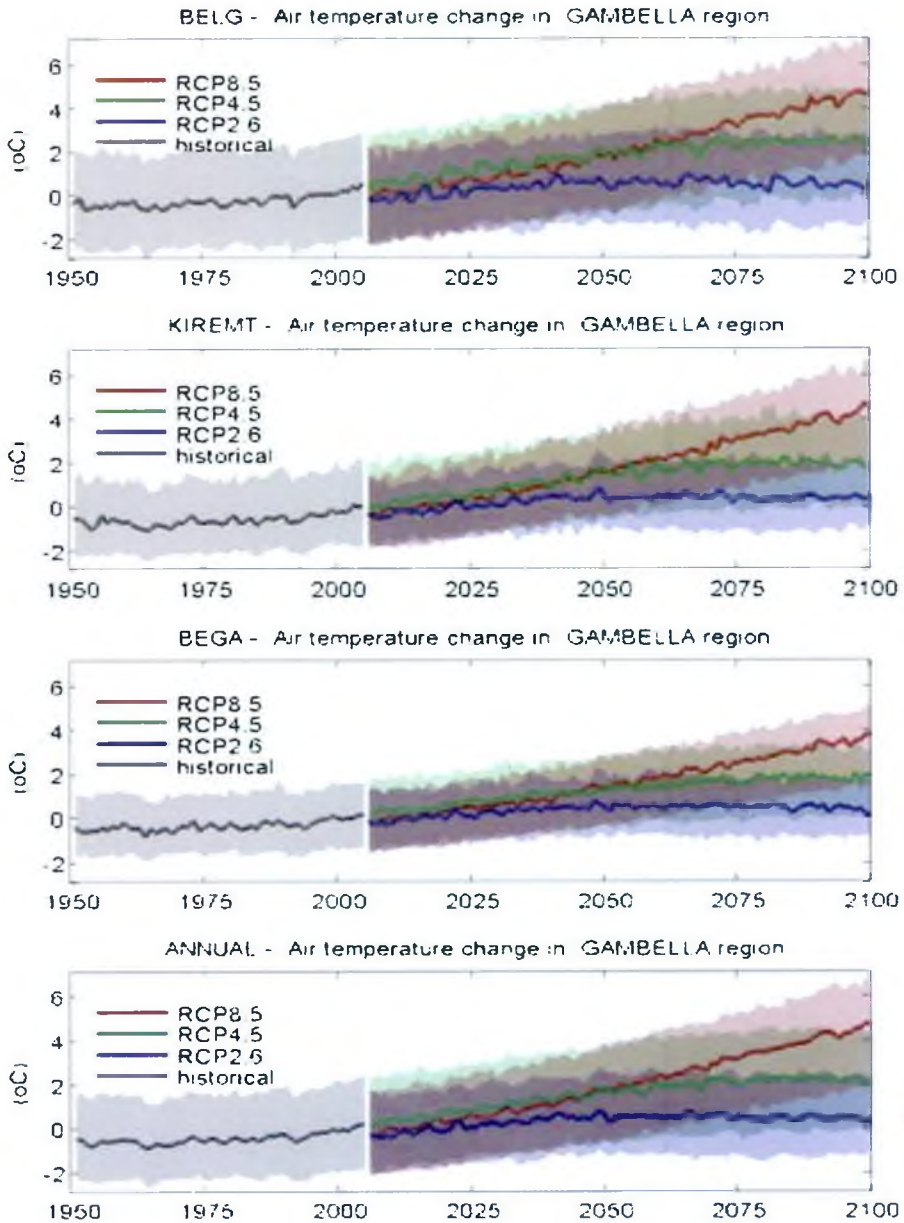
Figure A.12. Time series of seasonal and annual temperature change relative to 1986–2005 averaged over Afar region for the three RCP scenarios.
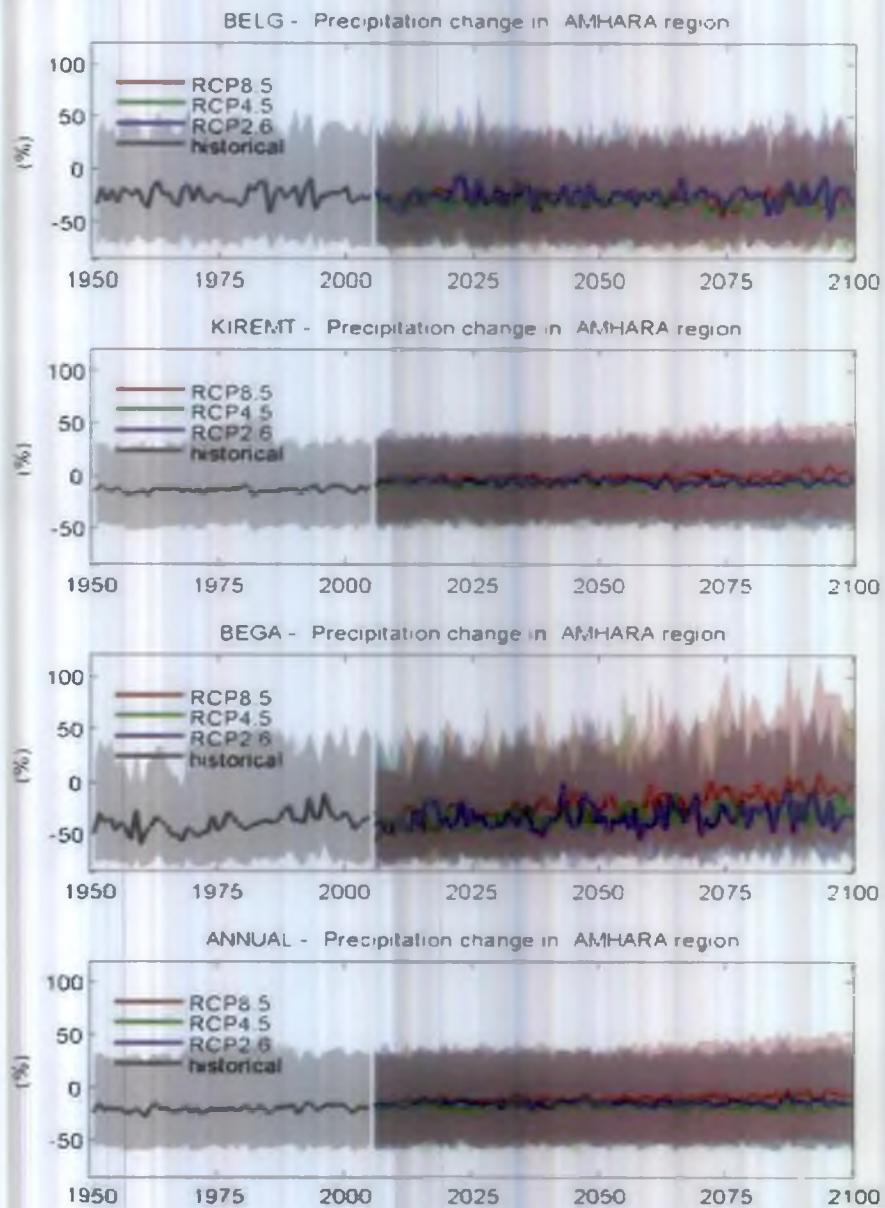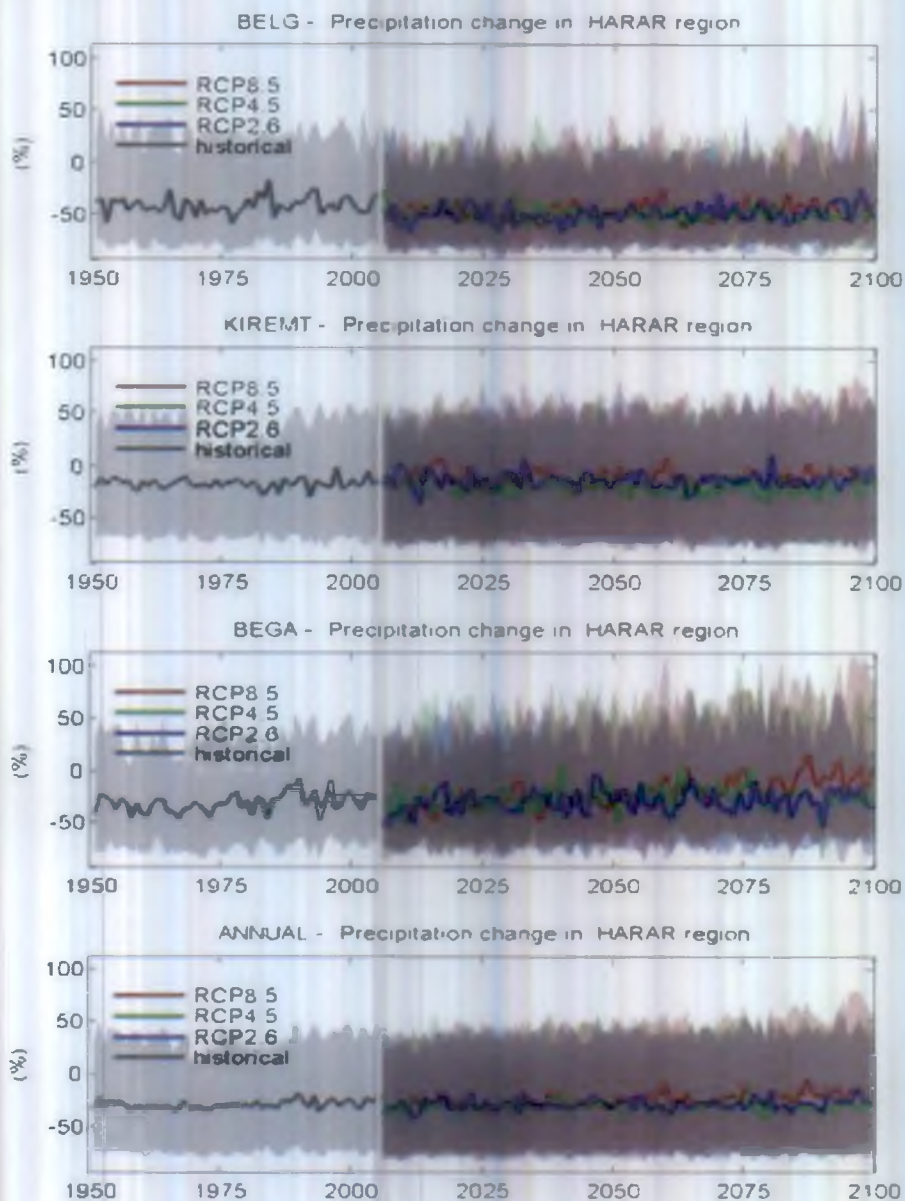
Figure A.13. Time series of relative change in seasonal and annual precipitation relative to 1986–2005 averaged over Amhara region for the three RCP scenarios.
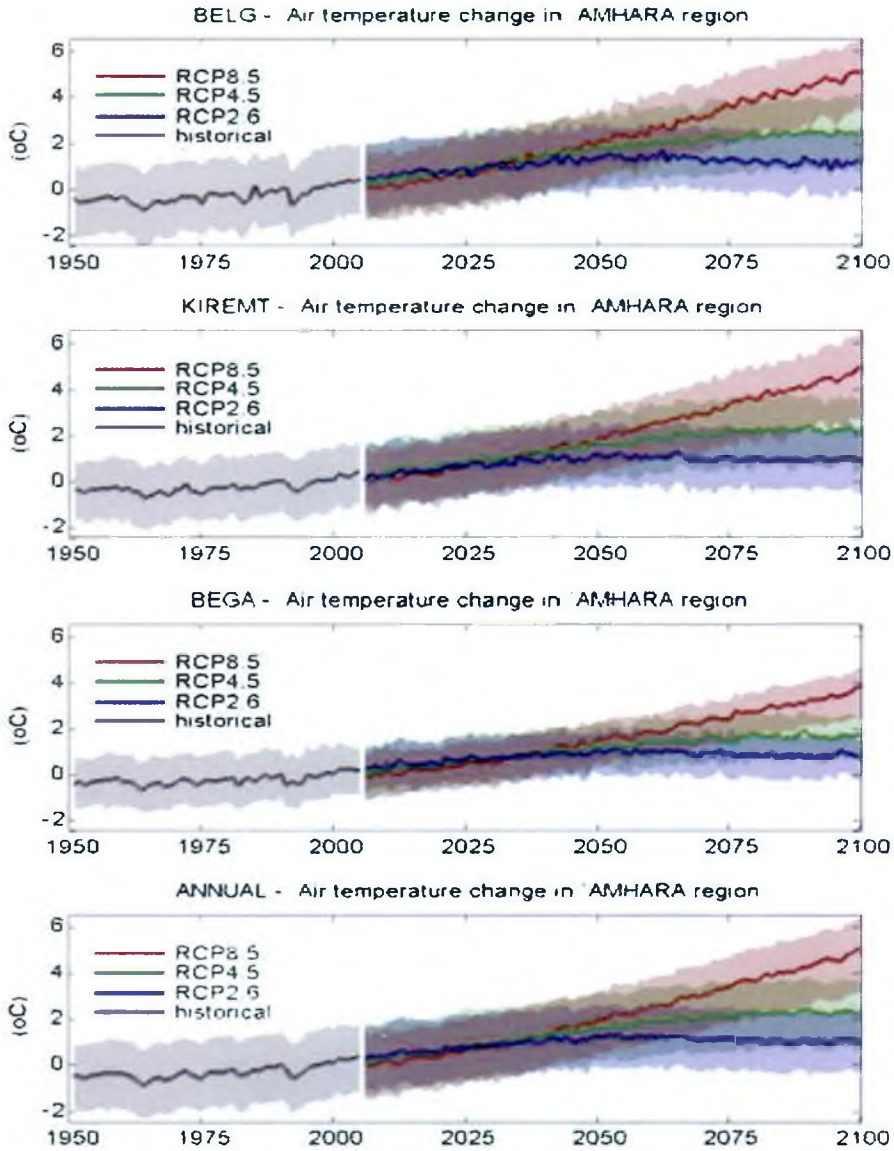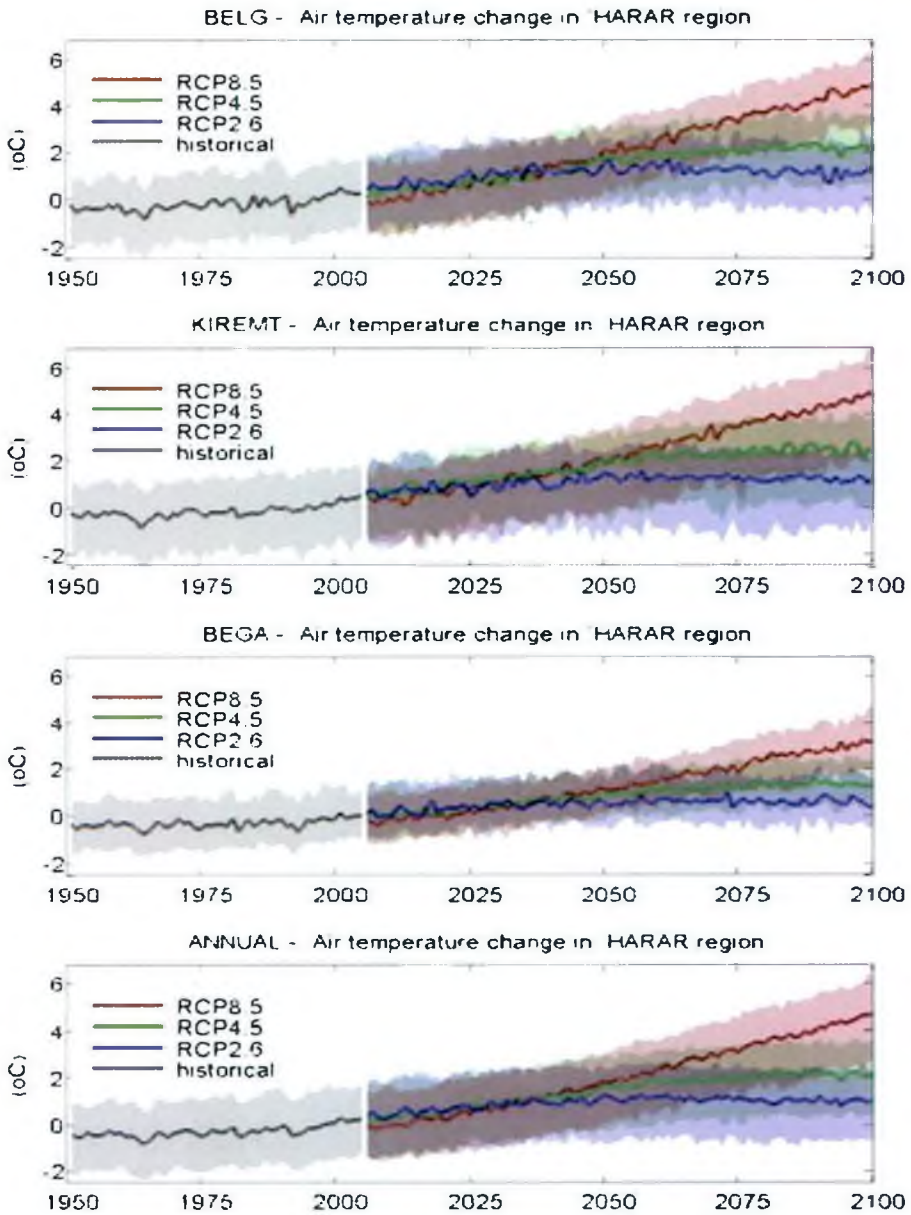
Figure A.14. Time series of seasonal and annual temperature change relative to 1986–2005 averaged over Amhara region for the three RCP scenarios.
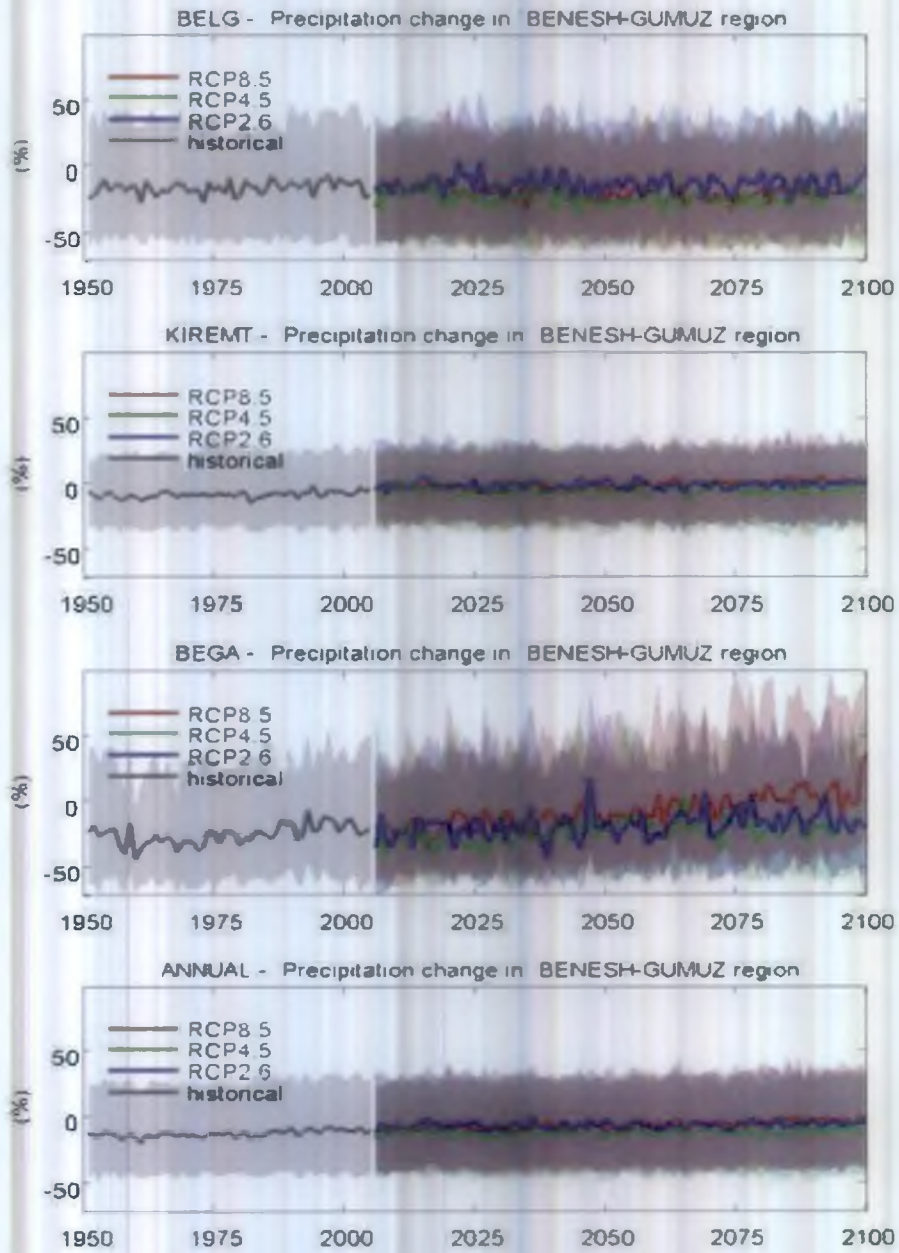
Figure A.15. Time series of relative change in seasonal and annual precipitation relative to 1986–2005 averaged over Beneshangul gumuz region for the three RCP scenarios.
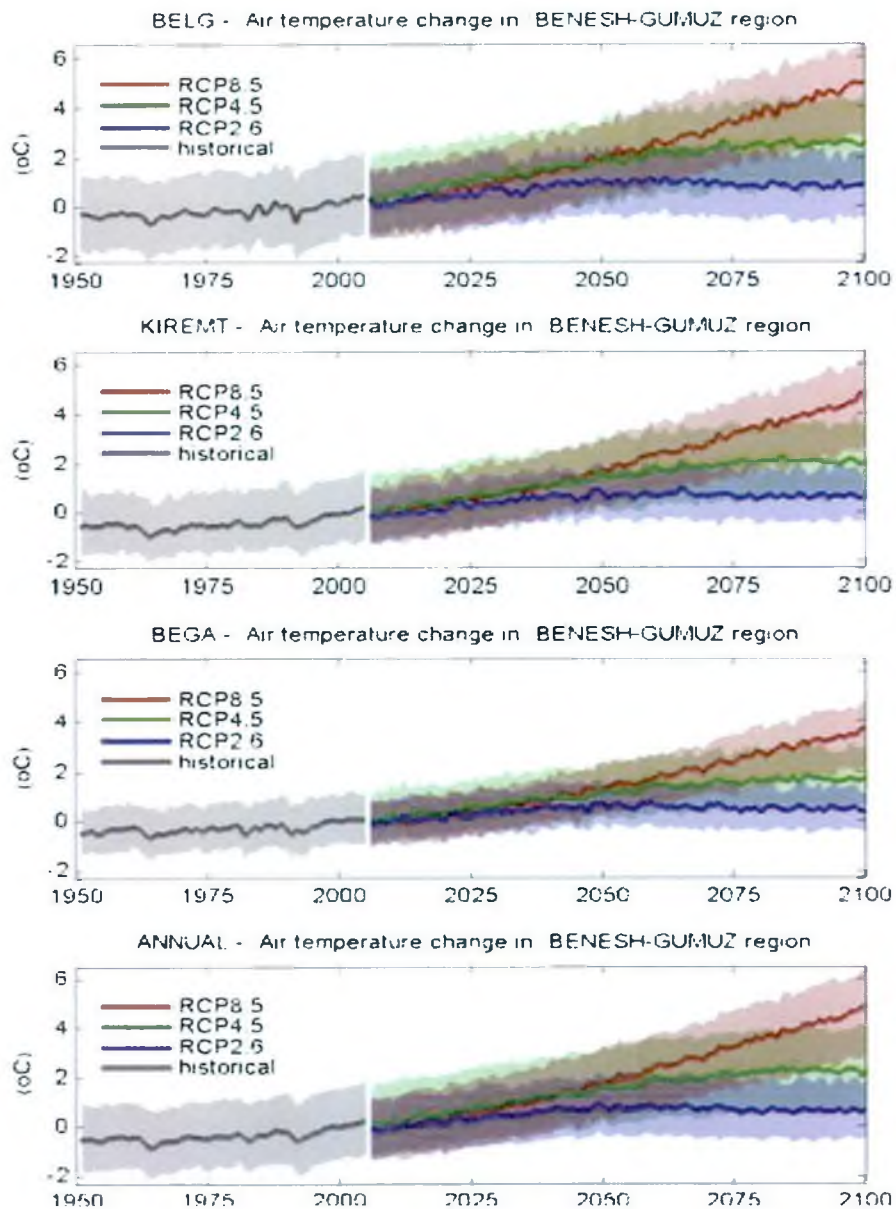
Figure A.16. Time series of seasonal and annual temperature change relative to 1986–2005 averaged over Beneshangul Gumuz region for the three RCP scenarios.
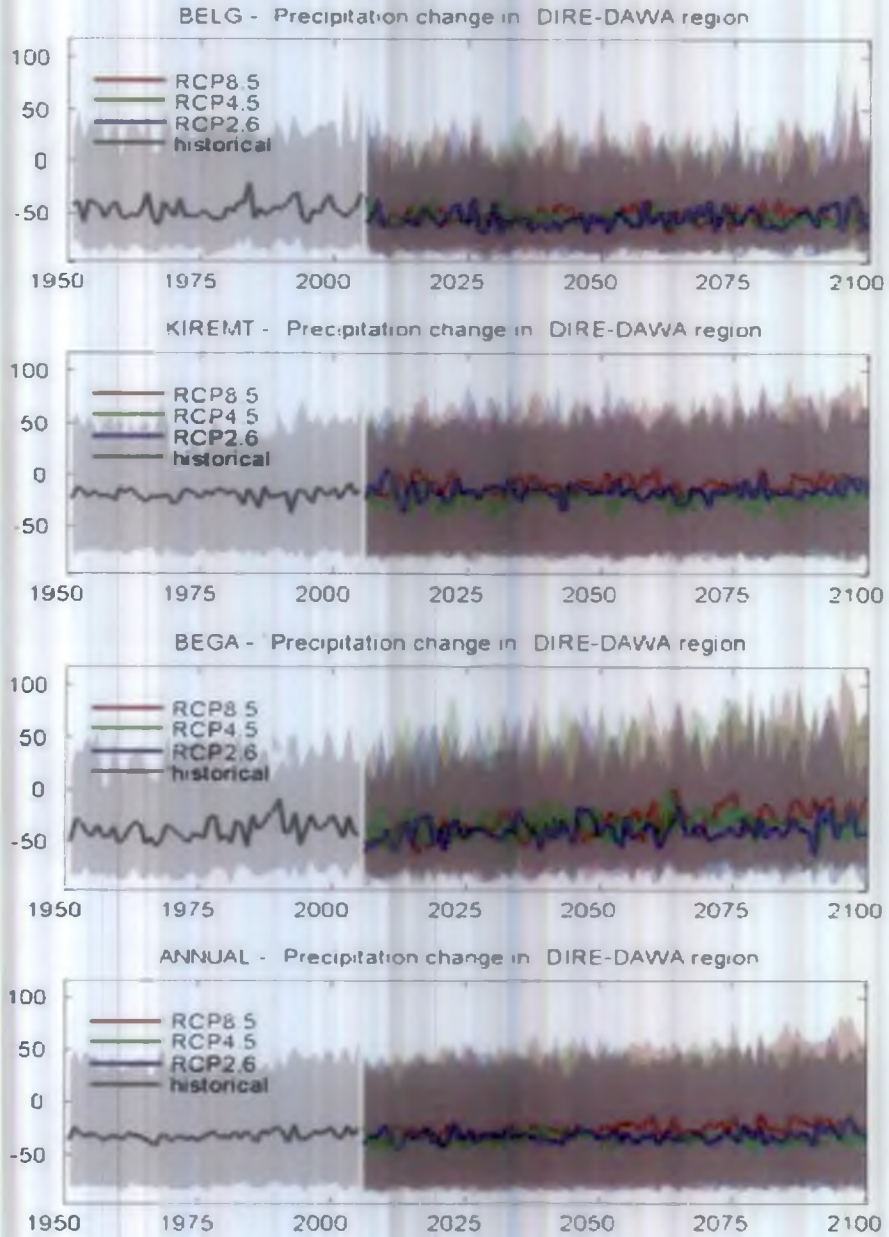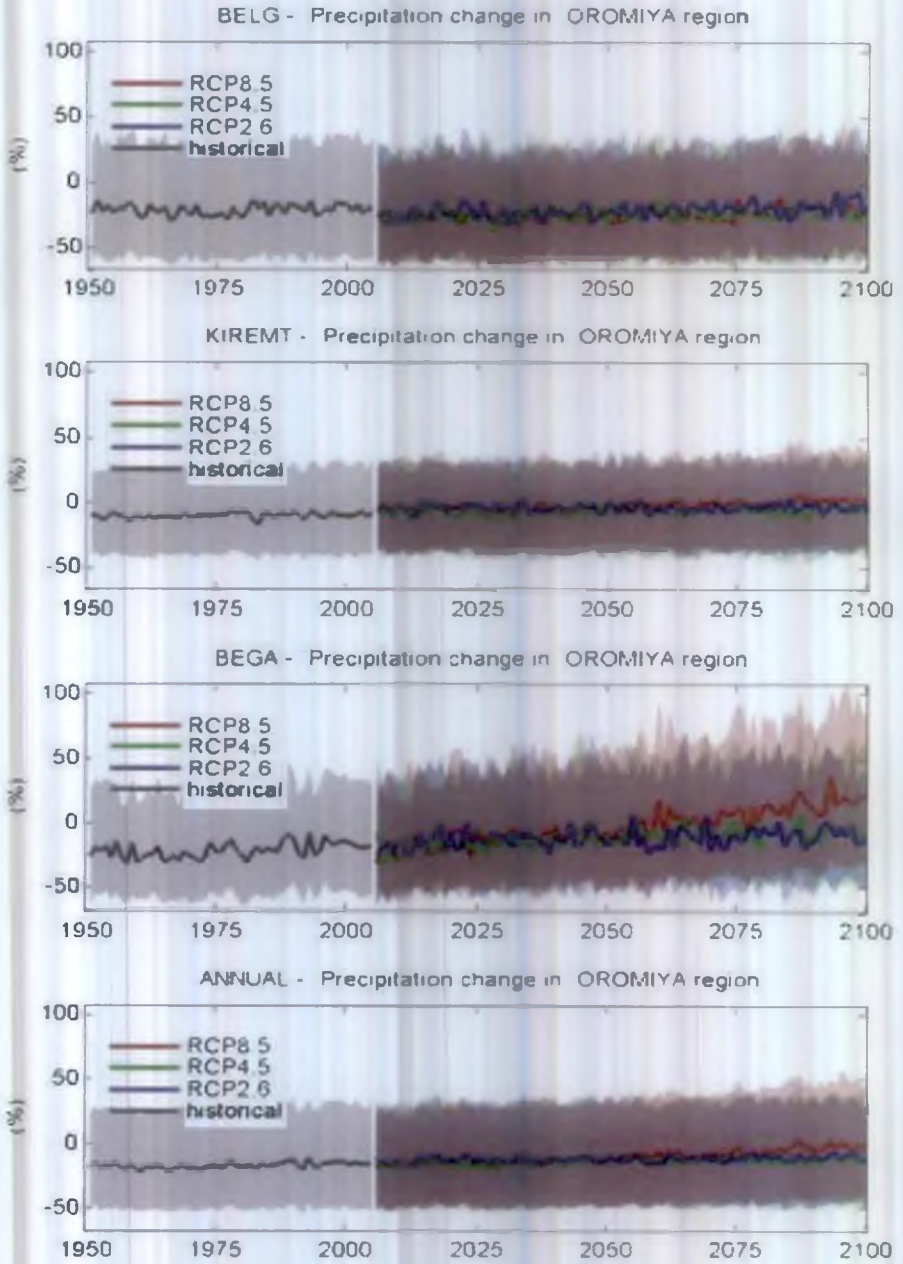
Figure A.17 Time series of relative change in seasonal and annual precipitation relative to 1986–2005 averaged over Dire Dawa region for the three RCP scenarios.
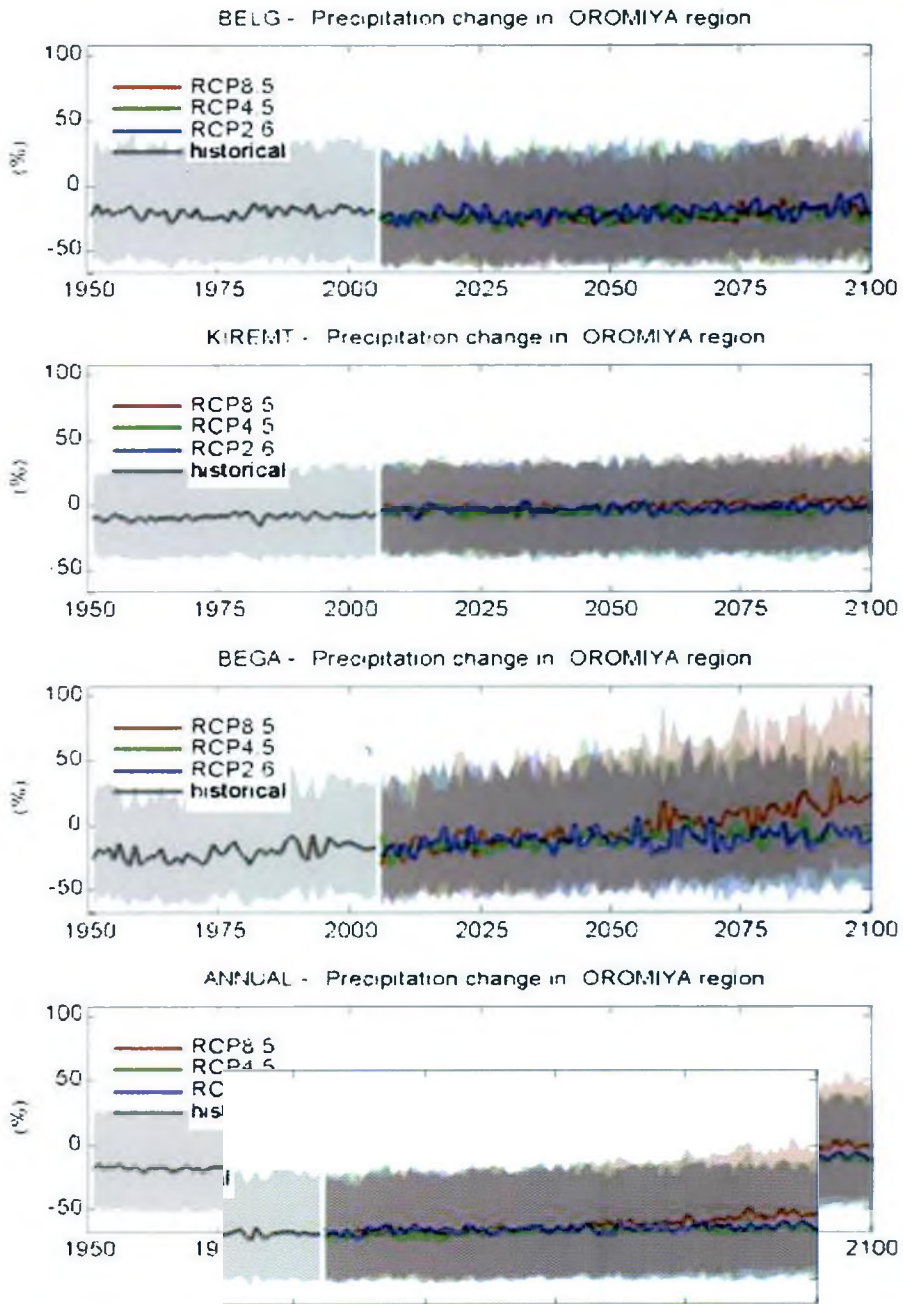
Figure A.18 Time series of seasonal and annual temperature change relative to 1986–2005 averaged over Dire Dawa region for the three RCP scenarios.

Figure A.19. Time series of relative change in seasonal and annual precipitation relative to 1986–2005 mean averaged over Gambella region for the three RCP scenarios.

Figure A.20. Time series of seasonal and annual temperature change relative to 1986–2005 averaged over Gambella region for the three rcp scenarios.
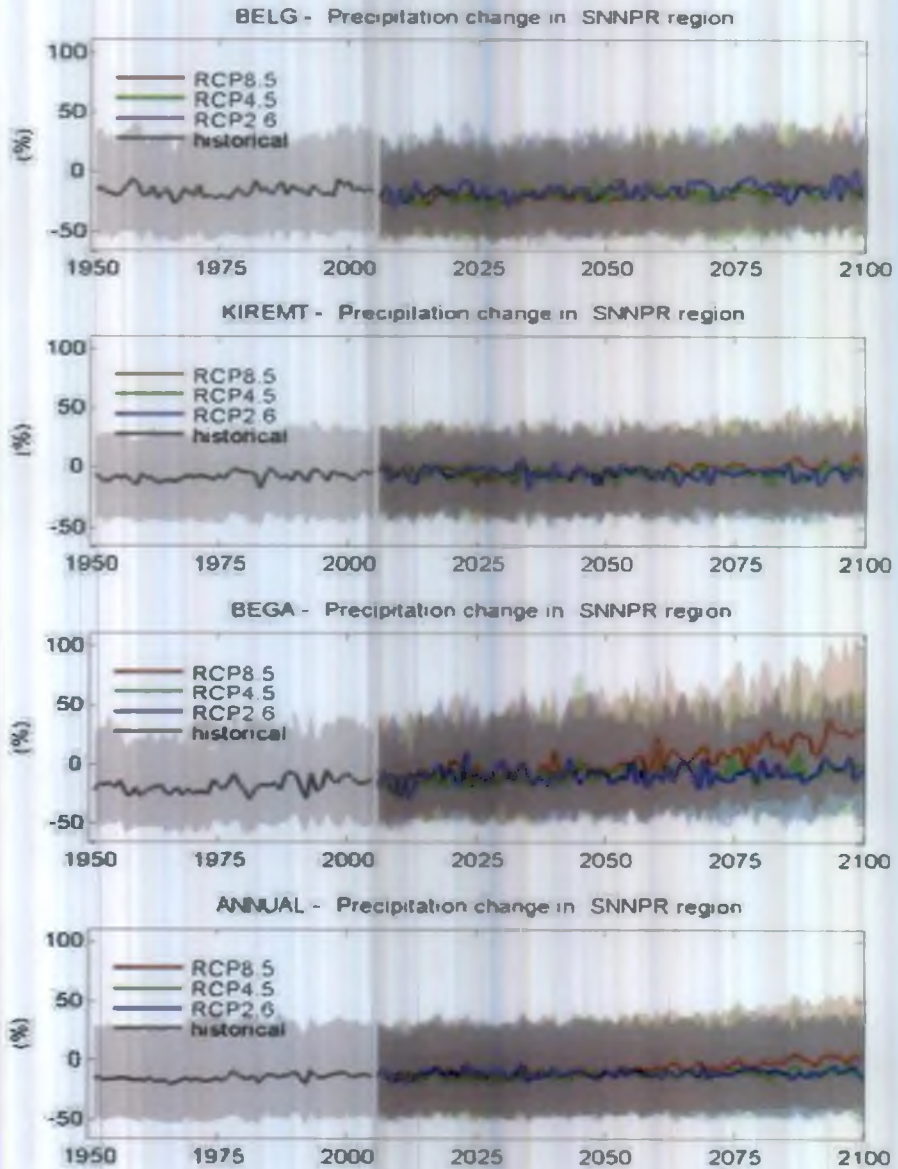
Figure A.21. Time series of relative change in seasonal and annual precipitation relative to 1986–2005 averaged over Harar region for the three RCP scenarios.
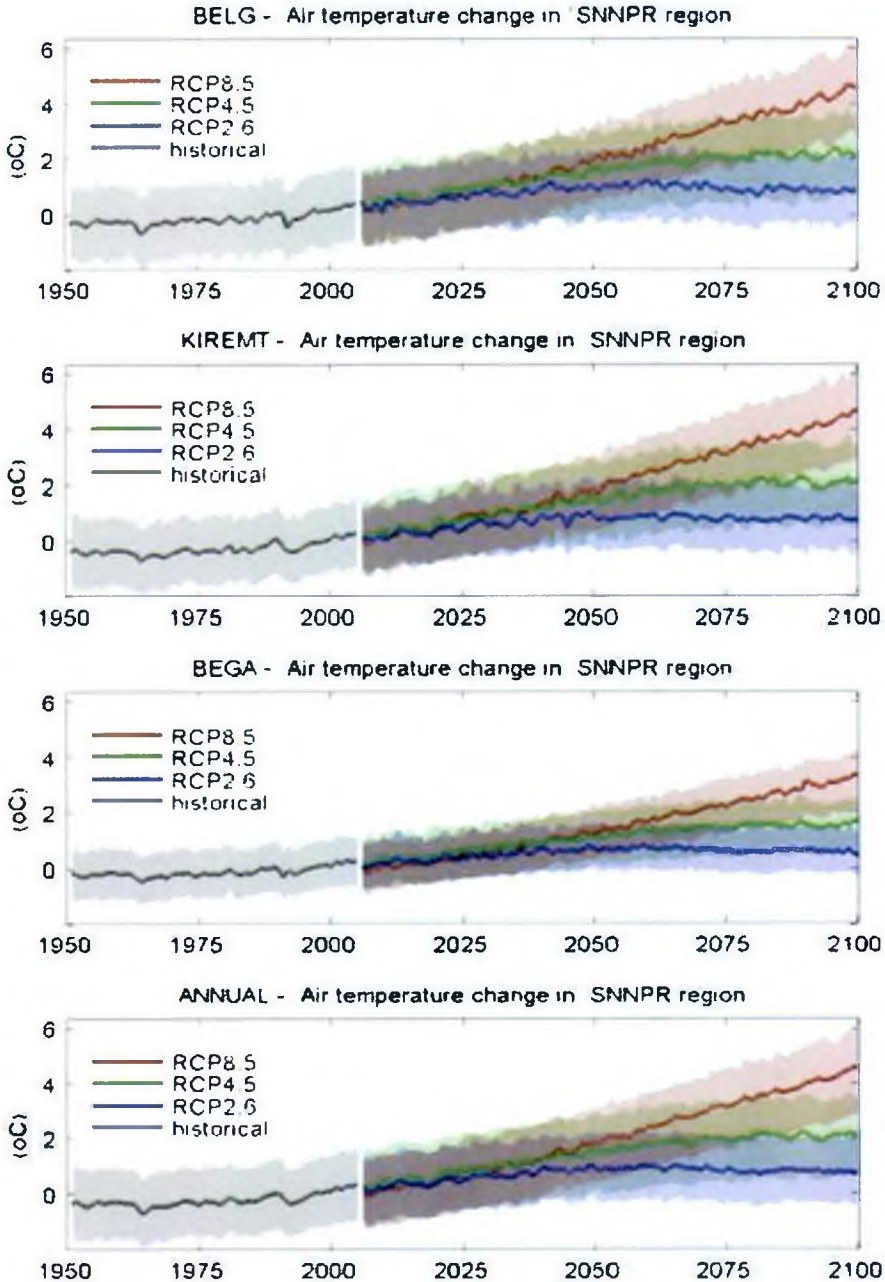
Figure A.22. Time series of seasonal and annual temperature change relative to 1986–2005 averaged over Harar region for the three RCP scenarios.
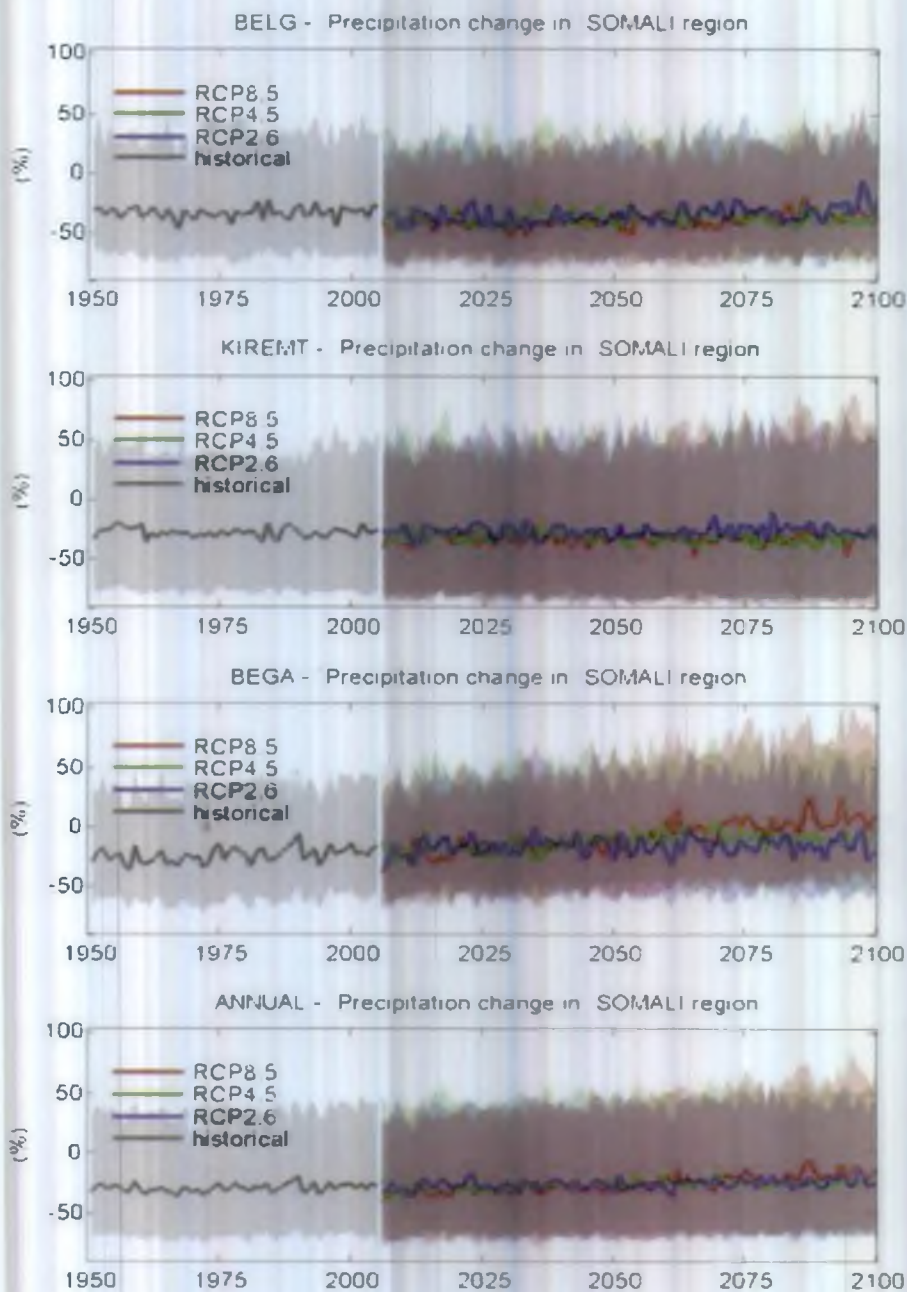
Figure A.23. Time series of relative change in seasonal and annual precipitation relative to 1986–2005 averaged over Oromiya region for the three RCP scenarios.

Figure A.24. Time series of seasonal and annual temperature change relative to 1986–2005 averaged over Oromiya region for the three rcp scenarios.

Figure A.25. Time series of relative change in seasonal and annual precipitation relative to 1986–2005 averaged over SNNRP region for the three RCP scenarios.
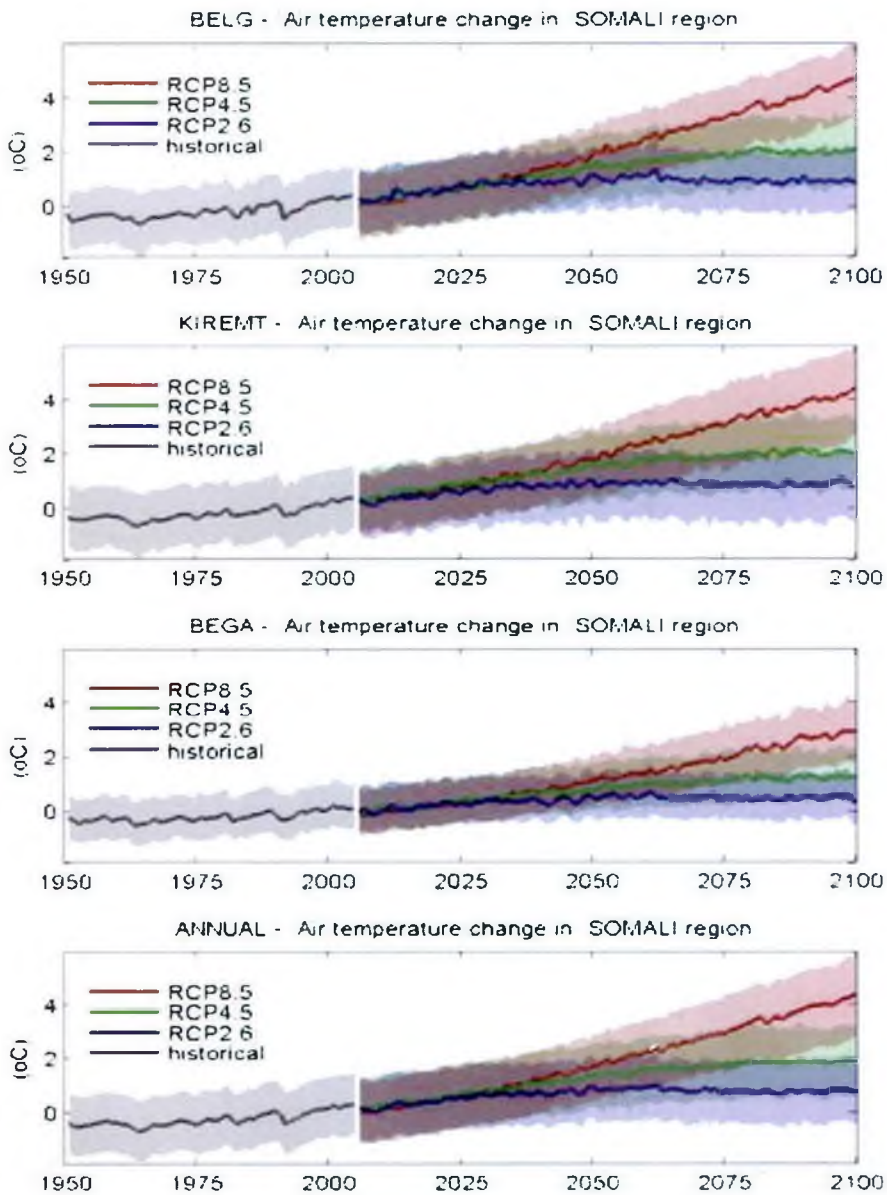
Figure A.26. Time series of seasonal and annual temperature change relative to 1986–2005 averaged over SNNRP region for the three RCP scenarios.

Figure A.27. Time series of relative change in seasonal and annual precipitation relative to 1986–2005 averaged over Somali region for the three RCP scenarios.

Figure A.28. Time series of seasonal and annual temperature change relative to 1986–2005 averaged over Somali region for the three RCP scenarios.
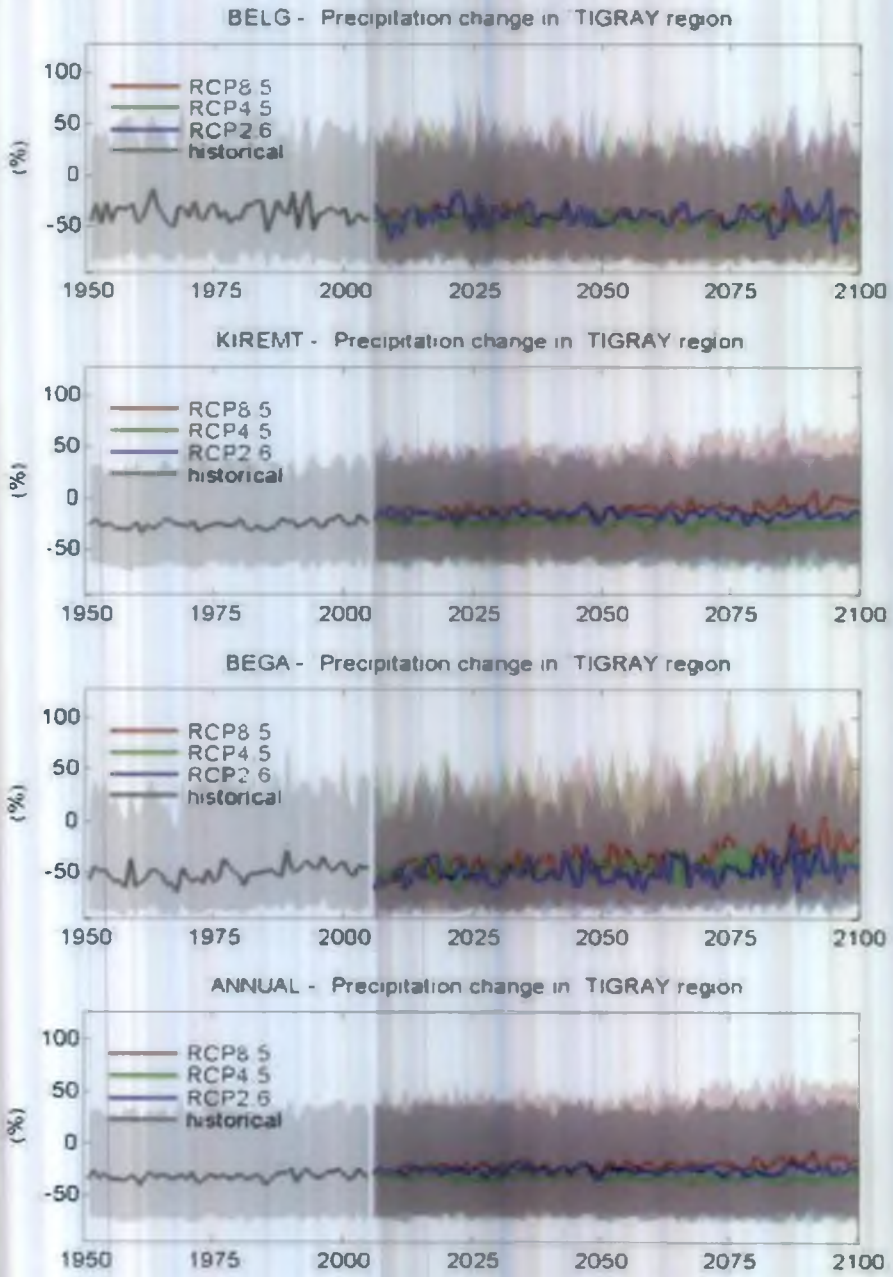
Figure A.29. Time series of relative change in seasonal and annual precipitation relative to 1986–2005 averaged over Tigray region for the three RCP scenarios.
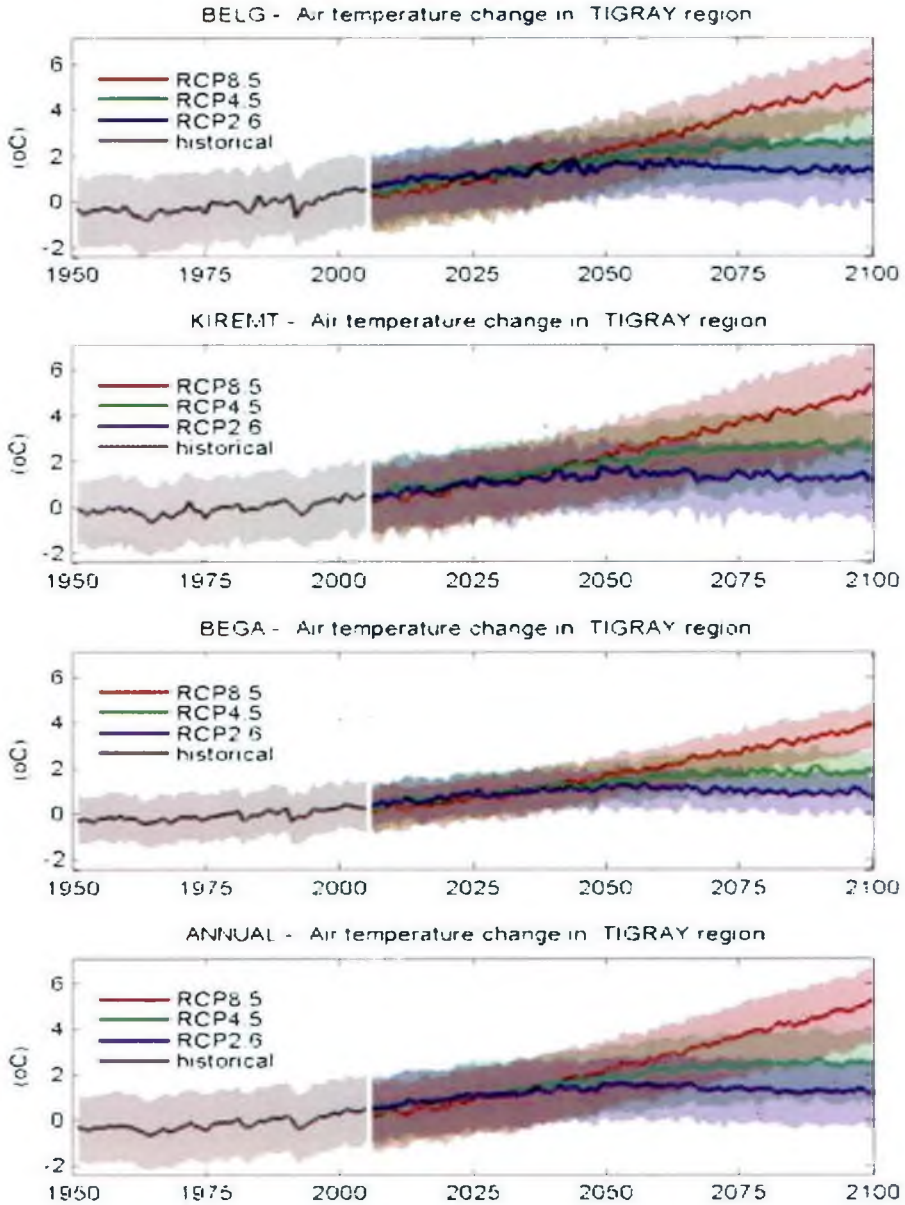
Figure A.30 Time series of seasonal and annual temperature change relative to 1986–2005 averaged over Tigray region for the three RCP scenarios.

Ethiopian
Academy
of Sciences
የኢትዮጵያ ሳይንስ አካዳሚ

PCC
ETHIOPIAN PANEL ON
CLIMATE CHANGE